



**DESIGN OF CYCLOPHANES:
SYNTHESIS AND STUDY OF PHOTOPHYSICAL AND
BIOMOLECULAR RECOGNITION PROPERTIES**

**Thesis Submitted to
Cochin University of Science and Technology
in Partial Fulfilment of the Requirements for the Degree of**

**Doctor of Philosophy
in Chemistry under the Faculty of Science**

By

PRAKASH P. N.

**Under the Supervision of
Dr. D. RAMAIAH**



**Photosciences and Photonics
Chemical Sciences and Technology Division
National Institute for Interdisciplinary Science and Technology
(Formerly, Regional Research Laboratory), CSIR,
Trivandrum 695 019, Kerala**

December 2008

STATEMENT

I hereby declare that the matter embodied in the thesis entitled: “**Design of Cyclophanes: Synthesis and Study of Photophysical and Biomolecular Recognition Properties**” is the result of investigations carried out by me at the Photosciences and Photonics, Chemical Sciences and Technology Division of the National Institute for Interdisciplinary Science and Technology (*formerly*, Regional Research Laboratory), CSIR, Trivandrum, under the supervision of Dr. D. Ramaiah and the same has not been submitted elsewhere for a degree.

In keeping with the general practice of reporting scientific observations, due acknowledgement has been made wherever the work described is based on the findings of other investigators.



(Prakash P. N.)

National Institute for Interdisciplinary Science and Technology



Photosciences and Photonics
Chemical Sciences and Technology Division
Trivandrum 695019, India



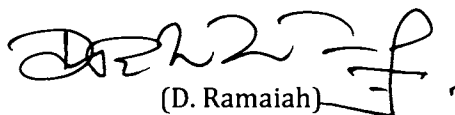
Dr. D. Ramaiah
Scientist

Tel: +91 471 2515362; Fax: +91 471 2490186
E-mail: d_ramaiah@rediffmail.com

December 05, 2008

CERTIFICATE

This is to certify that the work embodied in the thesis entitled: **“Design of Cyclophanes: Synthesis and Study of Photophysical and Biomolecular Recognition Properties”** has been carried out by Mr. Prakash P. N. under my supervision at the Photosciences and Photonics, Chemical Sciences and Technology Division of the National Institute for Interdisciplinary Science and Technology (*formerly*, Regional Research Laboratory), CSIR, Trivandrum and the same has not been submitted elsewhere for a degree.



(D. Ramaiah)

Thesis Supervisor

ACKNOWLEDGEMENTS

I have great pleasure in placing on record my deep sense of gratitude to Dr. D. Ramaiah, my thesis supervisor, for suggesting the research problem and for his guidance, support and encouragement, leading to the successful completion of this work.

I would like to express my sincere thanks to Professor M. V. George for his constant help and encouragement during the tenure of this work.

I wish to thank Professor T. K. Chandrashekar and Dr. B. C. Pai, Directors of the National Institute for Interdisciplinary Science and Technology (NIIST) for providing me the necessary facilities for carrying out the work.

I sincerely thank Dr. Suresh Das, Dr. A. Ajayaghosh, Dr. K. R. Gopidas, Dr. K. George Thomas and Dr. A. Srinivasan, Scientists of the Photosciences and Photonics, Chemical Sciences and Technology Division, for all the help and support extended to me.

I thank all the members of the Photosciences and Photonics and in particular, Dr. Joshy Joseph, Dr. K. T. Arun, Dr. Mahesh Hariharan, Dr. Elizabeth Kuruvilla, Dr. Jyothish Kuthanapillil, Ms. V. S. Jisha, Ms. Rekha Rachel, Mr. Akhil K. Nair, Mr. C. K. Suneesh, Mr. P. C. Nandajan and Mr. K. S. Sanju for their help and cooperation. I also thank members of other Divisions of NIIST for their help and cooperation. I would like to thank Mr. Robert Philip and Mrs. Sarada Nair for their help and support and also Mrs. Saumini Shoji and Mrs. S. Viji for NMR and mass spectral analyses.

I sincerely thank the Department of Science and Technology (DST), Government of India, for providing me "SERC Bioinorganic Pre-doctoral Fellowship" and NIIST, CSIR, for the financial support.

Prakash P. N.

CONTENTS

| | Page |
|--|------------|
| Statement | i |
| Certificate | ii |
| Acknowledgements | iii |
| Preface | vii |
| | |
| Chapter 1. Biomolecular Recognition of Nucleotides and Nucleic Acids: An Overview | |
| 1.1. Introduction | 1 |
| 1.2. Molecules of Life | 4 |
| 1.2.1. Nucleotides and Nucleic Acids | 5 |
| 1.2.2. Ligand-DNA Interactions | 9 |
| 1.3. Biomolecular Recognition: Strategies | 12 |
| 1.3.1. Indicator Displacement Assay | 14 |
| 1.3.2. Creation of Combinatorial Libraries | 15 |
| 1.3.3. Biomolecular Recognition: Non-covalent Interactions | 16 |
| 1.4. Nucleotides and Nucleic Acids Recognition | 19 |
| 1.4.1. Probes for Nucleotides | 19 |
| 1.4.2. Probes for Nucleic Acids | 27 |
| 1.4.3. Cyanine Dyes | 28 |
| 1.4.4. Phenanthridine and Acridine Dyes | 30 |
| 1.4.5. Indole and Imidazole Dyes | 34 |
| 1.5. Objectives of the Present Investigation | 36 |
| 1.6. References | 38 |

| | | |
|-------------------|---|-----|
| Chapter 2. | Design of Novel Cyclophanes: Synthesis and Study of their Photophysical Properties | |
| 2.1. | Abstract | 45 |
| 2.2. | Introduction | 47 |
| 2.3. | Results | 49 |
| 2.3.1. | Synthesis | 49 |
| 2.3.2. | Absorption and Fluorescence Properties | 57 |
| 2.3.3. | Characterization of Intramolecular Excimer | 61 |
| 2.3.4. | Time-resolved Fluorescence Measurements | 65 |
| 2.3.5. | Solid State Photophysical Properties | 69 |
| 2.3.6. | Solid State Time-resolved Fluorescence Properties | 73 |
| 2.4. | Discussion | 76 |
| 2.5. | Conclusions | 81 |
| 2.6. | Experimental Section | 82 |
| 2.7. | References | 94 |
| Chapter 3. | Biomolecular Recognition: Investigation of Interaction of a Few Cyclophanes with Nucleotides | |
| 3.1. | Abstract | 101 |
| 3.2. | Introduction | 103 |
| 3.3. | Results | 107 |
| 3.3.1. | Interactions with Nucleotides | 107 |
| 3.3.2. | Nature of Host-Guest Complexation | 110 |
| 3.3.3. | Nucleotides Recognition Through FID Assay | 113 |
| 3.4. | Discussion | 122 |
| 3.5. | Conclusions | 130 |

| | | |
|-------------------|--|------------|
| 3.6. | Experimental Section | 132 |
| 3.7. | References | 136 |
| | | |
| Chapter 4. | Biomolecular Recognition: Investigation of Interactions of a Few Cyclophanes with DNA | |
| 4.1. | Abstract | 143 |
| 4.2. | Introduction | 145 |
| 4.3. | Results | 147 |
| 4.3.1. | Interactions with DNA | 147 |
| 4.3.2. | Time-resolved Fluorescence Analysis | 153 |
| 4.3.3. | Nature of DNA Binding Interactions | 157 |
| 4.3.4. | DNA Thermal Denaturation Studies | 160 |
| 4.3.5. | Viscosity Measurements | 161 |
| 4.3.6. | Interactions with Micelles and Proteins | 163 |
| 4.3.7. | Gel Electrophoretic DNA Detection | 166 |
| 4.3.8. | DNA Sequence Selective Interactions | 167 |
| 4.4. | Discussion | 170 |
| 4.5. | Conclusions | 174 |
| 4.6. | Experimental Section | 175 |
| 4.7. | References | 178 |
| | | |
| | List of Publications | 185 |

PREFACE

Molecular recognition is a fundamental process in biology, which governs the functions of enzymes, proteins and nucleic acids. Most of the biomolecular recognition processes could be rationalized on the basis of Fischer's "lock and key" model which compares the lock to a molecular receptor, while the key to a complimentary substrate. Later on, design and development of molecular receptors capable of mimicking natural processes has found applications in basic research as well as in the development of potentially useful technologies. Of the various receptors, cyclophanes have attracted much attention recently. By virtue of having a rigid structure with a defined cavity, these systems encapsulate and stabilize a large number of guest molecules through non-covalent interactions. In this context, the present thesis entitled: "Design of Cyclophanes: Synthesis and Study of Photophysical and Biomolecular Recognition Properties" reports our efforts towards the design of a few cyclophane derivatives as probes for biomolecules such as nucleotides and DNA.

The first Chapter of the thesis briefly describes the structural features of nucleotides, DNA, ligand-DNA interactions and the common strategies adopted for the biomolecular recognition. A brief description of the probes developed for nucleotides and DNA are also indicated in this Chapter along with the objectives of the present thesis.

In the second Chapter, synthesis of a few novel cyclophane derivatives as well as the investigation of their photophysical properties under different conditions was described. These compounds were synthesized in moderate yields and were characterized on the basis of analytical and spectral evidence. All these conjugates exhibited high solubility in the aqueous medium and showed characteristic absorption and fluorescence properties of the anthracene chromophore. While the viologen bridged systems **1-4** showed significantly lower quantum yields of fluorescence, the imidazolium bridged systems **5-7** were found to be highly fluorescent in the aqueous medium. Of these derivatives, the imidazolium bridged symmetric cyclophane **5**, unusually exhibited dual emission in the aqueous medium, which could be attributed to a locally excited singlet state (monomer) and an

intramolecular excimer. Moreover, the imidazolium based cyclophanes were found to exhibit significant fluorescence emission in the solid state as well, as compared to the viologen based systems. The emission spectrum of the cyclophane **5** in the powdered state consisted of a broad band with maximum at λ_{max} 570 nm due to an intramolecular excimer. In contrast, the model cyclophane **6** exhibited two bands in its emission spectrum consisting of a peak having maximum at λ_{max} 440 nm and a broad band centered at 510 nm. The broad emission in the cyclophane **6** could be attributed to a "T" shaped intermolecular excimer as evidenced from the molecular packing obtained through single crystal x-ray analysis. The results presented in this Chapter demonstrate that these cyclophanes are soluble in aqueous media and have favorable photophysical properties in the solid state as well as in the solution and hence can have potential applications as probes for biomolecules.

The third Chapter of the thesis deals with the investigation of interaction of a few selected cyclophanes with nucleosides and nucleotides. The addition of ATP or GTP to a solution of the cyclophane **1** in buffer resulted in decrease in its absorbance. In

contrast, negligible changes were observed with the addition of ADP, AMP, adenosine and phosphate, indicating thereby that the cyclophane **1** undergoes selective interactions only with nucleotide triphosphates with association constants in the order of 10^3 M^{-1} .

To improve the sensitivity of the technique by making use of the beneficial properties of the cyclophane **1**, we have investigated its interactions with the fluorescence indicator, 8-hydroxy-1,3,6-pyrene sulfonate (HPTS). The addition of the cyclophane **1** to a solution of HPTS resulted in 25% hypochromicity in the absorption spectrum, along with complete quenching of its fluorescence intensity. The subsequent titration of this non-fluorescent complex [**1**·HPTS] with various nucleosides and nucleotides resulted in the displacement of the indicator, HPTS leading to the revival of its fluorescence. It was observed that GTP induced maximum displacement of HPTS from the complex [**1**·HPTS] with an overall fluorescence enhancement of *ca.* 150-fold, whereas ATP induced *ca.* 45-fold enhancement. The selectivity towards GTP has been attributed to the presence of a better π -electron cloud which facilitates effective electronic, π -stacking and electrostatic interactions inside the cavity of the cyclophane **1**.

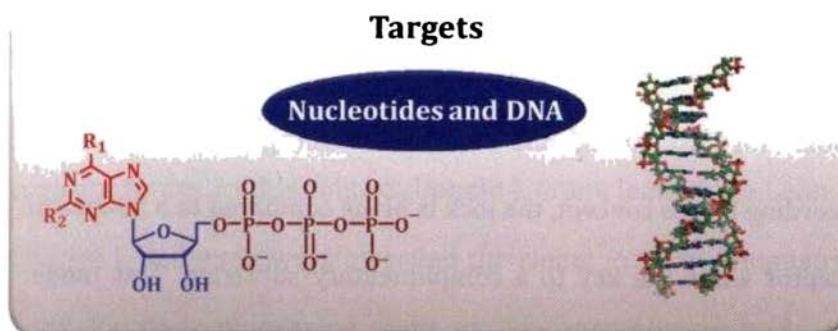
The cyclophane **2** having only one anthracene moiety on the other hand, behaved similarly, but with less sensitivity as compared to the cyclophane **1**. The reduced sensitivity of the cyclophane **2** could be attributed to its lower aromatic surface, resulting in less effective hydrophobic interactions. In contrast, the cyclophane **3** exhibited efficient interaction with HPTS, but was inefficient as a receptor for nucleotides through fluorescence indicator displacement assay. These results confirm the role of cavity size and aromatic surface in the molecular recognition ability of the cyclophanes and demonstrate the potential application of the probe **1** for detection of GTP and ATP in buffer and bio-fluids.

Investigation of interactions of a few selected representative cyclophane derivatives with DNA and polyoligonucleotides is the subject matter of the fourth Chapter. The addition of DNA to the viologen bridged cyclophane **1** resulted in significant hypochromicity in its absorption spectrum, whereas only negligible changes were observed in the emission spectrum. On the other hand, the imidazolium bridged cyclophane **2** exhibited hypochromicity in its absorption spectrum along with a significant enhancement in the excimer emission intensity and lifetimes.

Picosecond time resolved fluorescence measurements of the cyclophane **2** showed that the lifetime of the excimer increased from 52.6 to 143.1 ns in the presence of DNA. These observations indicate that the cyclophane **2** binds to DNA resulting in the formation of a highly organized *sandwich*-type conformer having bathochromic shifted emission maximum. DNA acts as a unique template when compared to micelles and proteins in inducing the excimer formation in the case of the cyclophane **2**. Detailed investigations revealed that the driving force for the formation of *sandwich*-type excimer of the cyclophane **2** in the presence of DNA could be attributed to the synergistic effects of hydrophobic interactions in the minor groove and electrostatic interactions between the cationic cyclophane and the phosphate backbone of DNA. The uniqueness of cyclophane **2** is that it undergoes interactions selectively with DNA as compared to micelles and proteins in buffer and under agarose gel electrophoresis conditions and signals the event interestingly through a “turn on” excimer emission mechanism.

Note: *The numbers of various compounds given here correspond to those given under the respective Chapters.*

1 BIOMOLECULAR RECOGNITION OF NUCLEOTIDES AND NUCLEIC ACIDS: AN OVERVIEW



1.1. INTRODUCTION

Molecular recognition – the specific noncovalent interaction between a receptor molecule and a particular substrate – is fundamental to almost every biological process. The importance of molecular recognition can be easily understood from various biological processes involving enzymes, nucleic acids, antibodies, etc.¹ Most of the processes involving these biological molecules are governed by molecular recognition events between these receptors and suitable substrates. Inspired by nature, chemists have attempted to develop novel molecular systems capable of

mimicking the binding events of biological systems and this has eventually led to the development of new exciting areas such as 'host-guest' and 'supramolecular' chemistry.²

The history of host-guest chemistry dates back to the nineteenth century when Emil Fischer proposed the "lock and key" model for explaining the molecular recognition processes.³ According to this concept, the lock is being compared to a molecular receptor while the key to a complimentary substrate. This model was quite successful in explaining the specific action of an enzyme with a single substrate. Later on, this understanding of a receptor-substrate complex has helped chemists to design synthetic systems with fascinating properties, which are important in basic research and also in the development of potentially useful technologies.⁴

As compared to the chemists of the past, who were primarily interested in the synthesis of novel molecules and investigating their fundamental properties, the modern day chemist has been more interested in understanding the "chemistry beyond the molecule". This has led to the development of a fascinating area known as "supramolecular chemistry"⁵ which is concerned with various non-covalent interactions and spatial fit between the

individual molecules.⁶ The various concepts of supramolecular chemistry such as complementarity and self-organization plays powerful roles in molecular recognition events. In general, molecular recognition can thus be defined as the study of polymolecular entities (supramolecular complexes) formed between two or more molecules which are held together by non-covalent forces. In this context, Donald J. Cram, Jean-Marie Lehn and Charles J. Pedersen were awarded the Nobel Prize in Chemistry in 1987 for their pioneering work on "*the development and use of molecule with structure-specific interactions of high selectivity*".⁷

Design and development of molecular receptors targeted at biologically relevant molecules such as amino acids, proteins, carbohydrates, nucleotides, nucleic acids etc. have gained particular importance in recent years due to their potential applications in biology and medicine. This Chapter describes briefly the structural aspects of different biomolecules such as nucleosides, nucleotides and nucleic acids and an overview of different strategies adopted for their selective recognition. The driving forces behind such selective molecular recognition have also been described in detail with a particular emphasis on nucleotides and DNA. Further, the objectives

of the present investigations are also briefly described in this Chapter.

1.2. MOLECULES OF LIFE

The simple organic compounds, from which living organisms are constructed, known as biomolecules, are identical in all organisms and are related to each other and interact among themselves. The size, shape and chemical activity of biomolecules enable them not only to serve as the building blocks of cells, but also to participate in various dynamic, self-sustaining transformations of energy and matter. Depending on their chemical composition and function, biomolecules can be broadly classified as amino acids, proteins, enzymes, carbohydrates, lipids, nucleic acids and so on.⁸ Because of their inherent importance in biology, the structure and function of all these biomolecules have been thoroughly studied. Our interest in this area is related to the study of interaction of small organic molecules with nucleic acids because such studies are useful in the design of novel chemotherapeutics and in the development of probes useful in biology and medicine. In the following section, a brief description of the structure and functions

of nucleotides and nucleic acids is provided along with an overview of different strategies adopted for their recognition.

1.2.1. Nucleotides and Nucleic Acids

Nucleic acids of all organisms are made up of a number of nucleotides joined together by phosphodiester linkages. Each nucleotide comprises of a sugar, phosphate and a purine or pyrimidine base. Nucleic acids may be divided into two classes depending upon the nature of their sugar residues. Those that contain β -2'-deoxy-D-ribose are called the deoxyribonucleic acids (DNA), while those containing β -D-ribose are known as ribonucleic acids (RNA). The common heterocyclic bases present in DNA are adenine (A), guanine (G), cytosine (C) and thymine (T), whereas in RNA, the thymine is replaced by uracil (U). While adenine and guanine belong to the class of purines, the pyrimidine bases are cytosine, thymine and uracil (Figure 1.1). Combination of one of these bases (N-1 of C, T or U and N-9 of A or G) with a sugar residue *via* the C-1 carbon constitutes a nucleoside and phosphorylation at the 5'-hydroxyl group of the nucleoside results in a nucleotide, the monomeric unit of the nucleic acids (Figure 1.2).

The primary structure of DNA has each nucleoside joined by a phosphodiester from its 5'-hydroxyl group to the 3'-hydroxyl group of one neighbor and by a second phosphodiester from its 3'-hydroxyl group to the 5'-hydroxyl of its other neighbor (Figure 1.3A). The 5' – 3' linkage is maintained throughout the entire length of DNA, which means that the uniqueness of a given DNA primary structure resides solely in the sequence of its bases. DNA consists of two chains, which run in opposite directions and are coiled around each other to form a double helix. These two chains are linked

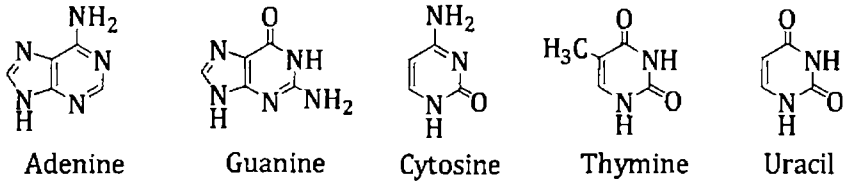


Figure 1.1. Structures of purine and pyrimidine bases present in nucleic acids.

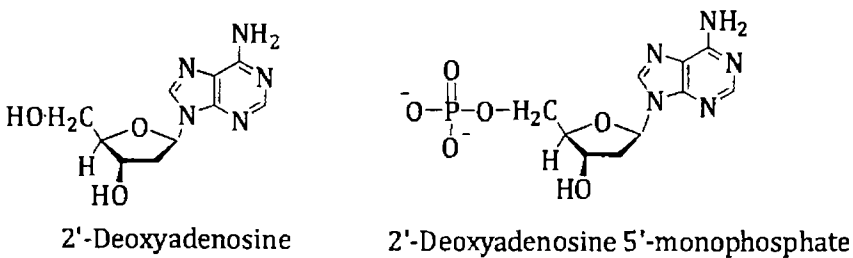


Figure 1.2. Structures of a representative nucleoside, 2'-deoxyadenosine (dA) and a nucleotide, 2'-deoxyadenosine 5'-monophosphate (dAMP).

together by a large number of weak hydrogen bonds formed between complementary bases (Figure 1.3B). The complementary base pairs are adenine-thymine and guanine-cytosine. The bases, which are hydrophobic and paired by hydrogen bonding lie inside and perpendicular to the helix axis, whereas the hydrophilic and negatively charged sugar and phosphate residues face out into the aqueous medium. The double helical structure of DNA (dsDNA) is stabilized by hydrogen bonding between the complementary base pairs and also by hydrophobic interactions between the stacked bases. The hydrogen bonding in nucleic acids is vital not only in the

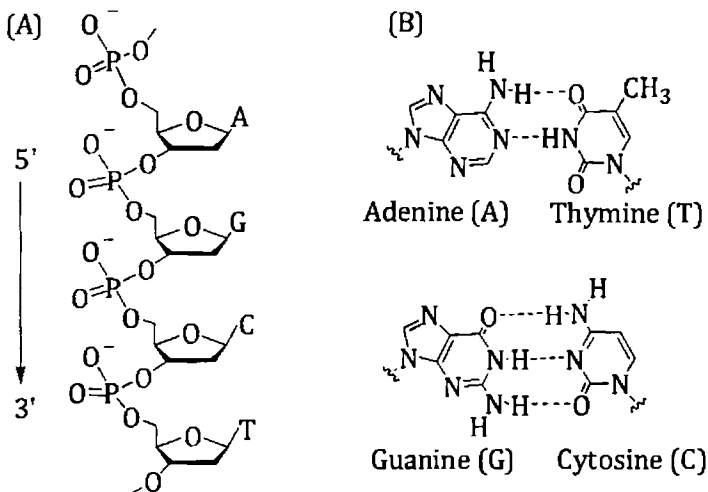


Figure 1.3. (A) Schematic representation of the primary structure of DNA and (B) Watson-Crick base pairing of adenine-thymine (A-T) and guanine-cytosine (G-C).

maintenance of the structure of DNA but also in the performance of its important biological functions such as the gene expression, replication and transcription.⁹

DNA adopts different secondary helical structures based on the environmental conditions such as humidity and salt concentration. A-DNA and B-DNA are the predominant DNA secondary structures with right handed double helices and Watson-Crick base pairing, whereas Z-DNA is a left handed double helical structure that is stabilized by high concentrations of $MgCl_2$ and $NaCl$.¹⁰ B-DNA is the only form that exists under physiological pH conditions, while A-DNA exists under dehydrated conditions. Figures 1.4A and 1.4B represent the secondary structure of B-DNA extrapolated from the crystal structure of stacked decamer of a sequence of $d(CCAACGTTGG)$.^{10a} The B-DNA structure shown in Figure 1.4B has 10 base pairs per turn with little tilting of bases. The wide major groove and narrow minor groove are of moderate depth and hence both these grooves are well solvated by water molecules. Another promising feature of B-DNA is that its structure is sufficiently flexible to permit a conformational response in the backbone to a particular base sequence.

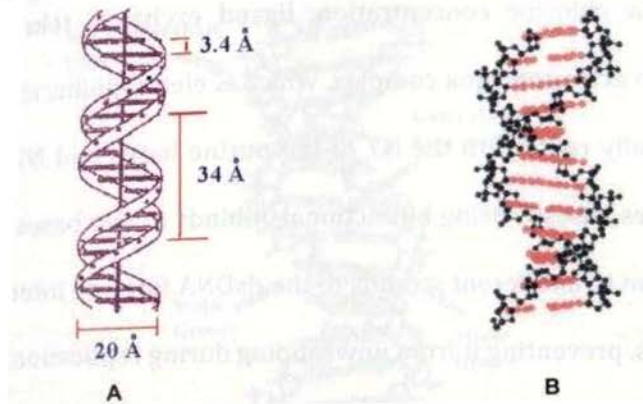


Figure 1.4. (A) Double helix model for the B-form of DNA and (B) twelve base pairs of B-DNA extrapolated from the crystal structure of stacked decamer of sequence $d(\text{CCAACGTTGG})$.^{10a}

1.2.2. Ligand-DNA Interactions

There are two principal ways through which a molecule can bind with DNA, first is the covalent interactions through the formation of covalent bonds and second is through the formation of non-covalent complexes *via* non-covalent interactions such as hydrogen bonding and π -stacking. Drugs which bind covalently to DNA are used to either add substituents onto the base residues or to form cross-links between different sections of DNA. One of the extensively studied example for covalent binding is *cis*-platin, $[\text{Pt}(\text{Cl})_2(\text{NH}_3)_2]$, a well known anti-cancer drug. The chlorine atoms of *cis*-platin are good leaving groups. When *cis*-platin enters cells

with a low chlorine concentration, ligand exchange takes place forming an activated aqua complex, which is electrophilic. *cis*-Platin preferentially react with the N7 of the purine bases and N3 of the pyrimidines bases.¹¹ Being bifunctional, it binds to two bases, which can be from two different strands of the dsDNA forming interstrand cross-links, preventing it from unwrapping during replication.

DNA can also undergo reversible or non-covalent interactions with a broad range of chemical species that include water, metal ions and their complexes, small organic molecules, drugs and proteins. All of the intricate nucleic acid conformations are stabilized by these reversible interactions. The three primary types of non-covalent interactions through which a ligand can bind to DNA are electrostatic, groove-binding and intercalative mechanisms (Figure 1.5).¹² DNA is a negatively charged polyelectrolyte, whose phosphate groups strongly affect its structure and interactions. Simple ions and positively charged molecules can bind to the anionic outer surface of DNA, which helps in maintaining the charge neutralization of DNA. The electrostatic mode of binding is relatively flexible and the bound molecules or ions can move freely along the nucleic acid chain. Metal ions such as Na⁺, Mg²⁺, Ca²⁺ and

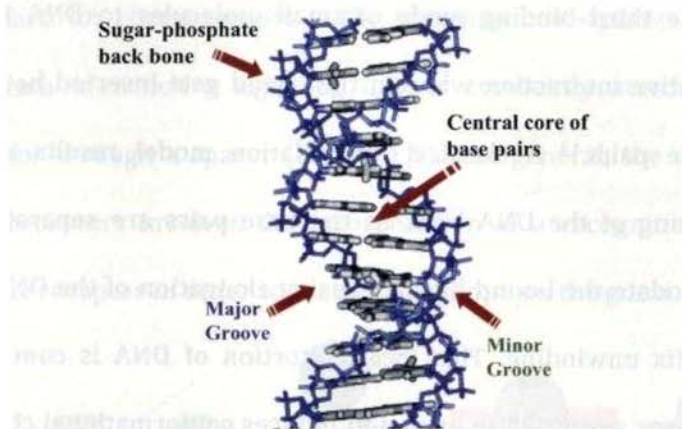


Figure 1.5. Schematic representation of B-DNA and probable ligand-binding sites.

organic molecules bearing positive charge are known to bind with DNA through the electrostatic mode. DNA possesses a wide major groove and a narrow minor groove through which small molecules can interact with the duplex. The major and minor grooves differ significantly in electrostatic potential, hydrogen bonding characteristics, steric effects and hydration. Many proteins exhibit binding specificity primarily through major groove interactions, while small molecules in general, prefer the minor groove of DNA. Inside the grooves, molecules can undergo van der Waals contacts with the helical chains, which define the 'wall' of the groove. The contact between the bound molecule and the edges of the base pairs gives additional stability and specificity for the groove interactions.

The third binding mode of small molecules to DNA is the intercalative interaction wherein the ligand gets inserted between two base pairs.¹³ A classical intercalation model results in the lengthening of the DNA helix as the base pairs are separated to accommodate the bound ligand, causing elongation of the DNA and local helix unwinding. This local distortion of DNA is commonly spread over several base pairs and induces conformational changes in the adjacent sequences, which result in a pronounced alteration of the DNA structure. On the other hand, a partial, non-classical model of intercalation is also proposed for molecules containing bulky substituents. In this mode of binding, the aromatic residue of the ligand is partially inserted between base pairs leading to a bend of the helix at the point of intercalation and results in the reduction of the effective length of DNA.¹⁴

1.3. BIOMOLECULAR RECOGNITION: STRATEGIES

The field of molecular recognition has reached a stage where one can confidently design and synthesize a receptor with a good degree of predictability and selectivity for many kinds of small to medium-sized molecules. Along this direction, the most widely used

approach for chemosensors is the signaling unit–spacer–receptor approach in which a signaling unit is covalently attached to a receptor through a spacer (Figure 1.6).¹⁵ In general, the design of such receptors involves the incorporation of a recognition entity into the receptor in order to bind each epitope on the guest. A

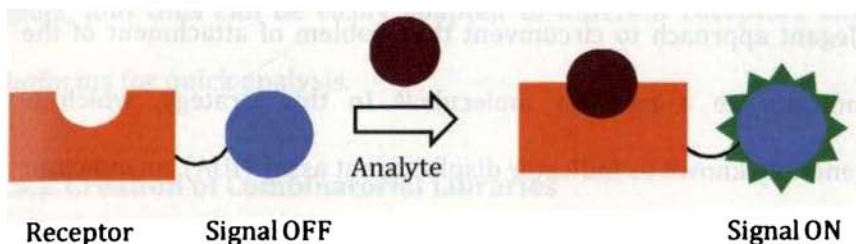


Figure 1.6. Schematic representation of a signaling unit–spacer–receptor approach.

proper spacer is also a pre-requisite in order to organize the recognition entities. The introduction of an analyte that binds to the receptor would induce measurable changes in the observable properties of the signaling motif. Employing this strategy, selective receptors for a wide range of guest molecules ranging from simple anions and cations to highly complex biomolecules such as amino acids and proteins has been developed and these systems utilize solvophobic effects, hydrogen bonding, and ion pairing interactions. Even though this approach is becoming more and more routine, its

major limitation is that attachment of the indicator to the receptor is often labor intensive.

1.3.1. Indicator Displacement Assay

Ansyn and co-workers have introduced an alternate and elegant approach to circumvent the problem of attachment of the indicator to a receptor molecule.¹⁶ In this strategy, which is generally known as indicator displacement assay (IDA), an indicator is first allowed to bind reversibly to a receptor (Figure 1.7). The complexation between the receptor and indicator results in notable changes in the optical properties of the indicator. Then, a competitive analyte is introduced into the system causing the displacement of the indicator from the host, which in turn modulates an optical signal. IDA offers many advantages over

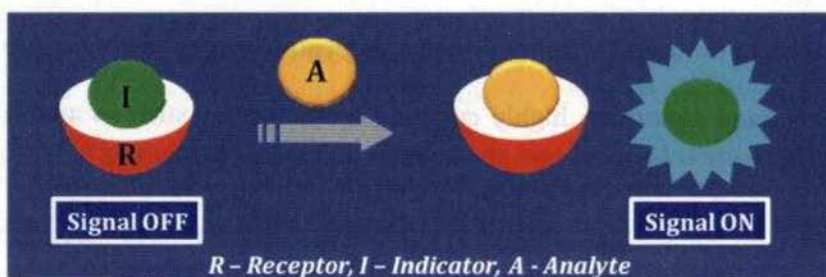


Figure 1.7. Schematic representation of the fluorescence indicator displacement (FID) assay.

traditional sensing assays. First, this method does not require the indicator to be covalently attached to the receptor. Second, because there are no covalent bonds between the receptor and the indicator, different indicators can be employed with the same receptor. Third advantage is that the assay works well in both organic and aqueous media, and thus can be easily adapted to different receptors and platforms for quick analysis.

1.3.2. Creation of Combinatorial Libraries

Another approach for targeting small and medium-sized molecules is the creation of a combinatorial library of receptors.¹⁷ This process allows for the creation of several different compounds through the combination of rapid parallel and combinatorial syntheses. The subsequent screening of the new materials can provide compounds for many applications. This recent strategy has been inspired by nature's methods of molecular recognition, which involves "differential" binding interactions. Differential, rather than specific or selective, indicates that these receptors have different binding characteristics, none of which are specific or selective. These receptors are "generalized" rather than "specialized". In this

approach, an array of sensors is created and the signal is evaluated and interpreted by pattern recognition protocols. This is the binding method used in the mammalian senses of taste and smell.

1.3.3. Biomolecular Recognition: Non-covalent Interactions

The important non-covalent interactions that form the basis of molecular recognition are hydrogen bonding, electrostatic, π -stacking and hydrophobic interactions. A hydrogen bond results from a dipole-dipole force between an electronegative atom and a hydrogen atom bonded to nitrogen, oxygen or fluorine.¹⁸ The energy of a hydrogen bond (typically 5 to 30 kJ/mol) is comparable to that of weak covalent bonds (155 kJ/mol) and a typical covalent bond is only 20 times stronger than an intermolecular hydrogen bond. The hydrogen bond is strong compared to van der Waals forces, but weaker than covalent, ionic and metallic bonds.

Electrostatic interactions arise from electrostatic attraction between either partial charges arising from the differing electronegativities of atoms (e.g. δ^+ and δ^-) or full charges arising from ionized residues. These interactions are particularly important when the target molecules contain charged moieties such as amino

acids or nucleic acids. On the other hand, stacking refers to a stacked arrangement of aromatic molecules, which interact through π - π stacking between organic compounds containing aromatic moieties.¹⁹ These interactions are caused by intermolecular overlapping of p-orbitals in π -conjugated systems, so they become stronger as the number of π -electrons increases and act strongly on flat polycyclic aromatic hydrocarbons because of the many delocalized π -electrons.

Another important non-covalent interaction that is gaining importance in molecular recognition is the cation- π interaction, which is the interaction between the face of an electron-rich π system with an adjacent cation.²⁰ Theoretical and experimental studies have shown that cation- π interactions can be quite strong, both in the gas phase and in aqueous media and the role for cation- π interactions in biological recognition has been well understood. Similarly, charge-transfer interactions form another important non-covalent bonding mode in molecular recognition.²¹ A charge-transfer complex (or CT complex, electron donor-acceptor complex) is a chemical association of two or more molecules in which the attraction between the molecules is created by an electronic

transition into an excited electronic state, such that a fraction of electronic charge is transferred between the molecules. The resulting electrostatic attraction provides a stabilizing force for the molecular complex. The strength of a charge-transfer complex is much weaker than covalent forces and is characterized as a weak electron resonance. As a result, the excitation energy of this resonance occurs very frequently in the visible region of the electromagnetic spectrum leading to intense colors which are often referred to as CT bands. CT complexes exist in many types of molecules, inorganic as well as organic, and in all phases of matter, i.e. in solids, liquids and even gases.

Finally, hydrophobic interaction is the most important non-covalent force in molecular recognition.²² The tendency of hydrocarbons to form intermolecular aggregates in an aqueous medium is known as hydrophobicity. The name arises from the attribution of the phenomenon to the apparent repulsion between water and hydrocarbons. At the molecular level, the hydrophobic effect is an important driving force for biological structures and is responsible for protein folding, protein-protein interactions, formation of lipid bilayer membranes, nucleic acid structures, and

protein-small molecule interactions. Though a non-covalent bond is weaker than a covalent bond, the sum of different non-covalent interactions creates a large net stabilizing energy and the association between a host and a guest molecule is usually stabilized by one or more of these non-covalent interactions.

1.4. NUCLEOTIDES AND NUCLEIC ACIDS RECOGNITION

There is widespread interest in studying the interactions of small molecules with biomolecules, which not only lead to the development of molecular probes but also provide basis for understanding the structure and functioning of biomolecules. As a result, various molecular systems have been developed for targeting biomolecules such as amino acids, proteins, nucleic acids etc. A few examples of molecules currently used as probes for nucleotides and DNA are described in the following sections.

1.4.1. Probes for Nucleotides

Because of the increasing awareness of the important role that nucleotides and nucleosides play in biology, their detection and quantification is becoming highly focused.²³ Multifunctional

receptors with electronic and steric characteristics able to develop different binding contributions like electrostatic, H-bonding, and hydrophobic interactions usually need to be included in the design. In the following section, an overview of receptors reported for the selective recognition of nucleotides is presented with a particular emphasis on ATP and GTP. The structural similarity between these molecules makes it highly challenging to develop host molecules which can successfully discriminate them.

In this context, Kim, Yoon and co-workers have synthesized a water-soluble anthracene-imidazolium derivative **1** (Chart 1.1), which not only differentiates GTP and ATP but also acts as a potential fluorescent chemosensor for GTP in buffer.²⁴ This chemosensor senses GTP by a chelation-enhanced fluorescence quenching (CHEQ) effect, while with ATP, ADP, AMP and other anions like fluoride and chloride, it displays a chelation-enhanced fluorescence (CHEF) effect. The host **1** shows a selective binding with GTP over ATP, ADP, AMP, pyrophosphate, H_2PO_4^- , F^- , and Cl^- . The selectivity for GTP is about 6 times than that for ATP, and over 100 times those for other ligands. The selectivity of the system **1** towards GTP over ATP has been attributed to the differences in

strength of the π -H interaction between **1**-GTP and **1**-ATP complexes as well as the differences in the dipole moments of guanine and adenine.

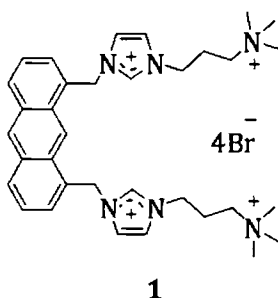


Chart 1.1

In another example, Chang and co-workers have discovered a “turn-on” GTP fluorescent sensor based on a combinatorial benzimidazolium dye library.²⁵ Condensation of benzimidazolium ring with 96 aromatic aldehydes provided extended conjugation and structural diversity. In order to achieve longer wavelengths of the final fluorophore, two Cl groups were introduced to the benzimidazolium ring. The synthesized dye derivatives were tested for detection of AMP, ADP, ATP, UTP, CTP and GTP in 10 mM HEPES buffer (pH 7.4) with 1% DMSO in 384-well microplates using a fluorescence plate reader. Two structurally related compounds (**2a** and **2b**, Chart 1.2) showed dramatic increase in fluorescence

intensity upon addition of GTP, while negligible changes were observed with other nucleotides. When excited at 480 nm, an approximately 80- and 70-fold fluorescence increase was observed for GTP and dGTP, while only ATP induced 2-fold enhancement, thereby indicating that the 2'-hydroxyl group of GTP is crucial for the molecular interaction. The quantum yields of **2a** before and after addition of GTP were 0.003 and 0.074, respectively leading to a visual detection of GTP.

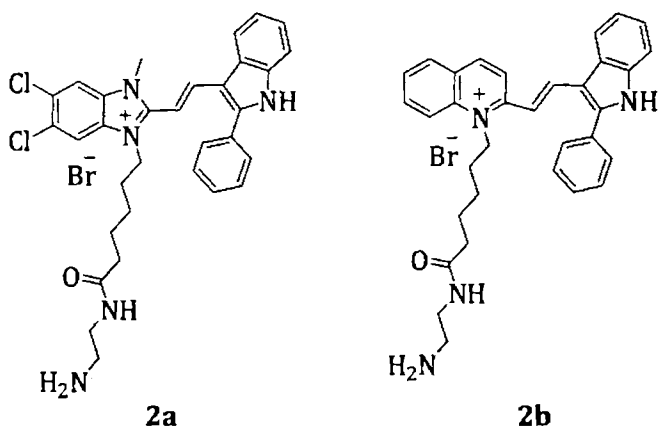
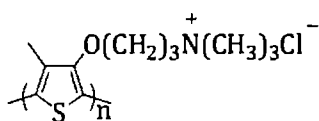


Chart 1.2

Recently, Shinkai and co-workers have reported a sensitive colorimetric and fluorescent probe for the detection of ATP based on a polythiophene derivative.²⁶ Poly(3-alkoxy-4-methylthiophene), **3** (Chart 1.3) was chosen for this study because its conformation is

sensitive to external stimuli as a result of the presence of sterically demanding side chains. In presence of ATP, the absorption maximum of the polymer showed red-shift from 400 to 538 nm with a dramatic color change from yellow to pink-red. This distinct shift and the appearance of two vibronic bands



3

Chart 1.3

are characteristic of the aggregation of the polymer backbone. Addition of other analytes such as AMP, chloride, carboxylate, and phosphate showed negligible changes whereas ADP and UTP showed less significant changes. The dramatic color change of **3** upon addition of ATP provides a very simple means for naked-eye detection of ATP in aqueous solution. GTP also gave similar change in color of the solution from yellow to pink-red. However, the presence of ATP can be efficiently distinguished from GTP by a chiroptical method as the two supramolecular complexes with **3** gave opposite induced circular dichroism pattern. The mechanism behind the color change observed for **3** is proposed to be the change

of the random coil conformation ($\lambda_{\max} = 400 \text{ nm}$) into the π -stacked aggregates ($\lambda_{\max} = 535 \text{ nm}$) induced by the triphosphates. The less significant changes observed with ADP indicates that the number of negative charges on the anion plays a crucial role in promoting the formation of a supramolecular aggregate.

Among the various strategies used for the selective recognition of nucleotides, the use of organometallic complexes has attracted much attention. In this context, Hamachi and co-workers have introduced Zn^{II} containing chemosensors for polyphosphates recognition. For example, the acridine based probes **4** and **5** (Chart 1.4) showed selectivity towards nucleotide polyphosphates.²⁷ Addition of ATP to **4**-2Zn^(II) under neutral aqueous conditions led to

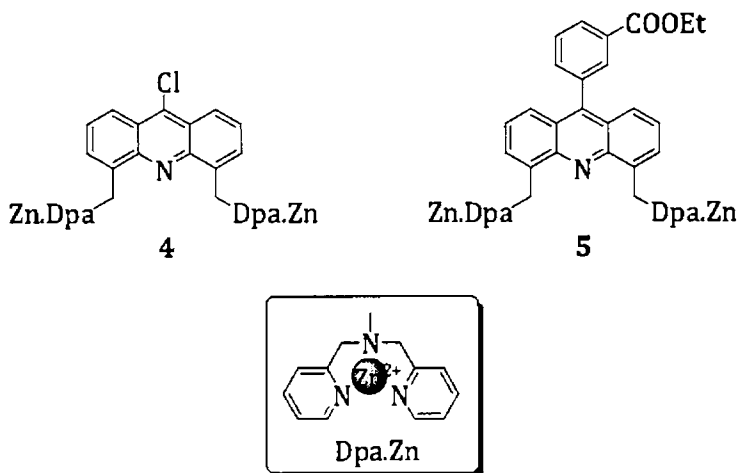


Chart 1.4

decrease in intensity of the emission maximum along with a blue shift. A much clearer wavelength shift and change in the emission intensity was observed in the case of $5\text{-Zn}^{(II)}$ leading to visual fluorescence change from green to blue in the presence of ATP and could detect upto 10^{-7} M of ATP with a dual-emission change.

Although these chemosensors could recognize nucleoside polyphosphates under neutral aqueous conditions, their utility in bioanalytical applications has been limited due to their small emission change as well as their moderate sensing selectivity among phosphate derivatives. To overcome these drawbacks, a new binuclear zinc complex $6\text{-Zn}^{(II)}$ (Chart 1.5) with a xanthene fluorophore was developed.²⁸ This chemosensor $6\text{-Zn}^{(II)}$ showed remarkably large fluorescence enhancement upon binding to ATP

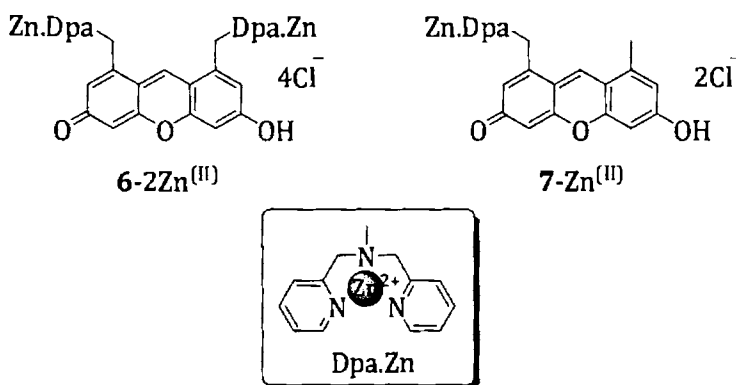


Chart 1.5

under neutral aqueous conditions. A large (30-fold) fluorescence enhancement was observed when ATP was added to a solution of **6-2Zn^(II)** and the association constant between **6-2Zn^(II)** and ATP was found to be $K_{app} = 1.3 \times 10^6 \text{ M}^{-1}$ with a stoichiometry of 1:1. The fluorescence quantum yield of the binding complex of **6-2Zn^(II)** with ATP was sufficiently high so as to enable a naked eye detection of ATP using **6-2Zn^(II)**. The sensing selectivity of **6-2Zn^(II)** for a variety of biologically relevant anions was subsequently evaluated and the chemosensor **6-2Zn^(II)** showed a strong binding affinity in the range from $4.9 - 17 \times 10^5 \text{ M}^{-1}$ towards various polyphosphate derivatives such as XTP (X = A, G, C) and XDP (X = A, U).

The strongest binding affinities were obtained for pyrophosphate (PPi) and inositol-1,3,4-trisphosphate (IP₃), due to the presence of negative charges which are essential for binding with the cationic **6-2Zn^(II)**. On the other hand, fluorescence changes were not induced even by a high concentration of monophosphorylated species such as HPO₄²⁻, AMP, cGMP, and phosphodiester suggesting that **6-2Zn^(II)** is a useful probe for the fluorescence detection of the polyphosphates. The turn-on fluorescence sensing of nucleoside polyphosphates by **6-2Zn^(II)** can

be ascribed to the recovery of the conjugated structure of the xanthene ring due to binding with ATP at two $\text{Zn}^{(II)}$ -Dpa sites. This binding disrupts the bridging of water between two Dpa- $\text{Zn}^{(II)}$ sites resulting in the recovery of the conjugated xanthene structure showing strong fluorescence emission. Further, the utility of $6\text{-Zn}^{(II)}$ as a bioanalytical tool was demonstrated by fluorescence imaging of ATP particulate stores in living cells.

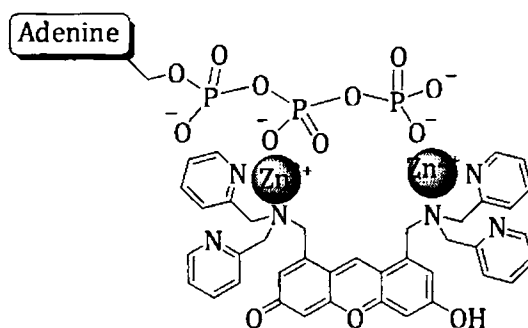


Figure 1.8. Schematic illustration of the binding of ATP with the receptor $6\text{-Zn}^{(II)}$.

1.4.2. Probes for Nucleic Acids

Nucleic acids, especially DNA, are used in numerous molecular biological experiments that involve its quantification and selective staining under *in vivo* and *in vitro* conditions. As a result various dyes have been developed for the qualitative and

quantitative analysis of DNA. A few examples of dyes currently used as probes for DNA along with their interactions are described in the following sections.

1.4.3. Cyanine Dyes

Cyanine dyes have recently become important as nucleic acid stains, particularly for double strand DNA (dsDNA).²⁹ Cationic cyanine dyes exhibit very large degrees of fluorescence enhancement on binding to nucleic acids. In addition, the covalent linkage of two cyanine dyes to form a bichromophore increases the nucleic acid binding affinity by approximately two orders of magnitude.³⁰ These characteristics of fluorescence enhancement and high binding affinity are crucial for high sensitivity nucleic acid detection applications. TOTO-1 (**8**) and TO-PRO-1 (**9**) (Chart 1.6) are representative examples of the cyanine dyes.^{31,32} Both these dyes bind to single strand DNA (ssDNA) as well as dsDNA, however, with marginal fluorescence enhancement with ssDNA. The TOTO-1 dye is capable of undergoing bis-intercalation, although it reportedly interacts with dsDNA and ssDNA with similarly high affinity.³³ NMR studies of interactions of **8** with a double stranded 8-

mer indicate that it acts as a bis-intercalator, with the aromatic units intercalating between the bases and the linker region undergoing interactions with the minor groove of DNA.³⁴ Binding of this dye partially unwinds the DNA thereby, distorting and elongating the helix. However, studies using fluorescence polarization measurements suggest that an external binding mode, where the dipole of the dye molecules is aligned with the DNA grooves is more important for its efficient interaction.

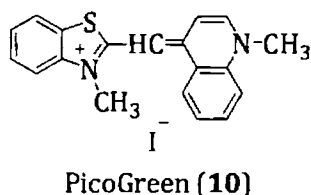
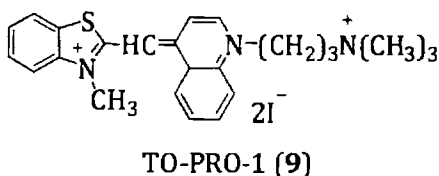
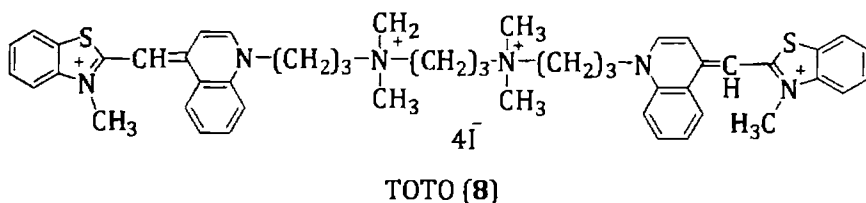


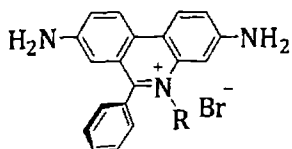
Chart 1.6

Pico-Green (10) is another example of a cyanine dye,³⁵ where its binding to dsDNA preferentially occurs by intercalation between alternating GC base pairs. Intercalation is also the most important

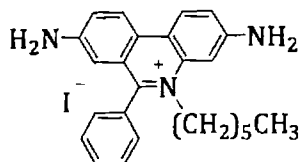
association mode for other base-pair configurations, but in many cases, binding to the exterior of DNA efficiently competes with intercalation. Intercalated Pico-Green molecules in calf thymus dsDNA are characterized by a monoexponential fluorescence decay, which is independent of the base pairs surrounding the dye.³⁶ However, it exhibited multiexponential decay in all types of ssDNA indicating that it binds to the calf thymus ssDNA as a monomer; further, the dominant mode of binding of this dye was found to be intercalation between two different bases, one of them being G or T. These dyes have found important applications as ultra sensitive reagents for solution quantitation and as stain for DNA in electrophoresis and blots.³⁷

1.4.4. Phenanthridine and Acridine Dyes

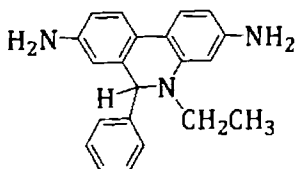
Ethidium bromide (**11**), propidium bromide (**12**), hexidium iodide (**13**) dihydroethidium (**14**), ethidium monoazide (**15**), ethidium homodimer-1 (**16**) and ethidium homodimer-2 (**17**) (Chart 1.7) are some of the phenanthridium dyes used as nucleic acid stains. These dyes exhibit *ca.* 20 to 30-fold enhancement in fluorescence emission when bound to nucleic acids. The mode of



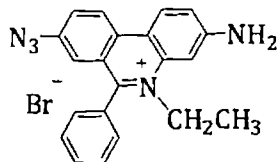
Ethidium bromide (R = C₂H₅, **11**)
 Propidium bromide (R = (CH₂)₃NMeEt₂, **12**)



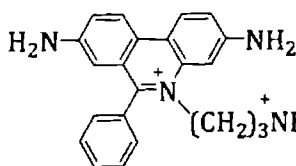
Hexidium iodide (**13**)



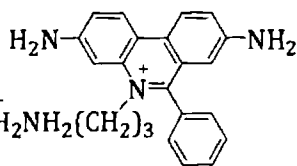
Dihydroethidium (**14**)



Ethidium monoazide (**15**)



Ethidium homodimer-1 (**16**)



Ethidium homodimer-2 (**17**)

Chart 1.7

binding is intercalation with no sequence specificity. Ethidium bromide is currently the most commonly used general nucleic acid gel stain, while propidium iodide is commonly used as a nuclear or

chromosome counter-stain and as a stain for dead cells. However, both ethidium bromide and propidium bromide are potent mutagens. Hexidium iodide (**13**), is a moderately lipophilic phenanthridium dye that permeate mammalian cells easily.

Ethidium homodimers-1 and 2 bind strongly to dsDNA, ssDNA and RNA with significant increase in fluorescence yields.³⁸ The ethidium homodimer-1 showed high affinity to triplex nucleic acid structures when compared to other DNA structures.³⁹ One molecule binds per four base pairs in dsDNA without any sequence selectivity. It was originally reported that only one of the two phenanthridium rings of ethidium homodimer-1 is bound at a time, however the subsequent reports indicate that bis-intercalation appears to be involved in staining both double strand and triplex DNA. The spectra and other properties of ethidium homodimers are almost identical. However, the DNA affinity of the homodimer-2 is found to be twice than that of the homodimer-1. The ethidium homodimer dyes **16** and **17** do not permeate cells with intact membranes making them useful as dead cell indicators. Dihydroethidium (**14**) is a reduced form of ethidium derivative that showed blue fluorescence when located in the cytoplasm.⁴⁰ Many

viable cells oxidize it to ethidium, which then fluoresces red upon DNA intercalation.⁴¹ Ethidium monoazide (**15**), on the other hand, has found application as an efficient photocrosslinking agent. It is used as a fluorescent photoaffinity label that, after photolysis, binds covalently to nucleic acids.⁴² The quantum yield for covalent photolabeling by ethidium monoazide was found to be unusually high (>0.4).

Acridine orange (**18**) (Chart 1.8) belongs to the class of acridine dyes that binds with DNA through intercalation and electrostatic interactions⁴³ and is used as flow cytometric dye. The acridine-homodimer (**20**) is an example of acridine dimer that has extremely high affinity for A.T rich regions of nucleic acids, making it particularly useful for chromosome banding.⁴⁴ It emits blue-green

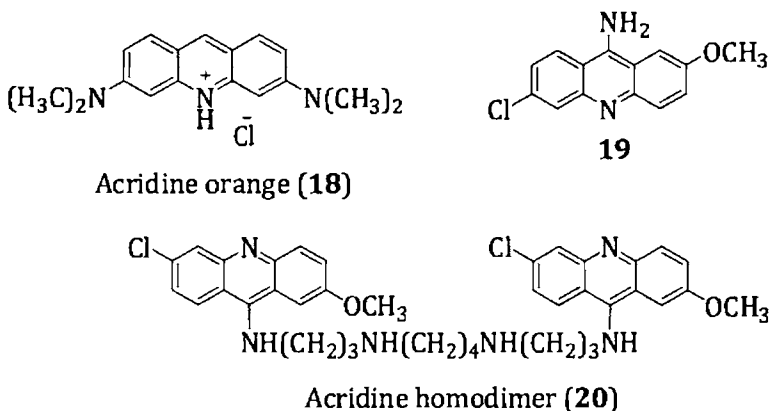


Chart 1.8

fluorescence when bound to DNA, yielding fluorescence that is proportional to the fourth power of the AT base pair content. 9-Amino-6-chloro-2-methoxyacridine (ACMA, **19**), on the other hand, is an efficient DNA intercalator that showed binding selectively to polyd(A-T)⁴⁵ sequences with an association constant of $2 \times 10^5 \text{ M}^{-1}$.

1.4.5. Indole and Imidazole Dyes

The bisbenzimidazole dyes such as Hoechst 33258 (**21**),⁴⁶ Hoechst 33342 (**22**)⁴⁷ and Hoechst 34580 (**23**)⁴⁸ (Chart 1.9) are minor groove binding DNA stains that fluoresce blue upon binding to DNA. These dyes show a wide spectrum of sequence dependent DNA affinities and bind with polyd(A-T) sequences with high association constants. They also exhibit multiple binding modes and distinct fluorescence emission spectra that are dependent on dye/base pair ratios. Hoechst 33258 is an antibiotic and chromosome stain and binds to AT minor groove sequences of DNA.⁴⁹ This molecule has a crescent shape with hydrogen bond donating groups on the inner face. This dye interacts with DNA through hydrogen bonding of the benzimidazole-NH groups with O-2 of thymine and N-3 of adenine and electrostatic interaction of the cationic dye with the anionic

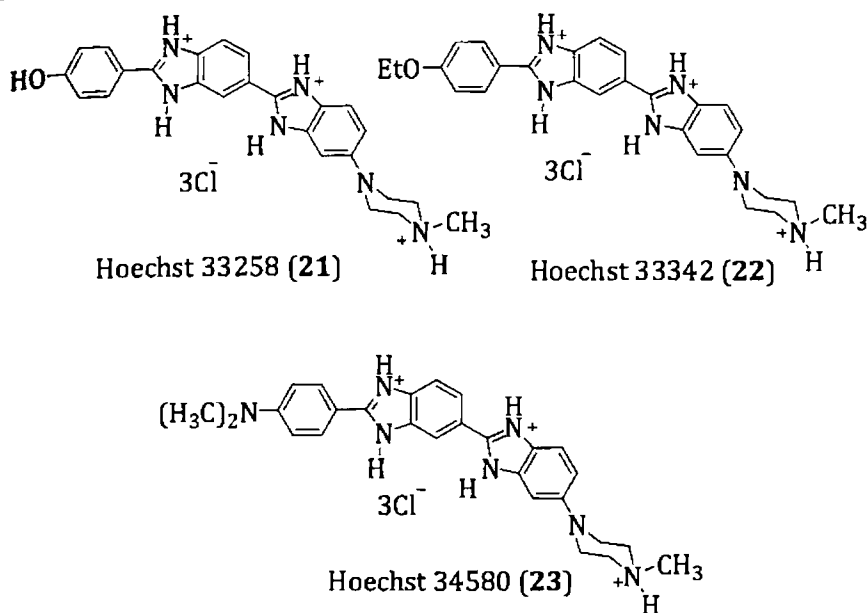
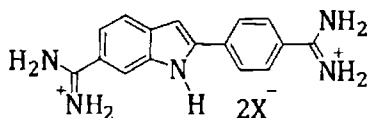


Chart 1.9

oligomer. The phenol ring of Hoechst 33258 makes an angle of 8° with the benzimidazole ring to which it is attached, while the two benzimidazole ring planes are twisted 32° with respect to each other. The piperazine moiety in this case is only slightly puckered and lies almost in the plane of the benzimidazole moiety to which it is attached. The dye maintains van der Waals contact with the walls of the minor groove, thus, placing itself in a favorable position so that its π -electron system can interact with the O-4' atoms of deoxyribose in the minor groove.

Similar to the imidazole based Hoechst dyes, the indole based DNA stain, DAPI (**24**) (Chart 1.10), associates with the minor groove of DNA preferentially binding to AT clusters.⁵⁰ DAPI is also reported to bind to DNA sequences that contain as few as two consecutive AT base pairs employing a different binding mode. Binding of DAPI to dsDNA produces ca. 20-fold fluorescence enhancement, apparently due to the displacement of water molecules from both DAPI and the minor groove of DNA. In the presence of high salt concentrations, it exhibits negligible interactions with ssDNA and GC pairs.



4,6'-Diamidino-2-phenylindole (DAPI, **24**)

Chart 1.10

1.5. OBJECTIVES OF THE PRESENT INVESTIGATION

Development of organic molecules that exhibit selective interactions with different biomolecules has immense significance in biochemical and medicinal applications. In this context, our main objective has been to design a few novel functionalized molecules that can selectively bind and recognize nucleotides and DNA in the

aqueous medium through non-covalent interactions. Our strategy was to design novel cyclophane receptor systems based on the anthracene chromophore linked through different bridging moieties and spacer groups. It was proposed that such systems would have a rigid structure with well defined cavity, wherein the aromatic chromophore can undergo π -stacking interactions with the guest molecules. The viologen and imidazolium moieties have been chosen as bridging units, since such groups, can in principle, could enhance the solubility of these derivatives in the aqueous medium as well as stabilize the inclusion complexes through electrostatic interactions.

We synthesized a series of water soluble novel functionalized cyclophanes and have investigated their interactions with nucleotides, DNA and oligonucleotides through photophysical, chiroptical, electrochemical and NMR techniques. Results indicate that these systems have favorable photophysical properties and exhibit selective interactions with ATP, GTP and DNA involving electrostatic, hydrophobic and π -stacking interactions inside the cavity and hence can have potential use as probes in biology.

1.6. REFERENCES

1. (a) *Molecular Recognition - Chemical and Biochemical Problems*, S. M. Roberts (Ed.), Royal Society of Chemistry, Cambridge, **1989**. (b) E. Katchalski-Katzir, In *Design and Synthesis of Organic Molecules Based on Molecular Recognition*, G. Van Binst (Ed.), Springer, New York, **1986**.
2. J. -M. Lehn, *Supramolecular Chemistry*, VCH, Weinheim, **1995**.
3. E. Fischer, *Ber. Dtsch. Chem. Ges.* **1894**, *27*, 2985-2987.
4. *Comprehensive Supramolecular Chemistry*, J. L. Atwood, J. E. D. Davies, D. D. Macnicol, F. Vögtle, J. -M. Lehn (Eds.), Vol. 1, Elsevier Science, Oxford, **1996**.
5. (a) F. Vögtle, *Supramolecular Chemistry - An Introduction*, Wiley, Chichester, **1993**. (b) *Supramolecular Chemistry*, V. Balzani, L. De Cola (Eds.) Kluwer, Dordrecht, **1992**.
6. (a) D. J. Cram, In *Chemistry for the Future*, H. Grunewald (Ed.), Pergamon, Oxford, New York, **1984**. (b) *Frontiers in Supramolecular Organic Chemistry and Photochemistry*, H.-J. Schneider, H. Dürr (Eds.), VCH, Weinheim, **1991**.
7. (a) C. J. Pedersen, *Angew. Chem. Int. Ed. Engl.* **1988**, *27*, 1021-

1027. (b) J. -M. Lehn, *Angew. Chem. Int. Ed. Engl.* **1988**, *27*, 89-112. (c) D. J. Cram, *Angew. Chem. Int. Ed. Engl.* **1988**, *27*, 1009-1020.
8. A. L. Lehninger, *Principles of Biochemistry*, CBS Publishers and Distributors, New Delhi, **1984**.
9. (a) J. D. Watson, N. H. Hopkins, J. W. Roberts, J. A. Steitz, A. M. Weiner, In *Molecular Biology of the Gene*, 4th Ed., Benjamin-Cummings, Menlo Park, CA, **1987**. (b) F. H. C. Crick, *Nature* **1970**, *227*, 561-563. (c) W. Saenger, *Principles of Nucleic Acid Structure*, Springer Verlag, New York, **1984**.
10. (a) R. E. Dickerson, H. R. Drew, B. N. Connor, R. M. Wing, A. V. Fratini, M. L. Kapka, *Science* **1982**, *216*, 475-485. (b) R. E. Dickerson, *Adv. Enzymol.* **1992**, *211*, 67-111.
11. (a) *Nucleic Acids in Chemistry and Biology*, G. M. Blackburn, M. J. Gait, (Eds.) Oxford University Press, Oxford, **1996**, 2nd Edition. (b) R. A. G. Friedman, G. S. Manning, *Biopolymers* **1984**, *23*, 2671-2714.
12. B. Armitage, *Top. Curr. Chem.* **2005**, *253*, 55-76.
13. H. Ihmels, D. Otto, *Top. Curr. Chem.* **2005**, *258*, 161-204.

14. (a) Y. Xiong, X.-F. He, X.-H. Zou, J.-Z. Wu, X.-M. Chen, L.-N. Ji, R.-H. Li, J.-Y. Zhou, K.-B. Yu, *J. Chem. Soc., Dalton Trans.* **1999**, 19-23. (b) L. Kapicak, E. J. Gabbay, *J. Am. Chem. Soc.* **1975**, *97*, 403-408.
15. (a) V. Amendola, D. Esteban-Gomez, L. Fabbrizzi, M. Licchelli, *Acc. Chem. Res.* **2006**, *39*, 343-353. (b) P. A. Gale, *Acc. Chem. Res.* **2006**, *39*, 465-475. (c) F.-G. Klarner, B. Kahlert, *Acc. Chem. Res.* **2003**, *36*, 919-932.
16. (a) B. T. Nguyen, E. V. Anslyn, *Coord. Chem. Rev.* **2006**, *250*, 3118-3127. (b) S. L. Wiskur, H. Ait-Haddou, J. J. Lavigne, E. V. Anslyn, *Acc. Chem. Res.* **2001**, *34*, 963-972.
17. (a) C. Schmuck, P. Wich, *Top. Curr. Chem.* **2007**, *277*, 3-30. (b) A. T. Wright, E. V. Anslyn, *Chem. Soc. Rev.* **2006**, *35*, 14-28. (c) P. Schuster, *Proc. Natl. Acad. Sci. USA* **2000**, *97*, 7678-7680. (d) D. R. Liu, P. G. Schultz, *Angew. Chem. Int. Ed.* **1999**, *38*, 37-54.
18. J. Emsley, *Chem. Soc. Rev.* **1980**, *9*, 91-124.
19. (a) C. A. Hunter, K. R. Lawson, J. Perkins, C. J. Urch, *J. Chem. Soc., Perkin Trans. 2* **2001**, 651-669. (b) C. G. Claessens, J. F. Stoddart, *J. Phys. Org. Chem.* **1997**, *10*, 254-272.

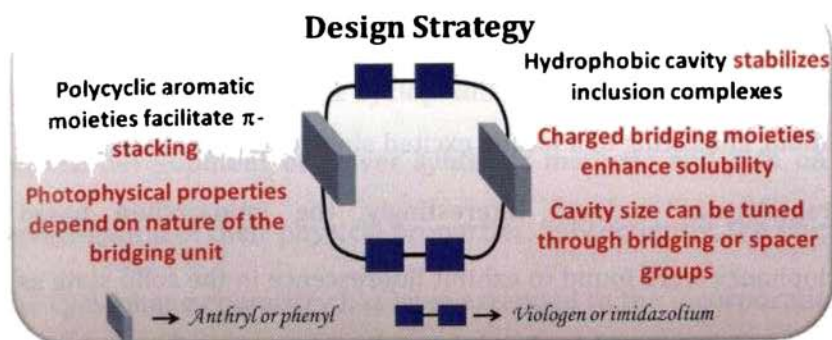
20. E. A. Meyer, R. K. Castellano, F. Diederich, *Angew. Chem. Int. Ed.* **2003**, *42*, 1210-1250.
21. (a) Y. H. Ko, E. Kim, I. Hwang, K. Kim, *Chem. Commun.* **2007**, 1305-1315. (b) Y. Imai, N. Tajima, T. Sato, R. Kuroda, *Org. Lett.* **2006**, *8*, 2941-2944. (c) B. Valeur, I. Leray, *Coord. Chem. Rev.* **2000**, *205*, 3-40.
22. H.-J. Schenider, T. Blatter, P. Zimmermann, *Angew. Chem. Int. Ed. Engl.* **1990**, *29*, 1161-1162.
23. (a) C. Bazzicalupi, A. Bencini, A. Bianchi, E. Faggi, C. Giorgi, S. Santarelli, B. Valtancoli, *J. Am. Chem. Soc.* **2008**, *130*, 2440-2441. (b) W. Willemse, E. Janssen, F. de Lange, B. Wieringa, J. Fransen, *Nat. Biotechnol.* **2007**, *25*, 170-172. (c) L. Vial, P. Dumy, *J. Am. Chem. Soc.* **2007**, *129*, 4884-4885.
24. J. Y. Kwon, N. J. Singh, H. N. Kim, S. K. Kim, K. S. Kim, J. Yoon, *J. Am. Chem. Soc.* **2004**, *126*, 8892-8893.
25. S. Wang, Y.-T. Chang, *J. Am. Chem. Soc.* **2006**, *128*, 10380-10381.
26. C. Li, M. Numata, M. Takeuchi, S. Shinkai, *Angew. Chem. Int. Ed.* **2005**, *44*, 6371-6374.

27. A. Ojida, Y. Miyahara, J. Wongkongkatep, S.-i. Tamaru, K. Sada, I. Hamachi, *Chem. Asian J.* **2006**, *1*, 555-563.
28. A. Ojida, I. Takashima, T. Kohira, H. Nonaka, I. Hamachi, *J. Am. Chem. Soc.* **2008**, *130*, 12095-12101.
29. (a) H. S. Rye, S. Yue, D. E. Wemmer, M. A. Quesada, R. P. Haugland, R. A. Mathies, A. N. Glazer, *Nucleic Acids Res.* **1992**, *20*, 2803-2812. (b) A. N. Glazer, H. S. Rye, *Nature* **1992**, *359*, 859-861. (c) G. Cosa, K. -S. Focsaneanu, J. R. N. McLean, J. P. McNamee, J. C. Scaiano, *Photochem. Photobiol.* **2001**, *73*, 585-599.
30. H. S. Rye, S. Yue, D. E. Wemmer, M. A. Quesada, R. P. Haugland, R. A. Mathies, A. N. Glazer, *Nucleic Acids Res.* **1992**, *20*, 2803-2812.
31. (a) A. Larsson, C. Carlsson, M. Jonsson, B. Albinsson, *J. Am. Chem. Soc.* **1994**, *116*, 8459-8465. (b) C. Carlsson, A. Larsson, M. Jonsson, B. Albinsson, B. Norden, *J. Phys. Chem.* **1994**, *98*, 10313-10321.
32. H. S. Rye, M. A. Quesada, K. Peck, R. A. Mathies, A. N. Glazer, *Nucleic Acids Res.* **1991**, *19*, 327-333.

33. (a) C. Carisson, M. Johnson, B. Akerman, *Nucleic Acids Res.* **1995**, *23*, 2413-2420. (b) H. S. Rye, A. N. Glazer, *Nucleic Acids Res.* **1995**, *23*, 1215-1222.
34. (a) H. P. Spielmann, D. E. Wemmer, J. P. Jacobsen, *Biochemistry* **1995**, *34*, 8542-8553. (b) H. P. Spielmann. *Biochemistry* **1998**, *37*, 16863-16876.
35. V. L. Singer, J. L. Jones, S. T. Yue, R. P. Haugland, *Anal. Biochem.* **1997**, *249*, 228-238.
36. H. M. Berman, J. Westbrook, Z. Feng, G. Gilliland, T. N. Bhat, H. Weissig, I. N. Shindyalov, P. E. Bourne, *Nucleic Acids Res.* **2000**, *28*, 235-242.
37. E. L. Romppanen, K. Savolainen, I. Mononen, *Anal. Biochem.* **2000**, *279*, 111-114.
38. B. Gaugain, J. Barbet, N. Capelle. B. P. Roques, J. B. Le Pecq, M. L. Bret, *Biochemistry* **1978**, *17*, 5078-5088.
39. E. Tuite, B. Norden, *Bioorg. Med. Chem.* **1995**, *3*, 701-711.
40. S. Perticarari, G. Presani, E. Banfi, *J. Immunol. Met.* **1994**, *170*, 117-124.
41. C. Bucana, I. Saiaki, R. Nayar, *J. Histochem. Cytochem.* **1986**, *34*, 1109-1115.

42. C. T. McMurray, E. W. Small, K. E. van Holde, *Biochemistry* **1991**, *30*, 5644-5652.
43. J. Delic, J. Coppey, H. Magdelenat, M. Copey-Moisan, *Exp. Cell. Res.* **1991**, *194*, 147-153.
44. N. Capelle, J. Barbet, P. Dessen, S. Blanquet, B. P. Roques, J. B. Le Pecq, *Biochemistry* **1979**, *18*, 3354-3362.
45. J. Markovits, C. Garbay-Jauregueberri, B. P. Roques, J. B. Le Pecq, *Eur. J. Biochem.* **1989**, *180*, 359-366.
46. F. G. Loonteins, P. Regenfuss, A. Zechel, L. Dumortier, R. M. Cleg, *Biochemistry* **1990**, *29*, 9029-9039.
47. H. Görner, *Photochem. Photobiol.* **2001**, *73*, 339-348.
48. H. M. Shapiro, N. G. Perlmutter, *Cytometry* **2001**, *44*, 133-136.
49. (a) M. S. Searle, K. J. Embrey, *Nucleic Acids Res.* **1990**, *18*, 3753-3762. (b) M. -K. Teng, U. Wahnert, *Nucleic Acids Res.* **1988**, *16*, 2670-2690.
50. (a) M. Kubista, B. Akerman, B. Norden, *Biochemistry* **1987**, *26*, 4545-4553. (b) W. D. Wilson, F. A. Tanious, H. J. Barton, R. L. Jones, K. Fox, R. L. Wydra, L. Strekowski, *Biochemistry* **1990**, *29*, 8452-8461.

2 DESIGN OF NOVEL CYCLOPHANES: SYNTHESIS AND STUDY OF THEIR PHOTOPHYSICAL PROPERTIES



2.1. ABSTRACT

With a view to develop efficient probes for molecular recognition, we have synthesized a few novel cyclophane derivatives containing electron donors (anthracene) attached to different acceptors (viologen and imidazolium) through different spacer groups. The synthesis of these molecules was achieved in moderate yields and was characterized using various spectroscopic and analytical methods. All these molecules showed good solubility in the aqueous medium and exhibited the characteristic photophysical properties of the anthracene chromophore. While the

viologen bridged systems showed significantly lower quantum yields of fluorescence, the imidazolium bridged systems were found to be highly fluorescent in the aqueous medium.

Of these derivatives, the imidazolium bridged symmetric cyclophane **5**, unusually exhibited dual emission in the aqueous medium, consisting of a locally excited singlet state (monomer) and intramolecular excimer. Interestingly, the imidazolium based cyclophanes were found to exhibit fluorescence in the solid state as well, when compared to the viologen based systems. The emission spectrum of the cyclophane **5** in the powdered state consisted of a broad band at λ_{max} 570 nm due to the formation of an intramolecular excimer. In contrast, the model cyclophane **6** exhibited dual emission having bands at $\lambda_{\text{max}} = 440$ and 510 nm due to the locally excited singlet state and "T" shaped intermolecular excimer, respectively. These results demonstrate that the cyclophanes under investigation have high solubility in the aqueous medium and exhibit favorable photophysical properties and hence can have potential applications in biomolecular recognition.

2.2. INTRODUCTION

Ever since the synthesis of [2.2]metacyclophane¹ and [2.2]paracyclophane,² the chemistry of cyclophanes has received significant attention due to their numerous applications. In the beginning, research on the cyclophane systems was focused mainly on the development of newer synthetic methods and also on the investigation of their physical properties. Subsequently, the scope of the cyclophane chemistry has been extended to the incorporation of heterocycles into these molecules and later on to the synthesis of multibridged and multilayered cyclophanes.³ The first practical application of the cyclophanes was found in the host-guest chemistry.⁴ Molecular recognition of ions and neutral molecules by the functionalized cyclophanes has been demonstrated through numerous examples. As the molecular recognition in water has a special interest, since it can directly mimic the recognition events in biological systems,⁵ much attention has been devoted to the development of water soluble cyclophanes as hosts with high binding selectivity for biological applications.⁶

The current area of interest in the cyclophanes is the use of these substituted systems in supramolecular chemistry,⁷ molecular recognition,⁸ molecular electronics and machines,⁹ and as catalysts in organic synthesis.¹⁰ By virtue of having a rigid structure with defined cavity, these systems encapsulate and stabilize a large number of guest molecules through non-covalent interactions.¹¹ Even though several cyclophane derivatives have been effectively utilized for host-guest complexation, designing functional cyclophanes, which are soluble in the aqueous medium and capable of undergoing specific interactions with biomacromolecules has been challenging.¹²

In this context, we have synthesized a series of novel cyclophanes and model derivatives (Chart 2.1), wherein we have systematically varied the bridging moieties and the spacer groups between the two aromatic (anthryl and phenyl) chromophores. Results of our investigations indicate that these systems can be prepared in moderate yields and the nature of the bridging moiety, the cavity size and spacer groups have a profound influence on their photophysical and hence biomolecular recognition properties.

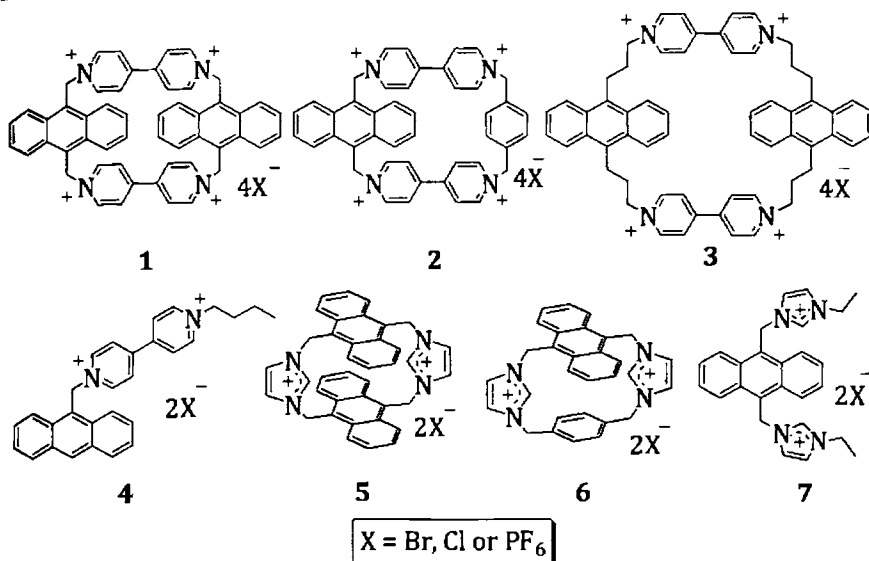
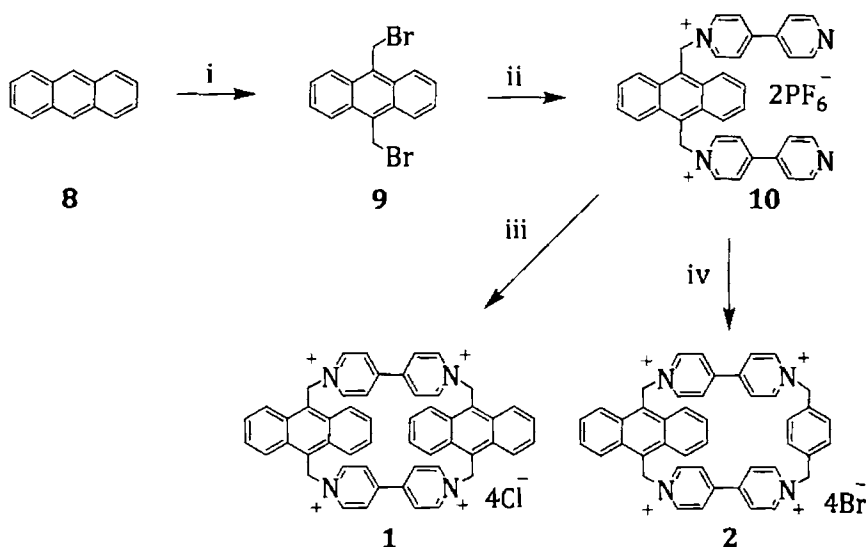


Chart 2.1

2.3. RESULTS

2.3.1. Synthesis

The synthesis of the viologen linked cyclophane derivatives **1** and **2** were carried out as shown in Scheme 2.1. Bromomethylation of anthracene with HBr in glacial acetic acid gave 9,10-bis(bromomethyl)anthracene with 95% yield. The reaction of **9** with 4,4'-bipyridine gave the open derivative **10** in 88% yield, which was further reacted with 9,10-bis(bromomethyl)anthracene (**9**) or 1,4-bis(bromomethyl)benzene in dry CH₃CN to give 37% and 36% of



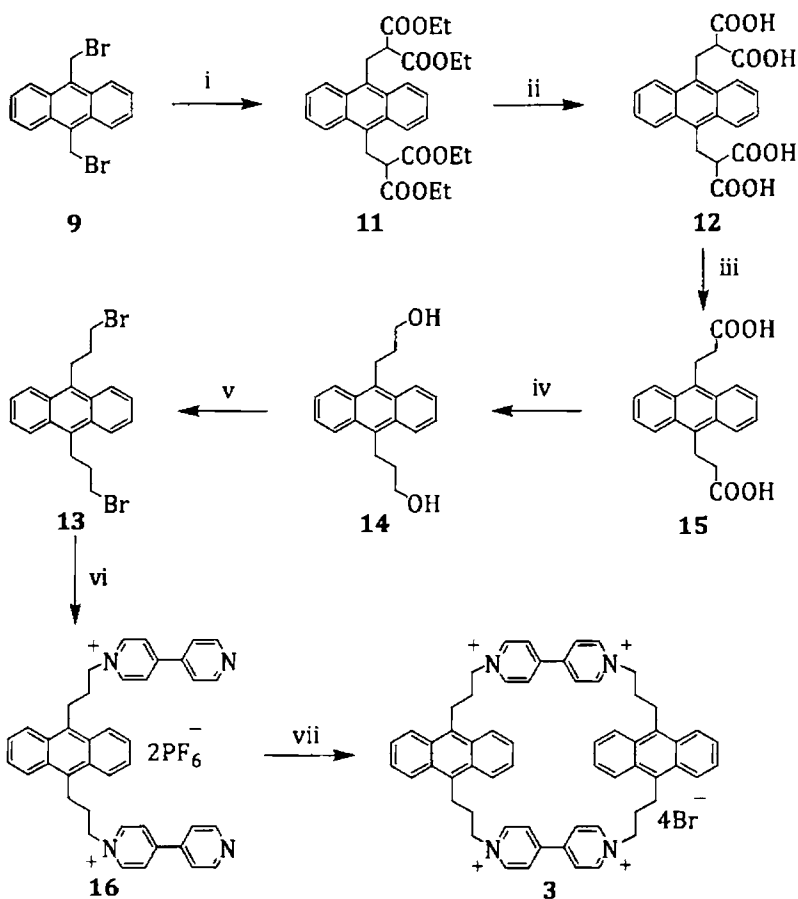
i) Paraformaldehyde, HBr in glacial acetic acid, rt, 2 h; ii) (a) 4,4'-bipyridine, CH₃CN, reflux, 4 h, (b) Aq. NH₄PF₆; iii) (a) 9, CH₃CN, reflux, 24 h, (b) Aq. NaCl; iv) (a) 1,4-bis(bromomethyl)benzene, CH₃CN, reflux, 24 h, (b) N(Bu)₄Br, CH₃CN

Scheme 2.1

the cyclophane derivatives **1** and **2**, respectively.¹³ The synthesis of the cyclophane **3** with flexible polymethylene spacer group was achieved as outlined in Scheme 2.2. The reaction of 9,10-bis(bromomethyl)anthracene (**9**) with diethylmalonate in the presence of metallic sodium yielded 86% of tetraethyl-2,2'-(anthracene-9,10-diyl-bis(methylene))dimalonate (**11**). The hydrolysis of **11** using NaOH in ethanol-water mixture gave 2,2'-

(anthracene-9,10-diyl-bis(methylene)) dimalonic acid (**12**).

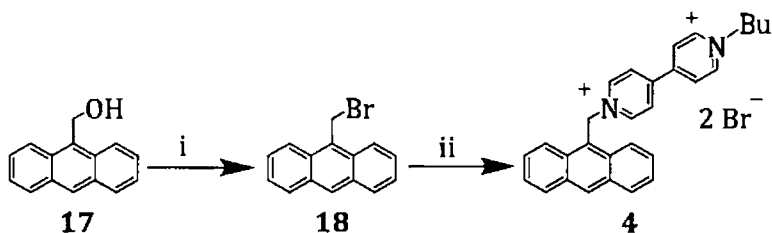
Decarboxylation of **12** gave 3,3'-(anthracene-9,10-diyl)dipropionic acid (**15**) in 45% yield, which on subsequent reduction using



i) Na/*p*-Xylene, diethylmalonate, reflux, 4 h; ii) NaOH, 2:1 EtOH/H₂O, reflux, 3 h; iii) diphenyl ether, reflux, 3 h; iv) LiAlH₄/ THF, reflux, 3 h; v) Aq. HBr, 120 °C, 2 h; vi) (a) 4,4'-bipyridine, CH₃CN, reflux, 12 h, (b) Aq. NH₄PF₆; vii) (a) **13**, CH₃CN, reflux, 3 days, (b) N(Bu)₄Br, CH₃CN

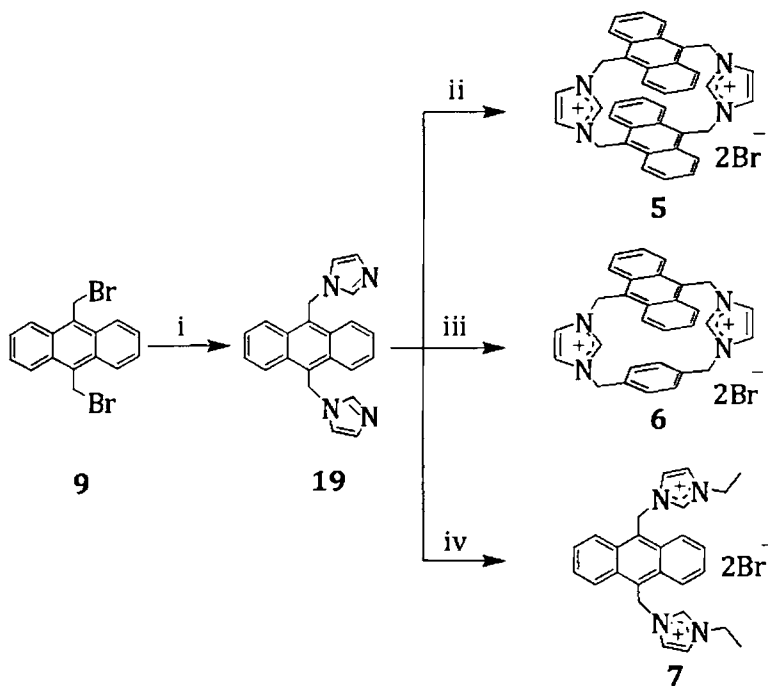
Scheme 2.2

lithium aluminium hydride in THF yielded 66% of 3,3'-(anthracene-9,10-diyl)dipropyl-1-ol (**14**). Bromination of **14** with aq. HBr, on the other hand, gave 9,10-bis(3-bromopropyl)anthracene (**13**) in 74% yield. The reaction of **13** with 4,4'-bipyridine gave the open derivative **16** in 60% yield. Further reaction of **16** with 9,10-bis(3-bromopropyl)anthracene (**13**) in dry CH₃CN gave the cyclophane **3** in 52% yield. The synthesis of the model viologen-linked conjugate **4** was achieved in moderate yields through the S_N2 reaction of 9-(bromomethyl)anthracene (**18**) with 1-butyl-4,4'-bipyridinium bromide (Scheme 2.3).¹³ The synthetic strategy adopted for the cyclophane systems **5-7** is shown in Scheme 2.4.¹⁴ The reaction of 9,10-bis(bromomethyl)anthracene (**9**) with imidazole in the presence of NaH in THF yielded 78% of 9,10-bis((1*H*-imidazol-1-yl)methyl)anthracene (**19**). The subsequent reaction of **19** with the



i) PBr₃, CH₂Cl₂, 0 °C, 12 h; ii) 1-butyl-4,4'-bipyridinium bromide, CH₃CN, reflux, 4 h

Scheme 2.3



i) Imidazole, NaH/THF, 0 °C, 2 h; ii) **9**, CH₃CN/DMF, 80 °C, 24 h; iii) 1,4-bis(bromomethyl)benzene, CH₃CN/DMF, 80 °C, 24 h; iv) CH₃CH₂Br, CH₃CN/DMF, 80 °C, 24 h

Scheme 2.4

9,10-bis(bromomethyl)anthracene (**9**) and 1,4-bis(bromomethyl)benzene, respectively, yielded the cyclophanes **5** and **6**, in 39% and 40% yields, whereas the open model derivative **7** was obtained in quantitative yields by the reaction of **19** with bromoethane.

All these compounds were characterized on the basis of spectral data and analytical results. For example, the ¹H NMR

spectrum of the cyclophane **1** in D₂O showed peaks corresponding to the anthracene and viologen protons in the region δ 7.81-9.01, whereas the methylene protons appeared as a singlet at δ 7.09. Similarly, the ¹³C NMR spectrum of **1** showed peaks at δ 72.9, 122.2, 124.6, 125.3, 127.7, 129.3, 131.3 and 142.7. Similarly, the symmetric nature of the cyclophane derivative **5** is evident from the NMR data as compared to that of the model compound **6**. The methylene protons appeared as a singlet at δ 6.39 in the ¹H NMR spectrum of the cyclophane **5**, whereas the anthracene protons appeared at δ 7.44 – 7.46 and 8.03 – 8.05 and the imidazole protons at δ 8.28 and 5.59. Similarly, the ¹³C NMR spectrum showed only seven peaks indicating the symmetric nature of the cyclophane **5**. On the other hand, the ¹H NMR spectrum of the model derivative **6**, showed the methylene protons as two singlets at δ 5.19 and 6.61, thereby clearly indicating the unsymmetrical structure of the cyclophane **6**. Similarly, the anthracene protons appeared at δ 7.66 – 7.68 and 8.34 – 8.36, while the imidazole protons appeared at δ 8.00 – 8.01, 8.29 – 8.30 and 6.66. As expected, in the ¹³C NMR spectrum of the model compound **6**, two peaks were observed at δ 45.5 and 52.2

corresponding to the methylene carbons. Furthermore, the final confirmation of the structures was obtained through single crystal X-ray analysis of the representative cyclophanes. Figure 2.1 shows the ORTEP diagram of the cyclophane **6** while Table 2.1 summarizes its crystal data. The structure of the cyclophane **6** shows a well defined rigid cavity flanked by anthryl and phenyl units, which lie in parallel planes.

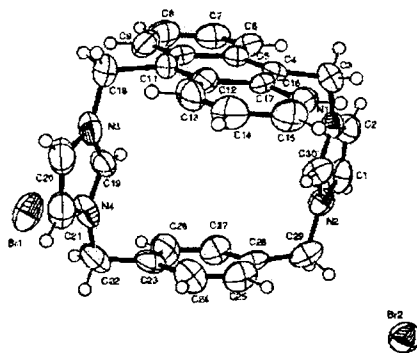


Figure 2.1. ORTEP diagram of the cyclophane **6**.

Table 2.1. Summary of crystallographic data for the cyclophane **6**

| Parameters | |
|-----------------------|-----------------------|
| Empirical formula | $C_{30}H_{26}Br_2N_4$ |
| Formula weight | 602.36 |
| T, K | 293 (2) |
| $\lambda, \text{\AA}$ | 0.71073 |
| Crystal system | Monoclinic |

Chapter 2

| | |
|---|--|
| Space group | P21 |
| a , Å | 10.3953(4) |
| b , Å | 17.2537(6) |
| c , Å | 16.1405(6) |
| α , deg | 90 |
| β , deg | 100.491(2) |
| γ , deg | 90 |
| V , Å ³ | 2846.53(18) |
| Z | 2 |
| d_{calc} , Mg/m ³ | 1.282 |
| F (000) | 1136 |
| Crystal size, mm | 0.30 × 0.20 × 0.20 |
| μ (MoK α), mm ⁻¹ | 1.474 |
| Theta range for data collection, ° | 1.28 to 25.00 |
| Limiting indices | -12 ≤ h ≤ 12, -20 ≤ k ≤ 20, -19 ≤ l ≤ 19 |
| Reflections collected/ unique | 25966/ 9821 |
| Refinement method | Full-matrix least-squares on F^2 |
| Data/ restraints/ parameters | 9821/ 2/ 681 |
| Goodness-of-fit on F^2 | 1.056 |
| Final R indices [$I > 2\sigma(I)$] | R1 = 0.0637, wR2 = 0.1719 |
| R indices (all data) | R1 = 0.0956, wR2 = 0.1974 |

2.3.2. Absorption and Fluorescence Properties

The absorption properties of the cyclophane derivatives and the model compounds have been investigated in various polar and non-polar solvents. Figure 2.2 shows the absorption spectra of a few representative cyclophane derivatives in the aqueous medium. All these derivatives exhibited characteristic anthracene chromophore absorption with the maxima in the region between 375 – 380 nm. For example, the viologen based cyclophane **1** showed a structured absorption band at λ_{\max} 379 nm, while the imidazolium based cyclophane **5** exhibited an absorption maximum at 375 nm. Thus, the absorption spectra of these derivatives can be described as the

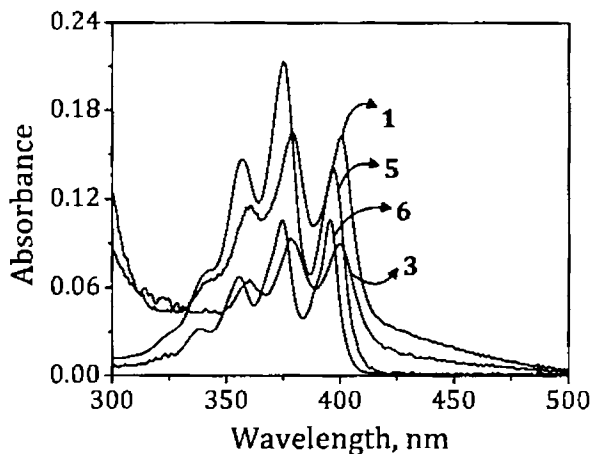


Figure 2.2. Absorption spectra of a few representative cyclophane derivatives in the aqueous medium.

sum of the absorption bands of the individual units, thereby ruling out the possibility of any ground-state charge-transfer interactions in these systems. Similarly, the absorption spectra of these derivatives in organic solvents such as methanol and acetonitrile were found to be similar to that observed in the aqueous medium.

The fluorescence spectra of different cyclophanes and the model derivatives recorded in organic media were characteristic of the anthracene chromophore. For example, in methanol and acetonitrile, all these derivatives exhibited emission maxima in the region between 418 – 430 nm (Figure 2.3). In the aqueous medium, the viologen bridged cyclophanes **1** and **3** exhibited emission

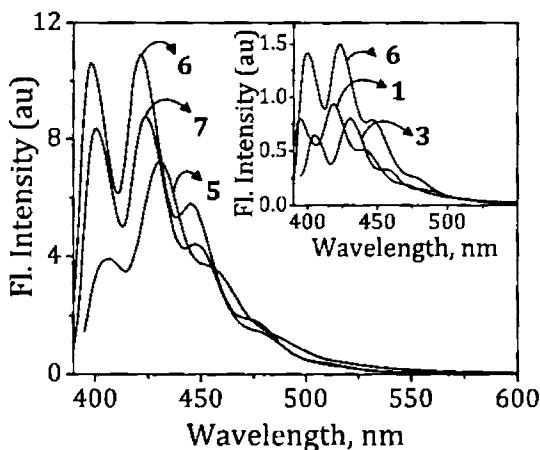


Figure 2.3. Fluorescence spectra of a few representative cyclophane derivatives in methanol and aqueous medium (inset).

maxima at 419 and 431 nm, respectively, whereas the imidazolium based model cyclophane **6** exhibited an emission maximum at 423 nm under identical conditions. As compared to the imidazolium derivatives, the viologen bridged systems showed significantly lower quantum yields of fluorescence ($\Phi_f = 0.7 - 1 \times 10^{-3}$) and the efficient quenching of fluorescence has been attributed to the thermodynamically favorable photoinduced electron transfer process from the excited singlet state of the anthracene chromophore to the viologen moiety. Interestingly, the imidazolium bridged derivatives, on the other hand, were found to be highly fluorescent in the aqueous medium with quantum yields ranging from 0.1 - 0.6. The cyclophane **5** in the aqueous medium, though showed similar absorption as observed in methanol and acetonitrile, exhibited dual emission consisting of a structured band having λ_{max} at 430 nm and a broad band centered at 550 nm with an I_{550}/I_{430} ratio of 0.8 (Figure 2.4). To ascertain the origin of dual emission observed in the case of the cyclophane **5** in the aqueous medium, the excitation spectra were recorded at 430 and 550 nm. As shown in Figure 2.5, these excitation spectra were found to be identical to the absorption spectrum of **5**, indicating thereby that

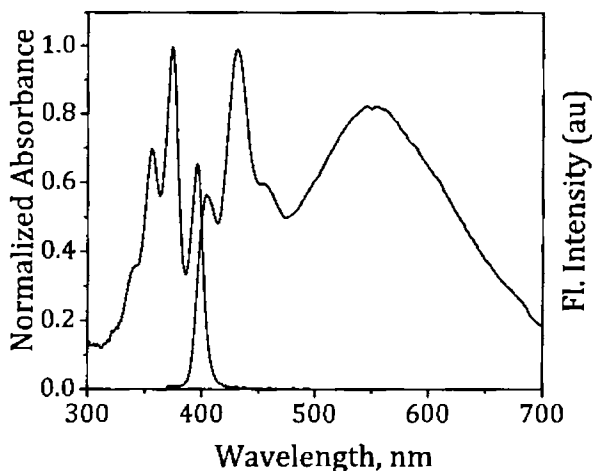


Figure 2.4. Normalized absorption and fluorescence spectra of the cyclophane **5** in aqueous medium. Excitation wavelength, 355 nm.

the absorbing species is the same for both these emission bands. On the basis of the experimental evidence and literature reports,¹⁵ we assign the dual emission observed in the case of the cyclophane **5** in the aqueous medium to the locally excited singlet state of the anthracene chromophore (monomer) at 430 nm and the intramolecular excimer at 550 nm. The observation of significant bathochromic shift in the emission maximum for the excimer clearly supports the fact that anthracene chromophores of **5** are in an extensively stacked conformation.¹⁶ The intramolecular nature of the excimer formed in the case of the cyclophane **5** was further evidenced by the negative results obtained with the other

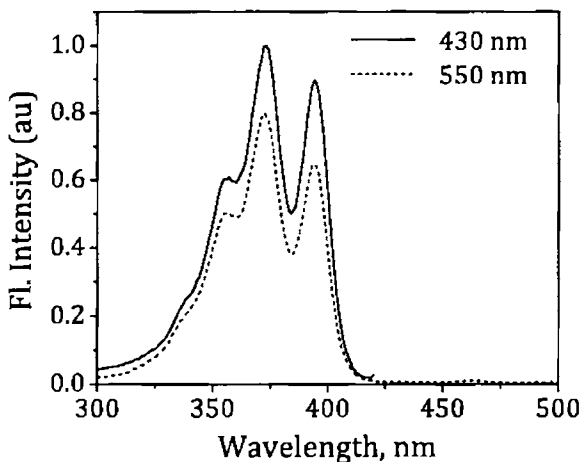


Figure 2.5. Excitation spectra of **5** monitored at 430 and 550 nm in the aqueous medium.

cyclophanes. For example, cyclophane **6** containing only one anthracene moiety exhibited exclusively monomer emission at 423 nm, indicating thereby that the presence of two extensively stacked anthryl moieties is a prerequisite for the intramolecular excimer formation. Further evidence for intramolecular excimer formation in **5** was obtained by monitoring its emission spectrum as a function of temperature, concentration and solvent polarity.

2.3.3. Characterization of Intramolecular Excimer

To understand the nature of the excimer formed in the case of the cyclophane **5**, we have investigated the effects of temperature,

concentration and solvent polarity on its emission spectrum. It is well known that the formation of intermolecular excimer is a diffusion controlled process. In such cases, at higher temperatures the rate of diffusion increases and as a result excimer formation gets enhanced.¹⁷ When the temperature of an aqueous solution of the cyclophane **5** was gradually increased from 298 to 353 K, we observed a regular decrease in the excimer emission intensity at 550 nm and a concomitant increase in the monomer emission at 430 nm along with an isoemissive point at 500 nm (Figure 2.6). This anomalous observation in the cyclophane **5** has been attributed to the formation of an intramolecular excimer formation which, in

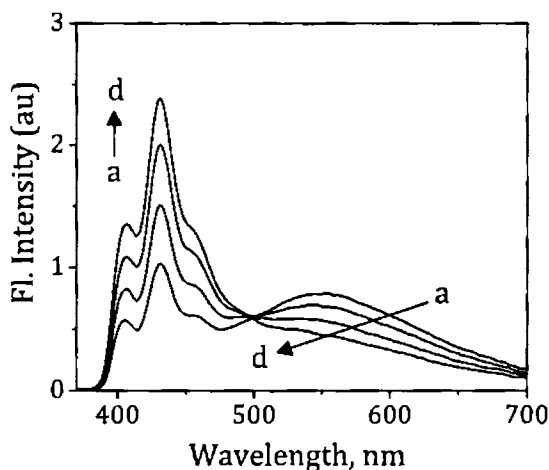


Figure 2.6. Effect of temperature on emission spectra of the cyclophane **5** in the aqueous medium. (a) 298 and (d) 353 K. Excitation wavelength, 355 nm.

turn, is strongly dependent on the highly ordered structure of the cyclophane **5**. A decrease in excimer emission intensity is observed at higher temperatures due to the perturbation of the ordered conformation of **5**, thereby leading to less significant interactions between the excited singlet state and the ground state of anthracene chromophores. Similarly, when the emission spectrum of **5** was recorded at different concentrations from 15 to 44 μM , we observed concentration independent spectral features (Figure 2.7). At all the concentrations investigated, we observed a constant excimer to monomer (I_{550}/I_{430}) ratio of 0.8 ± 0.01 . These facts confirm the intramolecular nature of the excimer in the case of the cyclophane **5**.

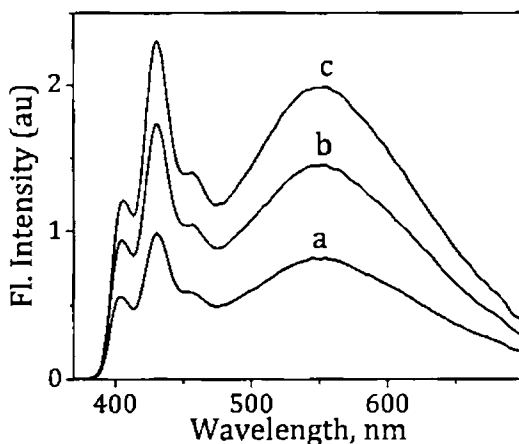


Figure 2.7. Emission spectra of the cyclophane **5** in the aqueous medium at different concentrations. (a) 15, (b) 29 and (c) 44 μM . Excitation wavelength, 355 nm.

Further, we have investigated the effect of solvent polarity on the fluorescence of the cyclophane **5** in order to understand the driving forces responsible for the excimer emission. Figure 2.8 shows the emission spectra of the cyclophane **5** in DMSO, ethylene glycol, glycerol, *n*-butanol, acetonitrile and methanol. Interestingly, the long wavelength emission was found to be highly dependent on the solvent polarity. It is evident from Figure 2.8 that the intensity of the excimer emission was found to be proportional to the solvent polarity. Of the different solvents used for comparison, the cyclophane **5** exhibited excimer emission only in DMSO and to a

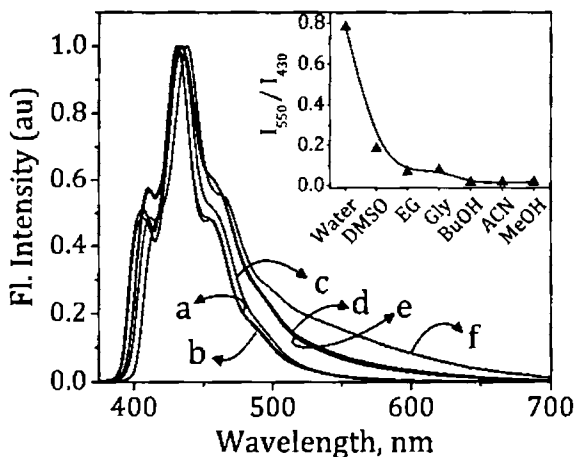


Figure 2.8. Emission spectra and (inset) the I_{550}/I_{430} ratio of the cyclophane **5** in (a) methanol (MeOH), (b) acetonitrile (ACN), (c) *n*-butanol (BuOH), (d) glycerol (Gly), (e) ethylene glycol (EG) and (f) DMSO. Excitation wavelength, 355 nm.

lesser extent in glycerol and ethylene glycol. These observations indicate that the polarity of the medium has a profound effect on excimer emission and thereby highlights the importance of hydrophobic forces in the excimer formation.

2.3.4. Time-Resolved Fluorescence Measurements

To understand the excited state behavior of various cyclophanes, we have carried out picosecond time-resolved fluorescence analysis under different conditions. For example, Figure 2.9 shows the fluorescence decay profiles of the viologen

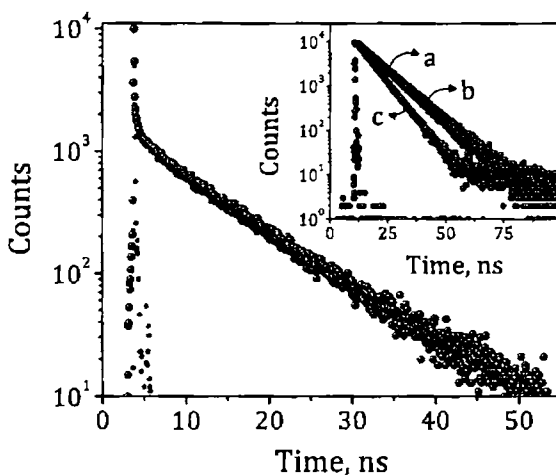


Figure 2.9. Fluorescence decay profiles of the cyclophane **1** in the aqueous medium monitored at 418 nm and (inset) the cyclophane **6** in (a) acetonitrile, (b) methanol and (c) aqueous medium monitored at 430 nm. Excitation wavelength, 375 nm.

bridged cyclophane **1** excited at 375 nm which exhibited a biexponential decay with lifetimes of 8.86 and 0.42 ns. The imidazolium bridged cyclophane **6**, on the other hand, showed only mono-exponential decay with lifetimes of 8.9 ± 0.2 , 9.7 ± 0.2 and 13.5 ± 0.3 ns, respectively, in acetonitrile, methanol and the aqueous medium. Similarly, the picosecond time-resolved fluorescence measurements of the cyclophane **5** in methanol and acetonitrile showed mono-exponential decay with lifetimes of 15.0 ± 0.5 and 18.7 ± 1 ns, respectively (Figure 2.10). In contrast, it showed biexponential decay having lifetimes of 13.4 ± 0.5 and 52.6 ± 2 ns in

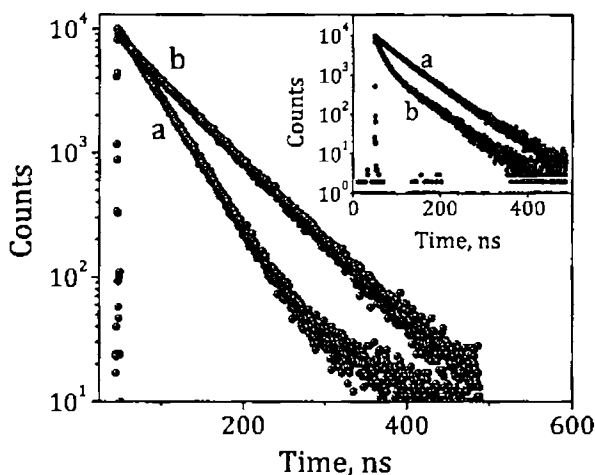


Figure 2.10. Fluorescence decay profiles of the cyclophane **5** in (a) acetonitrile and (b) methanol monitored at 430 nm and inset shows the corresponding decays in the aqueous medium monitored at (a) 550 and (b) 430 nm. Excitation wavelength, 375 nm.

the aqueous medium (inset of Figure 2.10). However, when we monitored the lifetimes at 550 nm, the species having longer lifetime was observed to be the major component (96%), while at 430 nm, we observed both these species in equal amplitudes. Of these, the species with a short lifetime of 13.4 ns has been attributed to the locally excited state (monomer), whereas the species with a lifetime of 52.6 ns corresponds to the intramolecular excimer.¹⁴

The excimer formation involves interaction between a molecule in the excited state with another molecule in the ground state. Therefore, the excimer formation can be effectively studied using time-resolved emission spectra (TRES). TRES deals with the measurement of the evolution of the emission spectrum with time and can be used for studying the time-dependent spectral changes.¹⁸ TRES is essentially the emission spectrum that would be observed at some instance in time following a pulsed excitation. In a TRES experiment, the time-resolved decay profiles at a number of wavelengths across the emission spectrum are measured. The intensity of decay profiles are then analyzed in terms of a suitable multiexponential model and the intensity at any wavelength and

time are calculated. For example, when the excited state behavior of **5** was analyzed immediately after excitation (60 ps) through TRES, we obtained a spectrum having only the emission band with λ_{\max} at 420 nm (Figure 2.11). However, gradually with time, we observed the formation of a new broad band around 550 nm. This band grew in intensity and after 26 ns, an emission spectrum that is similar to that obtained in the steady-state was observed with an I_{550}/I_{430} ratio of 0.8. These observations establish the fact that the locally excited singlet state of **5** undergoes geometric relaxation and forms a stable intramolecular excimer due to the existence of strong hydrophobic interactions in the aqueous medium.

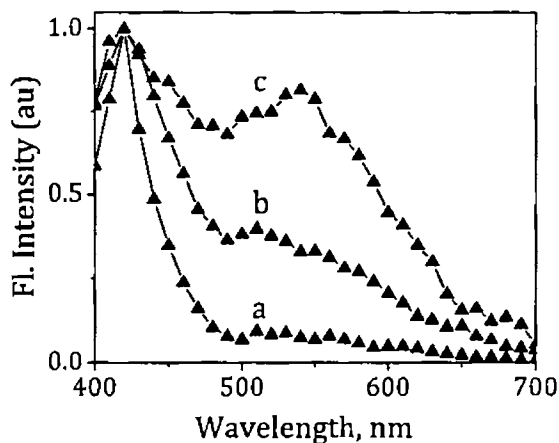


Figure 2.11. Time resolved emission spectra (TRES) of cyclophane **5** in the aqueous medium recorded at different time scales. (a) 60 ps, (b) 2.2 ns and (c) 26 ns. Excitation wavelength, 375 nm.

2.3.5. Solid State Photophysical Properties

Since the cyclophane derivatives under study exhibited favorable photophysical properties in various solvents, it was of our interest to investigate their photophysical properties in the solid state because such efficient molecules can have potential applications in devices.¹⁹ We have investigated their solid state photophysical properties in both powdered state and thin films. The reflectance spectra of the cyclophanes **1**, **5** and **6** and the model derivative **7** in the powdered state are shown in Figure 2.12. The reflectance spectra of all these derivatives exhibited absorption maximum in the region between 375 - 410 nm and were broader

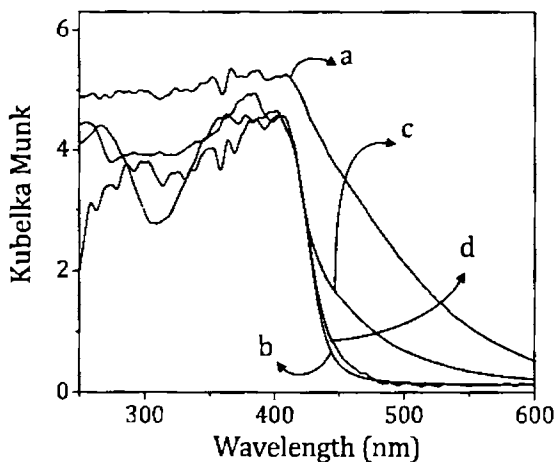


Figure 2.12. Normalized solid-state reflectance absorption spectra of cyclophanes (a) **1**, (b) **5** and (c) **6** and (d) the model derivative **7**.

and red-shifted as compared to that in solution. For example, the reflectance spectrum of the cyclophane **1** containing the viologen moiety exhibited bands that extended upto 600 nm. Similarly, the cyclophanes **5** and **6** exhibited maxima at 385 and 390 nm, respectively and extended upto 450 nm, whereas the model derivative **7** showed a $\lambda_{\text{max}} = 395$ nm. The significantly red shifted spectrum in the case of **1** indicates the existence of strong donor-acceptor interactions between the anthracene and viologen moieties in the solid state.

Further, the fluorescence properties of the cyclophanes and the model derivatives were studied in the powdered state and thin films prepared by drop-casting their solutions. Figure 2.13 shows the emission spectra of the cyclophanes **5** and **6** and the model derivative **7** in the powdered state. The cyclophane **5** exhibited an emission spectrum that is completely different from that obtained in solution. In the powdered state, the cyclophane **5** exhibited emission spectrum consisting exclusively of a broad band with λ_{max} 565 nm, as against the observation of a structured band at 430 nm in organic solvents and a dual emission in the aqueous medium. On the other hand, the emission spectra of the cyclophane **6** and the

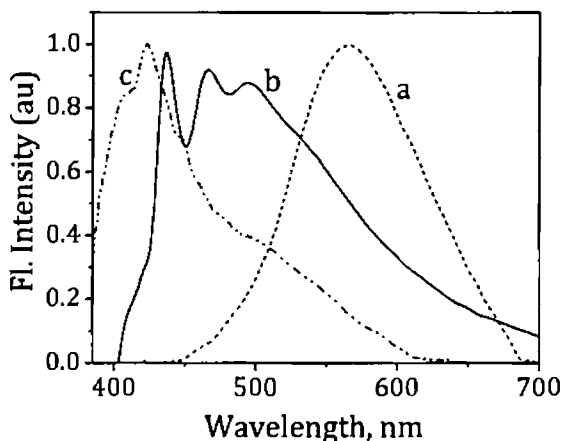


Figure 2.13. Normalized fluorescence spectra of the cyclophane derivatives (a) **5**, (b) **6** and (c) the model compound **7** in the powder state. Excitation wavelength, 375 nm.

open model compound **7** showed emission maxima around 435 nm along with a broad band centered around 500 nm.

The emission spectra of the cyclophanes in thin films, which were prepared by drop casting acetone solutions, exhibited broad emission around 550 nm (Figure 2.14). To ascertain the origin of the emission in the solid state, we have monitored the excitation spectra of the cyclophanes **5** and **6** at short and long wavelength regions. For example, Figure 2.15 shows the excitation spectra of **5** and **6** in the powdered state monitored at 565 and 435 nm, respectively. Both these compounds exhibited a structureless broad band in the excitation spectrum in the range 350 – 450 nm.

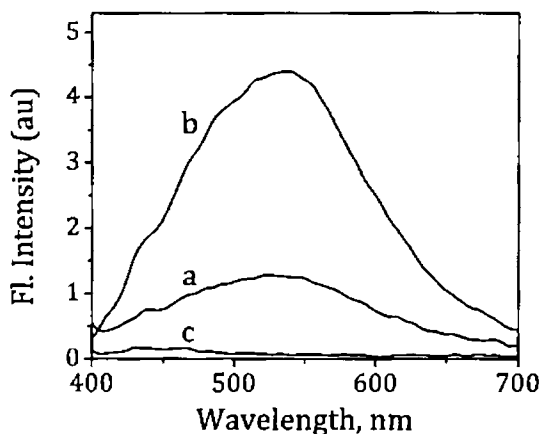


Figure 2.14. Fluorescence spectra of the cyclophane derivatives (a) **5**, (b) **6** and (c) the model open compound **7** in thin films. Excitation wavelength, 375 nm.

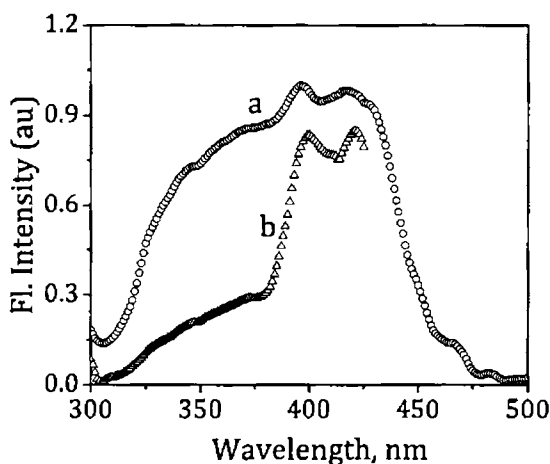


Figure 2.15. Normalized excitation spectra of the cyclophanes (a) **5** and (b) **6** in the powdered state monitored at 570 nm and 435 nm.

Similarly, the excitation spectrum of the cyclophane **6**, when monitored at 465 nm was observed to be similar to that monitored at 435 nm. Interestingly, all these spectra were found to be identical

to the respective reflectance spectra, thereby ruling out the possibility of ground state interactions in these cyclophanes. On the basis of the experimental evidence, the broad band in the long wavelength region of the emission spectrum may thus be attributed to the excimer formation.

2.3.6. Solid State Time-Resolved Fluorescence Properties

Picosecond time-resolved fluorescence and TRES measurements were used to further understand the photophysical properties of different cyclophane derivatives in the powdered state. As shown in Figure 2.16, the cyclophane **5** exhibited

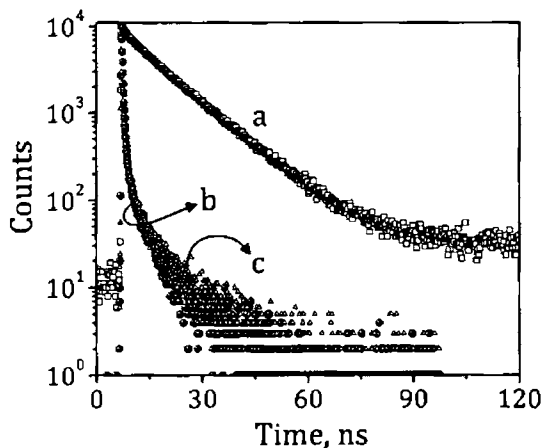


Figure 2.16. Fluorescence decay profiles of cyclophanes (a) **5**, (b) **6** and the model compound (c) **7** in the powdered state monitored at 570, 435 and 435 nm, respectively. Excitation wavelength, 375 nm.

biexponential decay in the powdered state, whereas the cyclophane **6** and the model derivative **7** exhibited triexponential decay under similar conditions. In the case of the cyclophane **5**, a species with a lifetime of 14.5 ns was observed as the major component (95%) while the short component (5%) showed a lifetime of 3.05 ns. On the other hand, the cyclophane **6** exhibited a lifetime of 0.2 ns as the major component (49%), whereas two minor components have lifetimes of 1.4 (23%) and 9.46 ns (28%). Similarly, in the case of the model open derivative **7**, we observed lifetimes of 0.27, 0.9 and 5.62 ns with relative amplitudes of 84, 10 and 6%. Figure 2.17 shows the TRES analysis of the cyclophane **5** in the powdered state

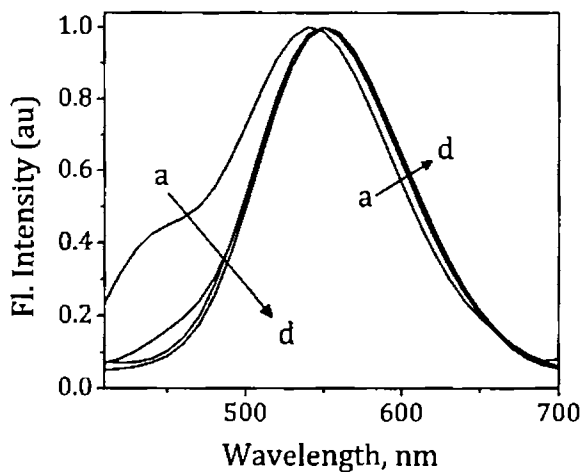


Figure 2.17. TRES analysis of the cyclophane **5** in the powdered state recorded at different time scales, (a) 0.23 and (d) 16.3 ns. Excitation wavelength, 375 nm.

recorded at different time scales. When monitored at a shorter time scale of 0.23 ns, the cyclophane **5** exhibited a peak at 550 nm with a shoulder in the 430 – 450 nm range. However, the short wavelength band disappeared gradually with time and the peak with $\lambda_{\max} = 550$ nm was observed exclusively at longer timescales. On the other hand, the TRES analyses of the cyclophane **6** and the model derivative **7** exhibited time dependent changes. Immediately after excitation, such as under a time scale of 0.11 ns, both these molecules exhibited a peak with $\lambda_{\max} = 440$ nm. But, gradually with time, we observed a red shift in the emission maxima and at longer time scales, i.e., after 12.1 ns, the emission spectra consisted exclusively of a broad band in the 500 – 510 nm range (Figure 2.18).

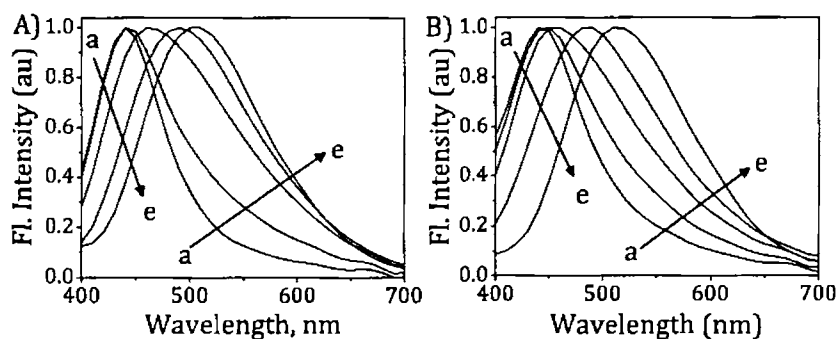


Figure 2.18. TRES analysis of (A) cyclophane **6** and (B) model derivative **7** in the powdered state recorded at different time scales. (a) 0.11 and (e) 12.1 ns. Excitation wavelength, 375 nm.

2.4. DISCUSSION

We have synthesized a series of novel cyclophane derivatives containing anthracene moieties linked together through two different bridging moieties, namely viologen and imidazolium moieties. All the cyclophane derivatives and the model derivatives were highly soluble in the aqueous medium and exhibited photophysical properties characteristic of the anthracene chromophore. The viologen linked derivatives were found to be negligibly fluorescent and their efficient fluorescence quenching has been attributed to photoinduced electron transfer from the excited anthracene chromophore to the viologen moiety. The anomalous behavior of the cyclophane **5** containing two anthracene moieties bridged together through imidazolium moieties in aqueous medium is rather unexpected and indeed interesting. The highly bathochromic shifted broad band in its emission spectrum in the aqueous medium has been attributed to the intramolecular excimer formation.

The optimized geometry obtained through B3LYP level theoretical calculations²⁰ using 6-31G basis set showed a rigid

conformation for the cyclophane derivatives and the interplanar distances in **1**, **5** and **6** were found to be 10.4, 5.26 and 5.24 Å, respectively (Figure 2.19). Based on the literature evidence,²¹ the formation of the excimer in the cyclophane **5** is unexpected since such a process is reported to be feasible only in systems having interplanar distance of less than 4 Å. This unusual behavior of the cyclophane **5** in the aqueous medium could be attributed to the existence of a highly ordered conformation due to hydrophobic interactions, which favor the excimer formation as evidenced through the excitation and TRES spectral analysis as well as concentration and temperature dependent experiments. Negligible formation of the excimer emission at and above 353 K confirms the fact that the ordered conformation of the cyclophane **5** is essential and that such a conformation no longer exists at these

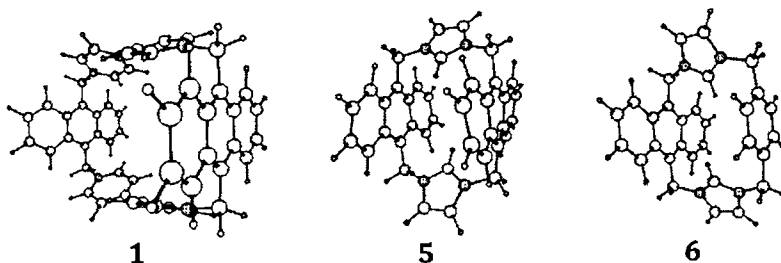


Figure 2.19. Optimized geometries of the cyclophanes **1**, **5** and **6** obtained with B3LYP/6-31G theoretical calculations.

temperatures. Similarly, the optimized geometries of the cyclophanes **1** and **6** showed interplanar distances of 10.35 and 5.24 Å, respectively. Both these derivatives exhibited typical fluorescence properties of the anthracene chromophore in the monomer state and the absence of red-shifted emission in these molecules confirm the intramolecular excimer formation in the cyclophane **5**.

In the case of the cyclophane **5**, the excimer formation is found to be efficient in the solid state as well. Our results show that the highly ordered *sandwich*-type conformation in the cyclophane **5** is retained in the solid state leading to highly red-shifted solid state excimer fluorescence with λ_{\max} 550 nm. The confirmation for excimer formation in the solid state in the cyclophane **5** is obtained from the excitation spectra and TRES analysis. The highly red-shifted emission maximum supports the extensively stacked conformation in the solid state. The cyclophane **6** and the model derivative **7**, on the other hand, showed broad emission in the region between 500 and 510 nm in addition to the monomer emission in the 430 – 440 nm region. The comparatively lesser red-shifted emission maxima in the case of these molecules can be attributed to the formation of a “T-type intermolecular excimer”.²²

The evidence for the proposed “T-type excimer” in the cyclophane **6** was obtained from the single crystal X-ray analysis (Figure 2.20). Single crystals of the cyclophane **6** were grown at room temperature by using methanol as the solvent. Figure 2.20 shows the unit cell and the extended crystal packing in the cyclophane **6**.²³

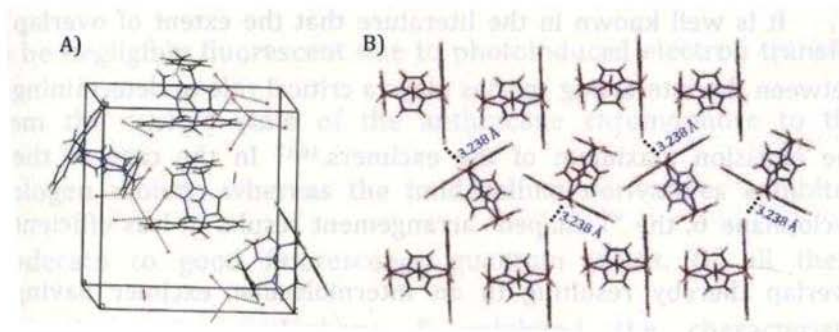


Figure 2.20. Crystal structure of the cyclophane **6** showing (A) a unit cell and (B) the extended packing.

The cyclophane **6** has four molecules per unit cell with the molecules arranged into two nonequivalent stacks in a herringbone fashion. A part of the x-ray structure of the cyclophane **6** is shown in Figure 2.20B and this figure can be used to explain the intermolecular interactions in the system. From this figure, it is evident that the anthracene moiety of a cyclophane molecule in one stack interacts with the anthracene moiety of another molecule in the adjacent row in a “T” fashion as shown using dotted lines. In

such an arrangement, the distance between the interacting molecules was found to be 3.238 Å, which is favorable for an excimer formation. On the basis of the X-ray data, the broad band in the 500 – 510 nm region of the cyclophane **6**, can thus be due to the formation of an intermolecular excimer.

It is well known in the literature that the extent of overlap between the interacting species plays a critical role in determining the emission maximum of the excimers.^{16,17} In the case of the cyclophane **6**, the “T-shaped” arrangement results in less efficient overlap thereby resulting in an intermolecular excimer having emission maximum around 500 nm. In the time resolved fluorescence measurements, the species with a lifetime of 9.46 ns can be assigned to the intermolecular excimer whereas that with a lifetime of 0.20 ns to the monomer. As compared to **6** and **7**, the cyclophane **5** exhibited a significantly bathochromic shift in the emission maximum ($\lambda_{\text{max}} = 565 \text{ nm}$) along with a longer lifetime of 14.5 ns. The red shift in its emission spectrum can be attributed to a highly ordered *sandwich*-type conformation wherein the anthracene molecules exist in an extensively stacked state.

2.5. CONCLUSIONS

We have synthesized a series of novel water soluble cyclophane derivatives containing anthracene moieties linked together through two different bridging moieties, namely viologen and imidazolium units. The viologen linked derivatives were found to be negligibly fluorescent due to photoinduced electron transfer from the excited state of the anthracene chromophore to the viologen moiety, whereas the imidazolium derivatives exhibited moderate to good fluorescence quantum yields. Of all these derivatives, the cyclophane **5** exhibited the characteristic anthracene fluorescence in acetonitrile and methanol, whereas it showed excimer emission under aqueous conditions with a maximum at 550 nm. The significantly red-shifted excimer emission maximum and long lifetimes indicate the existence of a highly stacked conformation in the case of **5**. Interestingly, the cyclophane **5** exhibited solid state fluorescence arising solely from the intramolecular excimer in the powdered state, while the model cyclophane **6** exhibited emission having two bands, one at 440 nm and the other in the 500 - 510 nm range. The solid state packing

obtained from the X-ray analysis showed the formation of a “T-shaped” excimer for the cyclophane **6**. These novel cyclophane systems which are soluble in aqueous medium exhibit favorable photophysical properties and consist of a hydrophobic cavity and hence can have potential use as receptors and probes for biomolecular recognition.

2.6. EXPERIMENTAL SECTION

2.6.1. General Techniques

The equipment and procedures for melting point determination and spectral recordings have been described elsewhere.^{24,25} All melting points were determined on a Mel-Temp II melting point apparatus. An Elico pH meter was used for pH measurements. ¹H and ¹³C NMR spectra were measured on a 300 MHz or 500 MHz Bruker advanced DPX spectrometer. HRMS were recorded on a JEOL mass spectrometer. The electronic absorption spectra were recorded on a Shimadzu UV-VIS-NIR spectrophotometer. Fluorescence spectra were recorded on a SPEX-Fluorolog F112X spectrofluorimeter. The fluorescence quantum yields were

determined by using optically matched solutions. Quinine sulphate ($\Phi_f = 0.54$) in 0.1 N H_2SO_4 was used as the standard.²⁶ The quantum yields of fluorescence were calculated using the equation 2.1, where,

$$F_u = \frac{A_s F_u n_s^2}{A_u F_s n_u^2} F_s \quad (2.1)$$

A_s and A_u are the absorbance of standard and unknown, respectively. F_u and F_s are the areas of fluorescence peaks of the unknown and standard and n_s and n_u are the refractive indices of the standard and unknown solvents, respectively. Φ_s and Φ_u are the fluorescence quantum yields of the standard and unknown. Fluorescence lifetimes were measured using a IBH Picosecond single photon counting system. The fluorescence decay profiles were deconvoluted using IBH data station software V2.1, and minimizing the χ^2 values of the fit to 1 ± 0.1 .

2.6.2. Materials

Anthracene, paraformaldehyde, sodium, diethylmalonate, imidazole and *p*-xylene were obtained locally and used as received. Anthracen-9-ylmethanol, lithium aluminium hydride and 4,4'-

bipyridine were purchased from Sigma-Aldrich and used as received. The synthesis of 9,10-bis(bromomethyl)anthracene (**9**), mp >300 °C (lit. mp >300 °C),²⁷ tetraethyl 2,2'-(anthracene-9,10-diylbis-(methylene))dimalonate (**11**), mp 171-172 °C (lit. mp 172 °C),²⁸ 2,2'-(anthracene-9,10-diylbis(methylene))dimalonic acid (**12**), mp 249-250 °C (lit. mp 251-253 °C)²⁸ and 3,3'-(anthracene-9,10-diyl)dipropanoic acid (**15**), mp 242-243 °C (lit. mp 244 °C)²⁸ was achieved as per reported procedures. Petroleum ether used was the fraction with boiling range 60-80 °C.

2.6.3. Preparation of 1,1'-[9,10-anthrylbis(methylene)]bis-4,4'-bipyridiniumbis(hexafluorophosphate) (10**)**

A solution of 9,10-bis(bromomethyl)anthracene (1 g, 2.747 mmol) in dry CH₃CN (20 mL) was added to a solution of 4,4'-bipyridyl (2.14 g, 13.7 mmol) in dry CH₃CN (5 mL) over a period of 30 min. at 25 °C. The reaction mixture was refluxed for 4 h at 80 °C and then cooled to room temperature. The precipitated product was filtered, washed with dry CH₃CN (3 mL) and dissolved in water (25 mL). The aqueous solution was washed with CH₂Cl₂ thrice, 5 mL each time, and then water was removed under vacuum to give a

solid residue, which was then recrystallized from water. The product was redissolved in hot water, and a saturated aqueous solution of NH_4PF_6 was added to yield 1.64 g (88%) of **10**, mp >300 °C, after re-crystallization from acetonitrile; ^1H NMR (300 MHz, CD_3COCD_3) δ 7.40 (4H, s), 7.81-7.85 (4H, m), 7.98-8.00 (4H, d), 8.59-8.62 (4H, d), 8.70-8.74 (4H, m), 8.88-8.90 (4H, d), 9.21-9.23 (4H, d); ^{13}C NMR (75 MHz, CD_3COCD_3) δ 58.2, 114.3, 114.5, 115.8, 116.2, 117.7, 123.8, 127.1, 128.7, 131.2, 144.7; HRMS (FAB) m/z calcd for $\text{C}_{36}\text{H}_{28}\text{N}_4\text{PF}_6$: 661.5986, found: 661.5991[M-PF₆]⁺.

2.6.4. Synthesis of the cyclophane 1

A solution of 9,10-bis(bromomethyl)anthracene (0.3 g, 0.8 mmol) and **10** (1 g, 1.2 mmol) in dry CH_3CN (100 mL) was heated under reflux at 80 °C for 24 h. The reaction mixture was cooled to room temperature to give a precipitate which was filtered and washed with dry CH_3CN (10 mL). The precipitate was redissolved in water, washed with CH_2Cl_2 thrice, 3 mL each time. A saturated aqueous solution of NaCl was added to give 0.18 g (26%) of the cyclophane derivative **1**, after re-crystallization from a mixture (1:3) water and methanol, mp >300 °C; ^1H NMR (300 MHz, D_2O) δ 7.09

(8H, s), 7.81 - 9.01 (32H, m); ^{13}C NMR (75 MHz, D_2O) δ 72.9, 122.2, 124.6, 125.3, 127.7, 129.3, 131.3, 142.7; HRMS (FAB) m/z calcd for $\text{C}_{52}\text{H}_{40}\text{N}_4\text{Cl}_2$: 791.8064, found: 791.8072 $[\text{M}-2\text{Cl}]^+$.

2.6.5. Synthesis of the cyclophane **2**

A solution of **10** (1 g, 1.2 mmol) and 1,4-bis(bromomethyl) benzene (0.21 g, 0.8 mmol) in dry CH_3CN (80 mL) was heated under reflux at 80 °C for 24 h. The reaction mixture was cooled to room temperature, and the precipitate was filtered and washed with dry CH_3CN . The precipitate was recrystallized from a 1:1 mixture of water and methanol to yield 0.41 g (36%) of **2**, mp >300 °C; ^1H NMR (300 MHz, $\text{DMSO}-d_6$) δ 6.02 (4H, s), 7.25 (4H, s), 7.72 - 7.74 (8H, m), 8.57 - 8.66 (12H, m), 9.19 - 9.23 (4H, m), 9.56 - 9.59 (4H, m); ^{13}C NMR (75 MHz, D_2O) δ 63.2, 70.9, 121.2, 123.2, 125.0, 126.2, 127.2, 130.4, 134.4, 135.8, 138.6, 139.1, 140.3, 141.3; HRMS (FAB) m/z calcd for $\text{C}_{44}\text{H}_{36}\text{N}_4\text{Br}_2$: 780.5903, found: 780.6964 $[\text{M}-2\text{Br}]^+$.

2.6.6. Preparation of 3,3'-(anthracene-9,10-diyl)dipropanol (**14**)

To a suspension of lithium aluminum hydride (0.053 g, 1.4 mmol) in 10 mL dry THF, 3,3'-(anthracene-9,10-diyl)dipropanoic

acid (**15**) (0.15 g, 0.47 mmol) in 20 mL dry THF was slowly added over 30 min. After the addition was complete, the reaction mixture was refluxed for 3 h. After cooling to room temperature, water was added to quench excess lithium aluminum hydride and the layers were separated. The aqueous layer was extracted with ethyl acetate and the organic fractions were combined, dried over anhydrous Na_2SO_4 and concentrated to get a residue which was column chromatographed over silica gel. Elution of the column with 20% ethyl acetate and petroleum ether mixture gave 0.09 g (66%) of the product **14** which was re-crystallized from a mixture (1:4) of ethyl acetate and petroleum mixture, mp 172-173 °C; ^1H NMR (300 MHz, $\text{DMSO}-d_6$) δ 8.37 - 8.40 (4H, m), 7.53 - 7.57 (4H, m), 4.71 (2H, t), 3.60 - 3.64 (8H, m), 1.87 - 1.89 (4H, m); HRMS (FAB) m/z calcd for $\text{C}_{20}\text{H}_{22}\text{O}_2$: 294.3875, found: 294.1628.

2.6.7. Preparation of 9,10-bis(3-bromopropyl)anthracene (13)

A mixture of 3,3'-(anthracene-9,10-diyl)dipropan-1-ol (**14**) (0.1 g, 0.34 mmol) and aqueous HBr (5 mL) was refluxed at 120 °C for 2 h. After cooling to room temperature, 10 mL CH_2Cl_2 was added to the reaction mixture and neutralized with aqueous sodium

bicarbonate solution. The organic layer was separated and the solvent was evaporated to give the product which was purified by column chromatography over silica gel. Elution of the column with petroleum ether yielded 0.11 g (74%) of **13**, mp 149-150 °C; ^1H NMR (300 MHz, CDCl_3) δ 8.24 - 8.27 (4H, m), 7.43 - 7.47 (4H, m), 3.71 (4H, t), 3.54 (4H, t), 2.25 - 2.34 (4H, m); ^{13}C NMR (75 MHz, CDCl_3) δ 132.2, 129.5, 125.3, 124.9, 34.0, 33.8, 26.5; HRMS (FAB) m/z calcd for $\text{C}_{20}\text{H}_{20}\text{Br}_2$: 420.1808, found 420.1938.

2.6.8. Preparation of 1,1'-(3,3'-(anthracene-9,10-diyl)bis(propane-3,1-diyl))di-4,4'-bipyridin-1-ium bishexafluorophosphate (16)

To a solution of 4,4'-bipyridine (0.185 g, 1.19 mmol) in 5 mL dry acetonitrile was added 9,10-bis(3-bromopropyl)anthracene (**13**) (0.1g, 0.24 mmol) in 5 mL dry acetonitrile over 30 min. The reaction mixture was then refluxed for 12 h and after cooling to room temperature the precipitated product was filtered and washed with dry CH_3CN . The residue was then dissolved in water, filtered and an aqueous solution of NH_4PF_6 was added to precipitate the product. The product was filtered and re-crystallized from

acetone and dried in vacuum to yield 0.12 g (60%) of **16**, mp >300 °C; ¹H NMR (300 MHz, CD₃COCD₃) δ 9.38 - 9.40 (4H, d), 8.64 - 8.66 (4H, d), 8.95 - 8.96 (4H, m), 8.45 - 8.49 (4H, m), 8.15 - 8.17 (4H, m); ¹³C NMR (75 MHz, CD₃COCD₃) δ 149.1, 145.6, 132.1, 130.1, 129.5, 126.1, 125.9, 125.7, 125.1, 123.0, 61.3, 32.5, 24.4; HRMS (FAB) m/z calcd for C₄₀H₃₆N₄PF₆: 717.71, found 717.74 [M - PF₆]⁺.

2.6.9. Synthesis of the cyclophane 3

To a solution of **16** (0.05 g, 0.058 mmol) in 5 mL dry acetonitrile, 9,10-bis(3-bromopropyl)anthracene (**13**) (0.025 g, 0.058 mmol) in dry acetonitrile (10 mL) was added slowly through 20 min. The reaction mixture was stirred and refluxed for 3 days and after cooling to room temperature, a saturated solution of tetrabutylammonium bromide in dry acetonitrile was added and the precipitate obtained was filtered. It was then washed with dry acetonitrile, re-crystallized from methanol and dried under vacuum to yield 0.035 g (52%) of **3**, mp. >300 °C; ¹H NMR (300 MHz, DMSO-*d*₆) δ 7.61-9.52 (32H, m), 5.03-5.06 (8H, m), 3.72-3.75 (8H, m), 2.40-2.43 (8H, m); ¹³C NMR (75 MHz, DMSO-*d*₆) δ 148.5, 145.9, 132.0,

129.0, 126.6, 125.6, 125.1, 60.8, 32.4, 24.3; HRMS (FAB) m/z calcd for $C_{60}H_{56}N_4Br_4$: 992.9203, found 993.0862 $[M - 2Br]^+$.

2.6.10. Preparation of 1-[(anthr-9-yl)methyl]-1'-butyl-4,4'-bipyridinium dibromide (**4**)

To a solution of 9-(bromomethyl)anthracene (**18**) (0.16 g, 0.6 mmol) in dry acetonitrile (50 mL), 1-butyl-4,4'-bipyridinium bromide (0.18 g, 0.6 mmol) was added and stirred for 12 h at 25 °C. Precipitated product was filtered, dried and re-crystallized from a mixture (6:4) of methanol and ethyl acetate to give 0.27 g (79%) of **4**, mp 289-290 °C; 1H NMR (300 MHz, $DMSO-d_6$) δ 0.88 (3H, t), 1.28-1.29 (2H, m), 1.89-1.91 (2H, m), 4.67 (2H,), 7.08 (2H, s), 7.61-9.33 (17H, m); ^{13}C NMR (75 MHz, $DMSO-d_6$) δ 13.3, 18.7, 32.7, 56.1, 60.5, 121.6, 123.3, 125.8, 126.7, 126.9, 128.4, 129.6, 131.1, 131.4, 131.5, 144.8, 145.7, 148.6, 149.1; HRMS (FAB) m/z calcd for $C_{29}H_{28}N_2Br_2$: 484.4501, found: 484.4495 $[M-Br]^+$.

2.6.11. Synthesis of 9,10-bis(imidazolylmethyl)anthracene (**19**)

To a reaction mixture of imidazole (0.5 g, 7.4 mmol) in dry THF (100 mL) was added NaH (0.33 g, 13.8 mmol) at 0 °C. After the

reaction mixture was stirred for 30 min at 0 °C, 9,10-bis(bromomethyl)anthracene (**9**, 0.5 g, 1.4 mmol) was added. After additional stirring for 2 h at room temperature, the reaction mixture was poured into 100 mL of water and extracted with dichloromethane. The organic layer was then separated, dried over anhydrous sodium sulfate and concentrated to get a residue which was further purified by column chromatography over silica gel. Elution of the column with ethyl acetate yielded 0.37 g (78%) of **19**, which was then re-crystallized from a mixture of acetonitrile and ethyl acetate (4:1); mp 246-247 °C; ¹H NMR (300 MHz, DMSO-*d*₆) δ 6.29 (4H, s), 6.78 (2H, s), 6.93 (2H, s), 7.67 – 7.73 (6H, m), 8.61 – 8.64 (4H, m); ¹³C NMR (75 MHz, DMSO-*d*₆) δ 109.9, 113.6, 119.1, 124.7, 124.9, 128.3, 129.1, 130.1; HRMS (FAB): *m/z* calcd for C₂₂H₁₉N₄: 339.4132, found 339.4508.

2.6.12. Synthesis of the cyclophane 5

To a solution of 9,10-bis((1*H*-imidazol-1-yl)methyl)anthracene (**19**, 0.25 g, 0.74 mmol) in a mixture of acetonitrile (100 mL) and DMF (50 mL) was added 9,10-bis(bromomethyl)anthracene (**9**, 0.27 g, 0.74 mmol). The reaction mixture was then

warmed and maintained at 80 °C for 24 h. After cooling to room temperature, the precipitated product was filtered and washed with 50 mL dry acetonitrile. It was further purified by re-crystallization from a mixture of acetonitrile and methanol (1:5) to yield 0.2 g (39%) of **5**; mp >300 °C; ¹H NMR (500 MHz, DMSO-*d*₆) δ 5.59 (2H, s), 6.39 (8H, s), 7.44 – 7.46 (8H, m), 8.03 – 8.05 (8H, m), 8.28 (4H, s); ¹³C NMR (125 MHz, DMSO-*d*₆) δ 45.3, 123.6, 124.1, 126.4, 127.6, 129.3, 132.5; HRMS (FAB) *m/z* calcd for C₃₈H₃₀Br₂N₄: 622.5758, found 622.5753 [M – Br]⁺.

2.6.13. Synthesis of the cyclophane **6**

To a solution of 9,10-bis((1*H*-imidazol-1-yl)methyl)anthracene (**19**, 0.25 g, 0.74 mmol) in a mixture of acetonitrile (100mL) and DMF (50 mL) was added 1,4-bis(bromomethyl)benzene (0.195 g, 0.74 mmol). The reaction mixture was then refluxed for 24 h and after cooling to room temperature the precipitated product was filtered and washed with 30 mL dry acetonitrile. It was further purified by re-crystallization from a mixture of acetonitrile and methanol (1:2) to yield 0.18 g (40%) of **6**; mp >300 °C; ¹H NMR (500 MHz, DMSO-*d*₆) δ 5.19 (4H, s), 6.61

(4H, s), 6.66 (2H, s), 6.81 (4H, s), 7.66 – 7.68 (4H, m), 8.00 – 8.01 (2H, t) 8.29 – 8.30 (2H, t), 8.34 – 8.36 (4H, m); ¹³C NMR (125 MHz, DMSO-*d*₆) δ 45.5, 52.2, 123.57, 123.63, 124.3, 127.5, 129.7, 129.9, 134.1, 134.3; HRMS (FAB) *m/z* calcd for C₃₈H₃₀Br₂N₄: 622.5758, found 622.5753 [M – Br]⁺.

2.6.14. Synthesis of 1,1'-(anthracene-9,10-diylbis(methylene)) bis(3-ethyl-1*H*-imidazol-3-ium) dibromide (7)

To a solution of 9,10-bis((1*H*-imidazol-1-yl)methyl)anthracene (**19**, 0.25 g, 0.74 mmol) in a mixture of acetonitrile (100mL) and DMF (50 mL) was added bromoethane (0.81 g, 0.74 mmol). The reaction mixture was then refluxed for 24 h and after cooling to room temperature the precipitated product was filtered and washed with 30 mL dry acetonitrile. It was further purified by re-crystallization from acetonitrile to yield 180 mg (40%) of **7**; mp 276-277 °C; ¹H NMR (500 MHz, DMSO-*d*₆) δ 5.19 (4H, s), 6.61 (4H, s), 6.66 (2H, s), 6.81 (4H, s), 7.66 – 7.68 (4H, m), 8.00 – 8.01 (2H, t), 8.29 – 8.30 (2H, t), 8.34 – 8.36 (4H, m); ¹³C NMR (125 MHz, DMSO-*d*₆) δ 45.5, 52.2, 123.57, 123.63, 124.3, 127.5, 129.7, 129.9, 134.1,

134.3; HRMS (FAB) m/z calcd for $C_{38}H_{30}Br_2N_4$: 622.5758, found 622.5753 [M - Br]⁺.

2.7. REFERENCES

1. M. M. Pellegrin, *Rec. Trav. Chim.* **1899**, *18*, 457–459.
2. C. J. Brown, A. C. Farthing, *Nature*, **1949**, *164*, 915–916.
3. (a) P. M. Keehn, S. M. Rosenfeld, *Cyclophanes I, II*; Academic Press, New York, **1983**. (b) F. Vögtle, *Cyclophane Chemistry*, Wiley, New York, **1993**.
4. J. L. Atwood, J. E. D. Davies, D. D. Macnicol, F. Vögtle, J. -M. Lehn (Eds.), *Comprehensive Supramolecular Chemistry*, Vol. 1, 2 and 10, Elsevier Science, Oxford, **1996**.
5. (a) F. Diederich, D. R. Carcanague, *Helv. Chim. Acta.* **1994**, *77*, 800–818. (b) D. Müller, F. Vögtle, *Synthesis*, **1995**, 759–760.
6. F. Diederich, In *Cyclophanes, Monographs in Supramolecular Chemistry*, J. F. Stoddart (Ed.), The Royal Society of Chemistry, London, **1991**.
7. (a) T. D. Nguyen, K. C.-F. Leung, M. Liong, Y. Liu, J. F. Stoddart, J. I. Zink, *Adv. Funct. Mater.* **2007**, *17*, 2101–2110. (b) F.

-
- Diederich, B. Felber, B. *Proc. Natl. Acad. Sci. USA.* **2002**, *99*, 4778–4781.
8. (a) H.-J. Schneider, A. K. Yatsimirsky, *Chem. Soc. Rev.* **2008**, *37*, 263–277. (b) E. V. Anslyn, *J. Org. Chem.* **2007**, *72*, 687–699.
9. (a) G. P. Bartholomew, G. C. Bazan, *Acc. Chem. Res.* **2001**, *34*, 30–39. (b) M. D. Watson, F. Jackel, N. Severin, J. P. Rabe, K. Mullen, *J. Am. Chem. Soc.* **2004**, *126*, 1402–1407. (c) E. R. Kay, D. A. Leigh, F. Zerbetto, *Angew. Chem. Int. Ed.* **2007**, *46*, 72–191. (d) S. Saha, J. F. Stoddart, *Chem. Soc. Rev.* **2007**, *36*, 77–92.
10. (a) C. S. Popeney, D. H. Camacho, Z. Guan, *J. Am. Chem. Soc.* **2007**, *129*, 10062–10063. (b) Z. R. Laughrey, B. C. Gibb, *Top. Curr. Chem.* **2005**, *249*, 67–125.
11. (a) E. A. Meyer, R. K. Castellano, F. Diederich, *Angew. Chem. Int. Ed.* **2003**, *42*, 1210–1250. (b) M. Inouye, K. Fujimoto, M. Furusyo, H. Nakazumi, *J. Am. Chem. Soc.* **1999**, *121*, 1452–1458. (c) C. G. Claessens, J. F. Stoddart, *J. Phys. Org. Chem.* **1997**, *10*, 254–272.
12. (a) P. D. Beer, P. A. Gale, *Angew. Chem. Int. Ed.* **2001**, *40*, 486–516. (b) N. Lomadze, H.-J. Schneider, M. T. Albelda, E. Garcia-Espana, B. Verdejo, *Org. Biomol. Chem.* **2006**, *4*, 1755–1759.

- (c) E. J. Fechter, B. Olenyuk, P. B. Dervan, *Angew. Chem. Int. Ed.* **2004**, *43*, 3591–3594. (d) M. Fernandez-Saiz, H.-J. Schneider, J. Sartorius, W. D. Wilson, *J. Am. Chem. Soc.* **1996**, *118*, 4739–4745. (e) S. C. Zimmerman, C. R. Lamberson, M. Cory, T. A. Fairley, *J. Am. Chem. Soc.* **1989**, *111*, 6805–6809.
13. (a) P. P. Neelakandan, M. Hariharan, D. Ramaiah, *Org. Lett.* **2005**, *7*, 5765–5768. (b) P. P. Neelakandan, M. Hariharan, D. Ramaiah, *J. Am. Chem. Soc.* **2006**, *128*, 11334–11335.
14. P. P. Neelakandan, D. Ramaiah, *Angew. Chem. Int. Ed.* **2008**, *47*, 8407–8411.
15. (a) Y. Molard, D. M. Bassani, J. P. Desvergne, N. Moran, J. H. R. Tucker, *J. Org. Chem.* **2006**, *71*, 8523–8531. (b) T. Förster, *Angew. Chem. Int. Ed. Engl.* **1969**, *8*, 333–343. (c) E. C. Lim, *Acc. Chem. Res.* **1987**, *20*, 8–17.
16. (a) L. S. Kaanumalle, C. L. D. Gibb, B. C. Gibb, V. Ramamurthy, *J. Am. Chem. Soc.* **2005**, *127*, 3674–3675. (b) T. Hayashi, N. Mataga, Y. Sakata, S. Misumi, M. Morita, J. Tanaka, *J. Am. Chem. Soc.* **1976**, *76*, 5910–5913.
17. Z. Lin, S. Priyadarshy, A. Bartko, D. H. Waldeck, *J. Photochem. Photobiol. A Chem.* **1997**, *110*, 131–139.

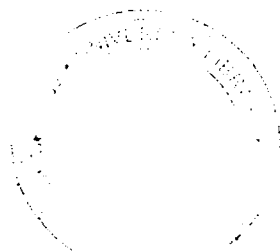
18. J. R. Lakowicz, *Principles of Fluorescence Spectroscopy*, Kluwer Academic/ Plenum Publishers, New York, **1996**.
19. (a) *Organic Light Emitting Devices: Synthesis, Properties and Applications*; K. Mullen, U. Scherf, (Eds.), Wiley-VCH, Weinheim, Germany, **2006**. (b) S. M. Kelly, M. O'Neill, In *Handbook of Advanced Electronic and Photonic Materials*; H. S. Nalwa, (Ed.), Academic Press, San Diego, CA, **2000**.
20. Gaussian 03 (Revision-D.01), M. J. Frisch, G. W. Trucks, H. B. Schlegel, G. E. Scuseria, M. A. Robb, J. R. Cheeseman, J. A. Montgomery, Jr., T. Vreven, K. N. Kudin, J. C. Burant, J. M. Millam, S. S. Iyengar, J. Tomasi, V. Barone, B. Mennucci, M. Cossi, G. Scalmani, N. Rega, G. A. Petersson, H. Nakatsuji, M. Hada, M. Ehara, K. Toyota, R. Fukuda, J. Hasegawa, M. Ishida, T. Nakajima, Y. Honda, O. Kitao, H. Nakai, M. Klene, X. Li, J. E. Knox, H. P. Hratchian, J. B. Cross, C. Adamo, J. Jaramillo, R. Gomperts, R. E. Stratmann, O. Yazyev, A. J. Austin, R. Cammi, C. Pomelli, J. W. Ochterski, P. Y. Ayala, K. Morokuma, G. A. Voth, P. Salvador, J. J. Dannenberg, V. G. Zakrzewski, S. Dapprich, A. D. Daniels, M. C. Strain, O. Farkas, D. K. Malick, A. D. Rabuck, K. Raghavachari, J. B. Foresman, J. V. Ortiz, Q. Cui, A. G. Baboul, S.

- Clifford, J. Cioslowski, B. B. Stefanov, G. Liu, A. Liashenko, P. Piskorz, I. Komaromi, R. L. Martin, D. J. Fox, T. Keith, M. A. Al-Laham, C. Y. Peng, A. Nanayakkara, M. Challacombe, P. M. W. Gill, B. Johnson, W. Chen, M. W. Wong, C. Gonzalez, and J. A. Pople, Gaussian, Inc., Pittsburgh, PA, **2003**.
21. N. J. Turro, *Modern Molecular Photochemistry*; The Benjamin Cummings publishing Co., Inc. **1978**.
22. G. Zhang, G. Yang, S. Wang, Q. Chen, J. S. Ma, *Chem. Eur. J.* **2007**, *13*, 3630–3635.
23. X-ray analysis was carried out at Sophisticated Analytical Instrument Facility, Indian Institute of Technology Madras, Chennai, India.
24. (a) R. R. Avirah, K. Jyothish, D. Ramaiah, *J. Org. Chem.* **2008**, *73*, 274–279. (b) M. Hariharan, P. P. Neelakandan, D. Ramaiah, *J. Phys. Chem. B* **2007**, *111*, 11940–11947. (c) K. Jyothish, M. Hariharan, D. Ramaiah, *Chem. Eur. J.* **2007**, *13*, 5944–5951.
25. (a) E. Kuruvilla, D. Ramaiah, *J. Phys. Chem. B* **2007**, *111*, 6549–6556. (b) V. S. Jisha, K. T. Arun, M. Hariharan, D. Ramaiah, *J. Am. Chem. Soc.* **2006**, *128*, 6024–6025.

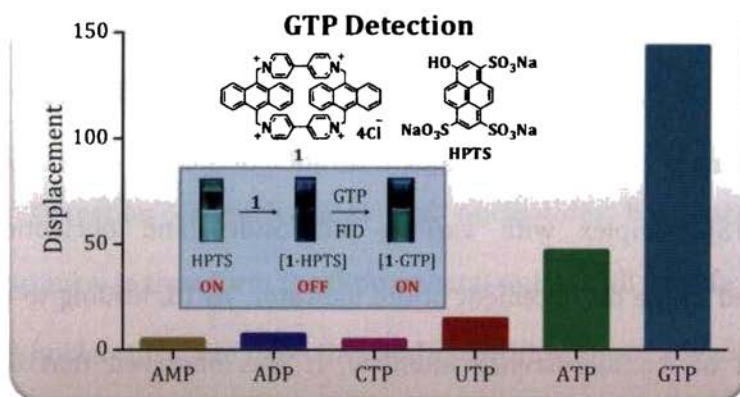
7269

Design of Novel Cyclophanes

26. A. R. Roshal, J. A. Organero, A. Douhal, *Chem. Phys. Lett.* **2003**, 379, 53-59.
27. B. Altava, M. I. Burguete, B. Escuder, S. V. Luis, *Tetrahedron*, **1997**, 53, 2629-2640.
28. S. Icli, S. Demica, B. Dindar, A. O. Doroshenko, C. Timur, *J. Photochem. Photobiol. A Chem.* **2000**, 136, 15-24.



3 BIOMOLECULAR RECOGNITION: INVESTIGATION OF INTERACTIONS OF A FEW CYCLOPHANES WITH NUCLEOTIDES



3.1. ABSTRACT

With the objective of developing sensitive fluorescence based probes for biomolecules, we have investigated the interactions of a few selected cyclophanes with nucleosides and nucleotides. The addition of ATP or GTP to a solution of the cyclophane **1** in buffer resulted in decrease in its absorbance at 375 nm as compared to the model derivative **4**. In contrast, negligible changes were observed with the addition of ADP, AMP, GDP, GMP, adenosine, guanosine and

phosphate, indicating thereby that the cyclophane **1** undergoes selective interactions only with nucleotide triphosphates with association constants in the order of 10^3 M^{-1} . The cyclophane **1** was further found to undergo efficient interactions with the fluorescence indicator, 8-hydroxy-1,3,6-pyrene trisulfonate (HPTS) resulting in 25% hypochromicity along with complete fluorescence quenching of HPTS. The subsequent titration of this non-fluorescent [1·HPTS] complex with various nucleosides and nucleotides resulted in the displacement of the indicator, HPTS, leading to the revival of its fluorescence intensity. It was observed that GTP induced the maximum displacement with an overall emission enhancement of *ca.* 150-fold, whereas *ca.* 45-fold increase was observed with ATP.

The selectivity towards GTP has been attributed to the presence of a better π -electron cloud which facilitates effective electronic, π -stacking and electrostatic interactions inside the cavity of the cyclophane **1**. The cyclophane **2**, having only one anthracene moiety, behaved similarly, but showed less sensitivity for GTP as compared to **1**. In contrast, the cyclophane **3**, exhibited efficient interactions with the indicator, HPTS, but was found to be

inefficient as a receptor for nucleotides because of the large cavity size. These results confirm the importance of the cavity size and aromatic surface in the molecular recognition ability of the cyclophanes and demonstrate the potential of the cyclophane **1** as a probe for the detection of GTP and ATP in buffer and bio-fluids.

3.2. INTRODUCTION

Detection of nucleosides and nucleotides has paramount importance as they form the fundamental units of all the life forms.¹ Of all nucleotides, the detection and quantification of adenosine 5'-triphosphate (ATP) and guanosine 5'-triphosphate (GTP) (Chart 3.1) is vital from the view point of clinical diagnosis, taking into account the fact that these nucleoside 5'-triphosphates play important roles in various biological processes.² GTP is required for many biological activities in the cell, such as synthesis of DNA, RNA,

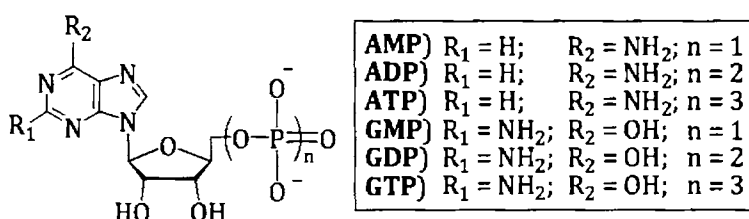


Chart 3.1

and proteins, nutrient metabolism, and cell signaling. It is well established that GTP-binding proteins play diverse roles as switches in cell growth, receptor activation, exocytosis, ion channel conductivity and change in cell shape.^{2a} Moreover, the cascade of reactions initiated through the recognition of GTP by G-proteins regulates the stress factor.

ATP, on the other hand, is known as the biological energy currency and the binding of ATP by proteins is one of the most prominent molecular recognition events in nature. ATP also plays an important role in energy transduction in organisms and controls several metabolic processes, including synthesis of cyclic adenosine monophosphate. The abnormalities in the concentrations of ATP and GTP in the body due to the defect of purine salvage enzymes, particularly, adenosine phosphoribosyl transferase (APRTase) and hypoxanthine phosphoribosyl transferase (HPRTase), result in severe combined immunodeficiency disorder (SCID) and Lesch-Nyhan syndrome (brain gout), respectively.

The development of molecular systems capable of recognizing GTP and ATP under physiological pH and biological conditions therefore can have potential applications in basic research as well

as in medicinal and diagnostic applications. In this context, design of fluorescent probes and methods to distinguish between various nucleotides, in particular GTP and ATP, is gaining importance.^{4,5} Of the reported molecular receptors, most use complementary hydrogen bonding for their recognition. Such molecular recognition in the aqueous medium would be limited due to the competitive hydrogen bonding of the solvent.⁶ Moreover, the sugar moiety of the nucleosides and nucleotides can interfere in such recognition and hence masking of the hydroxyl groups, prior to the recognition event is essential.⁷

Progress in this area would require new strategies for the complexation under physiological pH conditions and subsequent signaling of the host-guest complex formation. Of the various outputs, the optical methods offer several advantages for studying complexation process and fluorescence based techniques are particularly important for biological applications because of their high sensitivity. In this context, it was of our interest to develop novel cyclophane based systems as probes for nucleosides and nucleotides. These systems are associated with a high degree of structural rigidity and well defined cavity and hence these systems

can encapsulate and stabilize guest molecules through non-covalent interactions.⁸⁻¹⁰ We have selected a few cyclophanes **1-3** (Chart 3.2) and investigated their interactions with various nucleosides and nucleotides under different conditions through photophysical, chiroptical and biophysical techniques. Our results indicate that the cavity size and aromatic surface of the cyclophane play a major role in their biomolecular recognition. Of all the systems, the cyclophane **1** interacts selectively with GTP and ATP and also in presence of other analytes and signals the event through a 'turn on' fluorescence mechanism in buffer and biofluids.

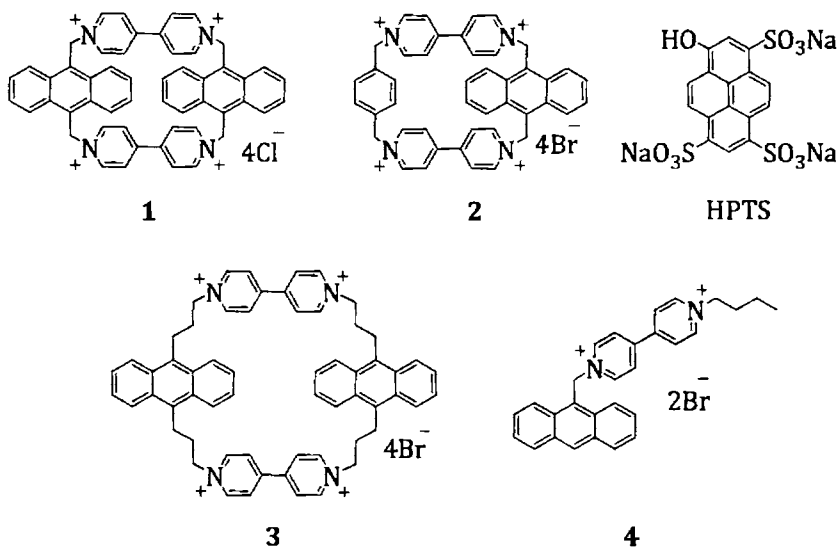


Chart 3.2

3.3. RESULTS

3.3.1. Interaction with Nucleotides

The synthesis of the cyclophanes **1-3**, under investigation as well as the model compound **4**, has been achieved as per the procedure described in Chapter 2 of this thesis. To investigate the biomolecular recognition ability, we have monitored the changes in the absorption and emission spectra of these derivatives with the addition of various nucleosides and nucleotides.¹¹ Addition of adenosine 5'-triphosphate (ATP) to a solution of the cyclophane **1** showed a gradual decrease in the absorbance corresponding to the anthracene chromophore (Figure 3.1). At 0.5 mM of ATP, we

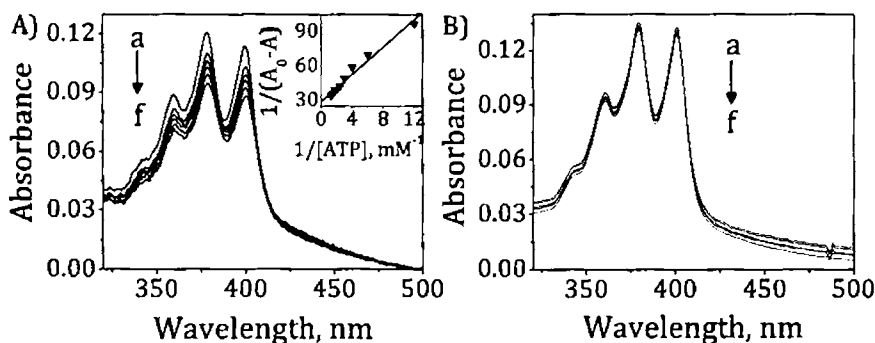


Figure 3.1. Changes in the absorption spectra of the cyclophane **1** (11 μM) with the successive addition of (A) ATP and (B) adenosine in phosphate buffer (10 mM, pH 7.4). [Ligand], (a) 0 and (f) 500 μM . Inset shows Benesi-Hildebrand plot for the binding of ATP with **1**.

observed 23% hypochromicity in the absorption spectrum of the cyclophane **1**, whereas 27% hypochromicity was observed with guanosine 5'-triphosphate (GTP) under identical conditions. Similarly, the addition of ATP to the cyclophanes **2** and **3** resulted in 15% and 17% hypochromicity, respectively (Figure 3.2), whereas

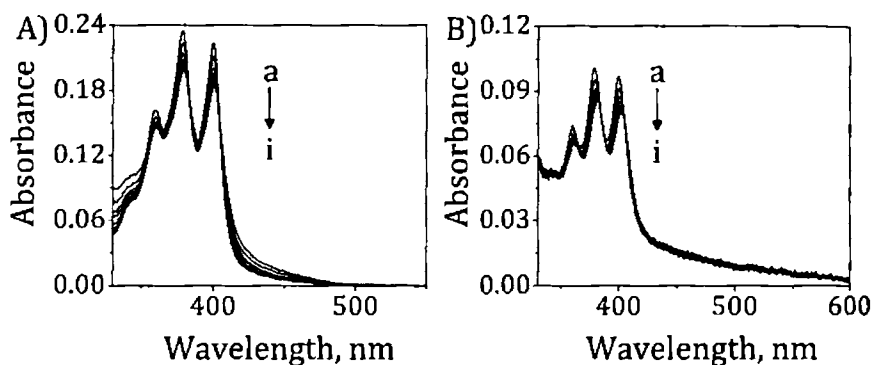


Figure 3.2. Changes in the absorption spectra of the cyclophanes (A) **2** (21 μM) and (B) **3** (17 μM) with the addition of ATP in 10 mM phosphate buffer and 20% DMSO-water mixture, respectively. [ATP], (a) 0 and (i) 625 μM. Excitation wavelength, 385 nm.

negligible changes were observed in the absorption spectrum of the model derivative **4** under identical conditions. The emission spectra of the cyclophanes **1-4**, on the other hand, exhibited negligible changes with the addition of both ATP and GTP. Benesi-Hildebrand analysis¹² of the absorption changes (inset of Figure 3.1A) showed a 1:1 stoichiometry for the complex formed between **1** and ATP with

a binding constant of $K_{\text{ass}} = 4040 \pm 140 \text{ M}^{-1}$ in buffer, while relatively a higher value of $K_{\text{ass}} = 4900 \pm 200 \text{ M}^{-1}$ was observed for GTP under identical conditions.

The addition of other guest molecules such as phosphate, pyrophosphate, adenosine, adenosine 5'-monophosphate (AMP), adenosine 5'-diphosphate (ADP), guanosine 5'-monophosphate (GMP) and guanosine 5'-diphosphate (GDP) resulted in negligible changes in the absorption and emission spectra of the cyclophane **1** (Figure 3.1B). Figure 3.3 shows the relative changes in the absorbance of the cyclophanes **1** and **3** as a function of concentration of various ligands. It is evident from Figure 3.3A that the cyclophane **1** shows selectivity towards GTP and ATP, whereas all other ligands have negligible influence on its absorption spectra.

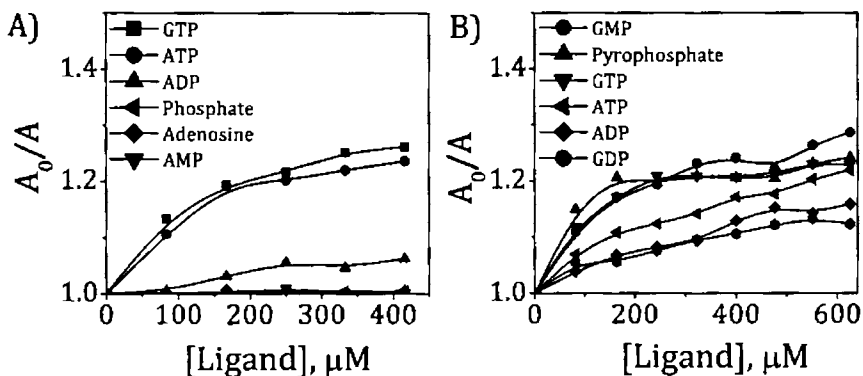


Figure 3.3. Relative changes in the absorbance of the cyclophanes (A) **1** (11 μM) and (B) **3** (17 μM) in the presence of various analytes.

In contrast, the addition of various nucleosides and nucleotides to the solution of the cyclophane **3** resulted in almost similar hypochromicity in its absorption spectrum, indicating thereby that its utility as a selective receptor is limited (Figure 3.3B).

3.3.2. Nature of Host-Guest Complexation

The complexation between the cyclophane **1** and ATP was further analyzed through cyclic voltammetry and NMR techniques. Figure 3.4 shows the differential pulse voltammograms (DPV) of the cyclophane **1** (0.2 mM) in the aqueous medium, which exhibited two reversible one-electron reduction processes centered at -0.50 and

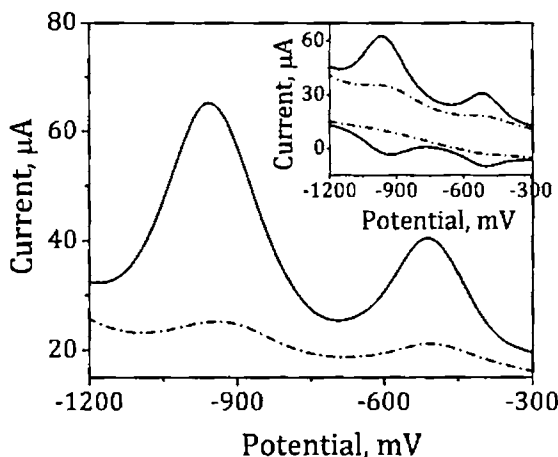


Figure 3.4. The differential pulse and square wave voltammograms (inset) of the cyclophane **1** (0.2 mM) in the (—) absence and (- - -) presence of ATP (1.3 μ M) in the aqueous medium.

-0.96 V, characteristic of the viologen moiety.¹³ When ATP (1.3 μM) was added, we observed a shift of reduction potentials by 16 and 8 mV, along with a significant decrease in current intensity of 40.04 μA (61%) and 19.33 μA (48%), confirming thereby the formation a stable complex between the cyclophane **1** and ATP. Similarly, in the ^1H NMR spectrum, the successive addition of ATP to a solution of the cyclophane **1** in D_2O resulted in broadening of protons of the methylene group, whereas the protons corresponding to the viologen moiety experienced an up-field shift of δ 0.03 ppm at 0.35 mM of ATP (Figure 3.5). Based on NMR titration data, the binding constant was determined ($K_{\text{ass}} = 4700 \pm 200 \text{ M}^{-1}$), which is in good agreement with that obtained through the absorption spectroscopy.

To understand the nature and strength of the complex formed between the cyclophane **1** and ATP, we investigated the effects of

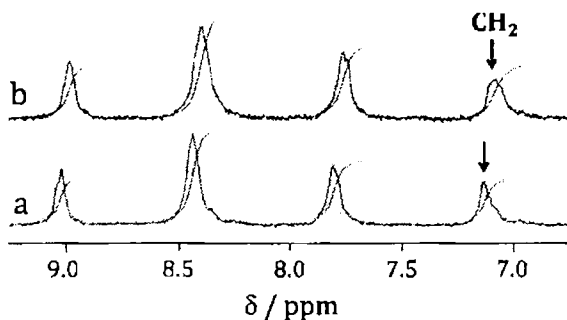


Figure 3.5. ^1H NMR spectra of the cyclophane **1** in D_2O in the (a) absence and (b) presence of ATP (0.35 mM).

ionic strength and temperature. As the salt concentration was increased gradually, the changes in the absorption spectrum of **1** induced by ATP were found to be less prominent (Figure 3.6). The values of K_{ass} at different ionic strengths were determined and are found to be 3558, 222 and 137 M^{-1} at 2, 50 and 500 mM of NaCl, respectively. The decrease in K_{ass} values with increase in ionic strength indicates that the viologen unit of **1** is shielded by Na^+ ions at higher ionic strength of the buffer from the phosphate groups of ATP,¹⁴ resulting less significant interactions between the cyclophane **1** and ATP. When the temperature of the complex [**1**·ATP] was

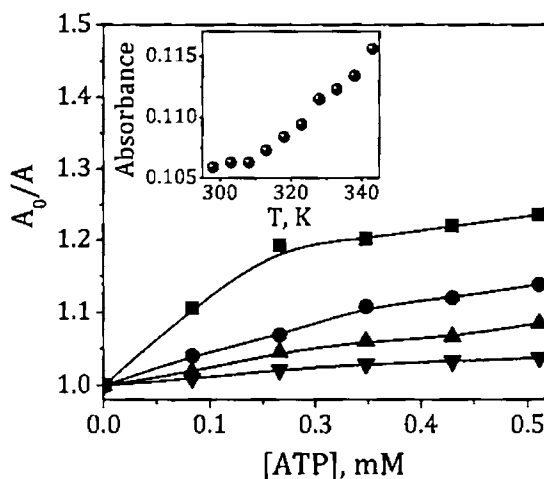


Figure 3.6. Relative changes in the absorbance of the cyclophane **1** with the addition of ATP in 10 mM phosphate buffer (pH 7.4) containing (■) 0, (●) 2, (▲) 50 and (▼) 500 mM of NaCl. Inset shows the effect of temperature on the absorbance of complex [**1**·ATP] from 298 to 343 K.

raised from 293 to 343 K, we observed an increase in the intensity of absorbance corresponding to the cyclophane **1** at 378 nm (inset of Figure 3.6), indicating the dissociation of the complex. However, the complex showed 19% hypochromicity at 343 K, indicating the stability of the complex even at this temperature.

3.3.3. Recognition of Nucleotides Through FID Assay

Eventhough the cyclophane **1** showed selectivity towards GTP and ATP in buffer and signaled the event through changes in the absorption spectroscopy, its utility as a sensitive probe was limited due to its negligible fluorescence yields ($\Phi_F = 0.0007$). By making use of the beneficial non-fluorescent and selective binding properties of the receptor **1**, it was of our interest to exploit its potential use as a probe for nucleotides through fluorescent indicator displacement (FID) assay. In this context, we have utilized a highly fluorescent indicator, 8-hydroxy-1,3,6-pyrene trisulfonate (HPTS; $\Phi_F = 0.7$). As described in the first Chapter of this thesis (Section 1.4),¹⁵ the FID assay involves first the reversible binding of a fluorescence indicator with a receptor followed by a competitive binding of analyte with the receptor resulting in the displacement of

the fluorescence indicator. Based on this principle, the major requirement is that the affinity between the indicator and the receptor be comparable to that between the analyte and the receptor.

The successive additions of the receptor **1** to a solution of HPTS in buffer resulted in a regular decrease in the absorbance and quenching of the fluorescence intensity of HPTS centered at 512 nm (Figure 3.7). At *ca.* 6.25 μM of the cyclophane **1**, we observed 25% hypochromicity in the absorption spectrum of HPTS along with the quantitative fluorescence quenching (99%). In contrast, the addition

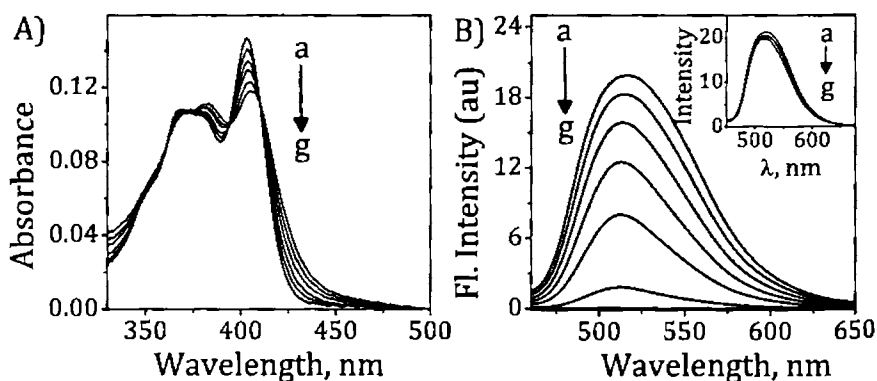


Figure 3.7. Changes in the (A) absorption and (B) fluorescence spectra of HPTS (7 μM) with addition of the cyclophane **1** in phosphate buffer (pH 7.4). Inset of (B) shows the corresponding fluorescence changes with the addition of the model compound **4** in buffer (pH 7.4). [**1** or **4**], (a) 0 and (g) 6.25 μM . Excitation wavelength, 364 nm.

of the model compound **4** resulted in only negligible changes in the absorption and fluorescence properties as shown in the inset of Figure 3.7B. Similarly, we have carried out the titrations of the cyclophanes **2** and **3** with HPTS under similar conditions (Figure 3.8). While the addition of the cyclophane **2** resulted in significant hypochromicity in the absorption spectrum and complete quenching of the fluorescence of HPTS, the cyclophane **3** showed less significant changes.

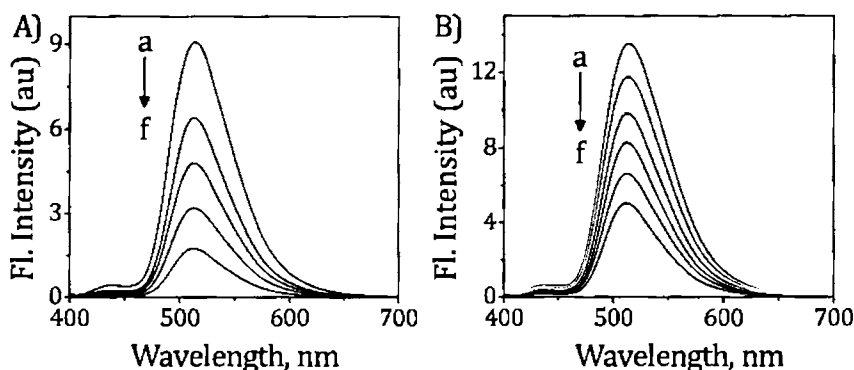


Figure 3.8. Changes in the fluorescence spectra of HPTS with the gradual addition of the cyclophanes (A) **2** in buffer (10 mM phosphate, pH 7.4) and (B) **3** in 20% DMSO-water. [**2** or **3**], (a) 0 and (f) 11.3 μM . Excitation wavelength, 364 nm.

The changes in the optical properties of HPTS in the presence of the cyclophanes **1-3** are indicative of the formation of a stable complex. Benesi-Hildebrand analysis of the emission data gave a 1:1

stoichiometry for the complex [1·HPTS], with an association constant (K_{ass}) of $4.66 \pm 0.2 \times 10^4 \text{ M}^{-1}$ and change in free energy of -27 kJ mol^{-1} in buffer, while a higher value of $K_{\text{ass}} = 6.56 \pm 0.3 \times 10^4 \text{ M}^{-1}$ was obtained in the aqueous medium. The complexation between the cyclophane **1** and HPTS was further analyzed by picosecond time-resolved fluorescence analysis and NMR techniques. HPTS alone exhibited a single exponential fluorescence decay with a lifetime of 5.3 ns (Figure 3.9),¹⁶ whereas a biexponential decay with lifetimes of 215 ps (70%) and 6.2 ns (30%) was observed in the presence of the cyclophane **1**. Similarly, the successive additions of the cyclophane **1** to a solution of HPTS in

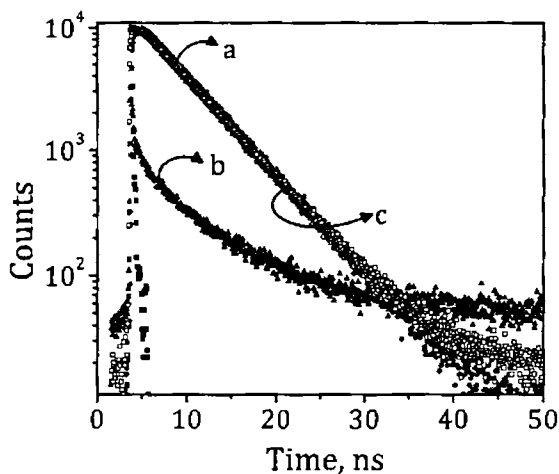


Figure 3.9. Fluorescence decay profiles of (a) HPTS, (b) complex [1·HPTS] and (c) complex [1·HPTS] in the presence of GTP.

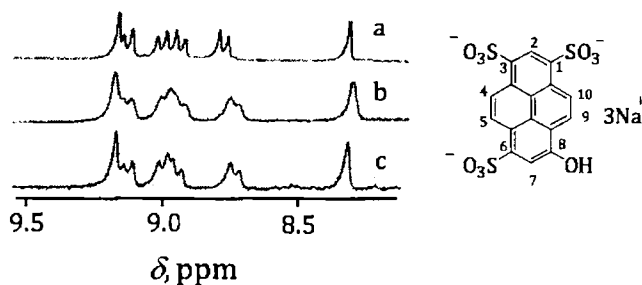


Figure 3.10. ^1H NMR spectra in D_2O of (a) HPTS alone, (b) complex $[1\cdot\text{HPTS}]$ and (c) $[1\cdot\text{HPTS}]$ in presence of GTP.

D_2O resulted in broadening of the peaks corresponding to H_4 , H_5 , H_9 and H_{10} protons of HPTS in its ^1H NMR spectrum (Figure 3.10).

To understand the nature and strength of the complex formed between the cyclophanes 1-3 and HPTS, we have investigated the effects of ionic strength and temperature on the complexation process (Figure 3.11). For example, the quenching of emission of HPTS by the cyclophane 1 was found to be less prominent as we increase in ionic strength of the buffer. We obtained a lower value of $K_{\text{ass}} = 1.9 \times 10^4 \text{ M}^{-1}$ at higher ionic strengths (500 mM), indicating thereby that the viologen units of the cyclophane 1 are shielded from the sulfonate groups of HPTS by Na^+ ions, resulting in less favorable interactions between the cyclophane 1 and HPTS. Moreover, when the temperature of the complex $[1\cdot\text{HPTS}]$ was raised from 293 to 358 K, we observed a regular increase in the

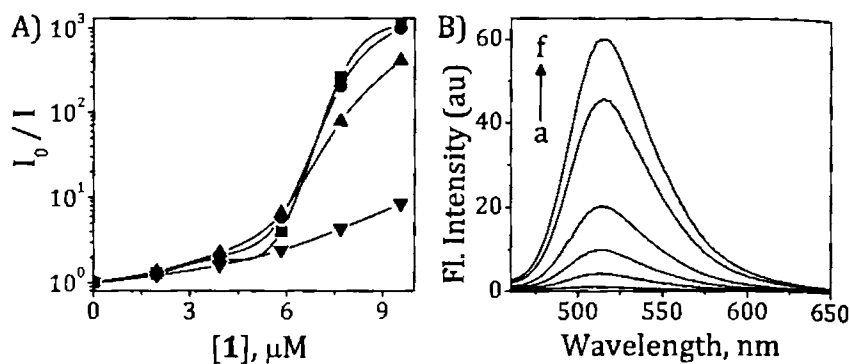


Figure 3.11. (A) The relative fluorescence quenching of HPTS by the cyclophane **1** in 10 mM phosphate buffer (pH 7.4) containing (■) 0, (●) 2, (▲) 50 and (▼) 500 mM NaCl. (B) Effect of temperature on the emission spectra of complex $[1\cdot\text{HPTS}]$. (a) 293 and (f) 358 K. Excitation wavelength, 364 nm.

emission intensity of HPTS, indicating a gradual dissociation of the complex at these temperatures.

Similarly, when the emission of the complex $[2\cdot\text{HPTS}]$ was recorded as a function of temperature, we observed a regular increase in the emission intensity of HPTS at higher temperatures due to the dissociation of the complex. In contrast, when the temperature of a mixture of the cyclophane **3** and HPTS was raised from 293 to 358 K, we observed negligible changes in the emission spectrum (Figure 3.12). The negligible effect of temperature on the emission spectrum of a mixture of **3** and HPTS strongly suggests that **3** is unable to form a stable complex with HPTS.

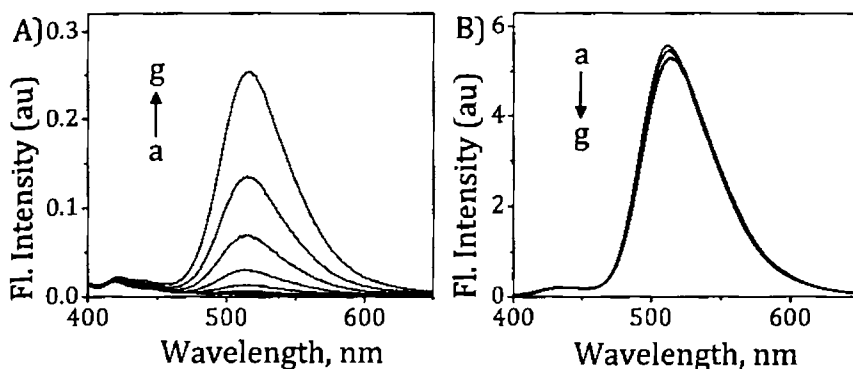


Figure 3.12. Effect of temperature on the emission spectra of (A) the complex [2.HPTS] and (B) a mixture of the cyclophane **3** and HPTS. (a) 293 to (g) 358 K. Excitation wavelength, 364 nm.

The beneficial competitiveness of the assay is demonstrated by comparing the efficiency of fluorescence indicator displacement (FID) by various nucleotides and nucleosides. Figure 3.13 shows regular release of HPTS from the complex [1·HPTS] by gradual addition of GTP. The successive additions resulted in a regular enhancement in fluorescence intensity corresponding to HPTS at 512 nm. In buffer, *ca.* 150-fold enhancement was observed at 1.6 mM of GTP, which led to the visual detection of GTP through “turn on” fluorescence intensity. In contrast, addition of adenosine, AMP, ADP, CTP and UTP showed negligible changes, whereas *ca.* 45 and 50-fold enhancement was observed with ATP and ITP, respectively (Figure 3.14). Similarly, the utility of the cyclophanes **2**

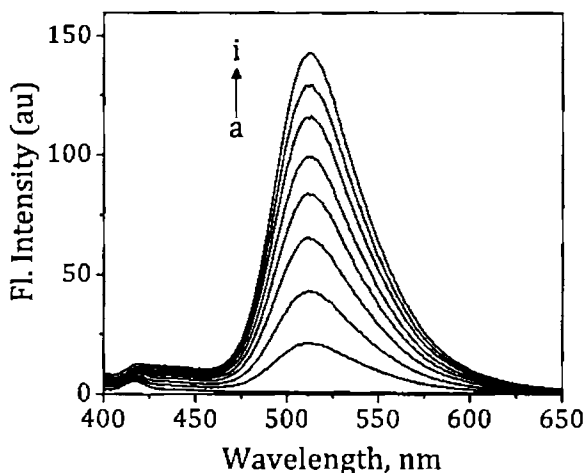


Figure 3.13. Fluorescence indicator displacement (FID) from the complex [1-HPTS] by GTP in buffer. [GTP], (a) 0 and (i) 1.6 mM. Excitation wavelength, 364 nm.

and **3** as receptors for nucleotides was investigated through FID assay. Figure 3.15 shows the changes in the emission spectra of a mixture of the cyclophanes **2** or **3** and HPTS with the addition of GTP. The successive additions of GTP to a solution of [2.HPTS] resulted in regular enhancement in the fluorescence of HPTS at 512 nm. At ca. 1.6 mM of GTP, we observed a net fluorescence enhancement of ca. 73-fold as compared to ca. 150-fold enhancement observed with the cyclophane **1**. The titrations carried out with the cyclophane **3**, on the other hand, resulted in contrasting results as compared to the cyclophanes **1** and **2**. When GTP was successively added to a solution of a mixture of HPTS and

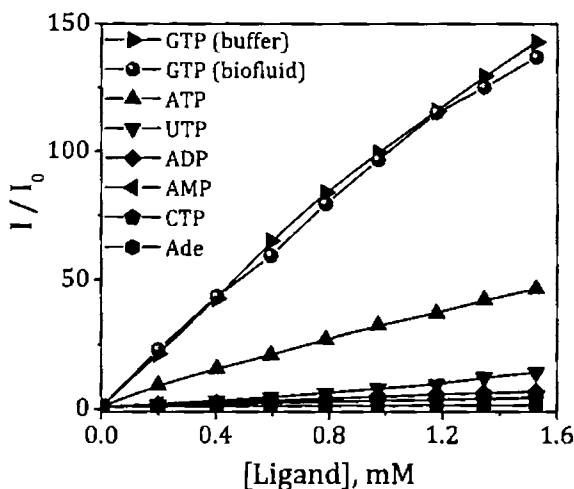


Figure 3.14. Relative concentration dependent FID efficiency by various analytes.

the cyclophane **3**, we observed negligible displacement of HPTS and showed non-negligible quenching in the fluorescence intensity of HPTS (Figure 3.15B).

To further demonstrate the selectivity of the FID assay, it was tested in the presence of other nucleotides and also in biological fluids. Even in the presence of various nucleotides, the complex [1.HPTS] exhibited selectivity towards GTP. Similarly, in biological fluids, we observed *ca.* 140-fold enhancement in fluorescence intensity, which is comparable to the results obtained in the buffer medium (Figure 3.14). The displacement of HPTS from the complex [1.HPTS] was confirmed by time-resolved fluorescence and NMR

techniques. When GTP was added to the complex [1·HPTS], we observed a biexponential decay having lifetimes 5.4 ns (98%) and 9.6 ns (2%) (Figure 3.9). The former lifetime has been attributed to the free HPTS in solution. Similarly, ^1H NMR spectrum of free HPTS was almost completely revived when GTP was added, thereby confirming the quantitative displacement of the indicator, HPTS from the complex (spectrum 'c' in Figure 3.10).

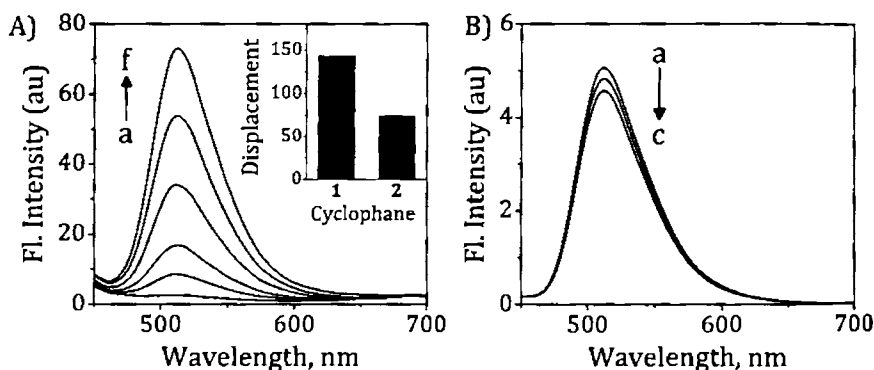


Figure 3.15. (A) FID from the complex [2.HPTS] by GTP in phosphate buffer (10 mM, pH 7.4). Inset shows the displacement of HPTS from [1.HPTS] and [2.HPTS] by GTP. (B) Changes in the emission spectrum of a mixture of **3** and HPTS with the addition of GTP. [GTP], (a) 0 and (c) 1.6 mM. Excitation wavelength, 364 nm.

3.4. DISCUSSION

The optimized geometries obtained through B3LYP level theoretical calculations¹⁷ revealed interplanar distances of 10.4, 9.9

and 13.9 Å between the two aromatic units for the cyclophanes **1-3**, respectively (Figure 3.16). In comparison to the cyclophane **1**, the replacement of one of the anthracene moieties by a phenyl unit in **2** results in a cavity having a lesser aromatic surface. On the other hand, cyclophane **3** having three methylene groups has a cavity with large dimensions. These variations in the cavity size could be correlated directly to the behavior of these derivatives towards various guest molecules like nucleotides and HPTS.

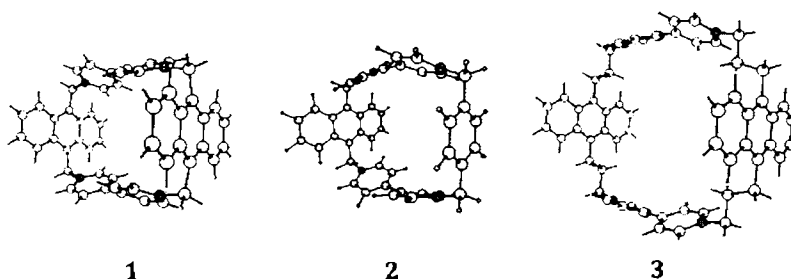


Figure 3.16. Optimized geometries of the cyclophanes **1 – 3**.

Based on our experimental evidence, the binding of ATP or GTP to the cyclophanes **1-3** is a result of π - π stacking in combination with electrostatic interactions inside the cavity as shown in Figure 3.17. The attraction between the phosphate groups of nucleotides and the viologen moiety of the cyclophane **1** involving multiple electrostatic interactions result in the formation of a tight complex,

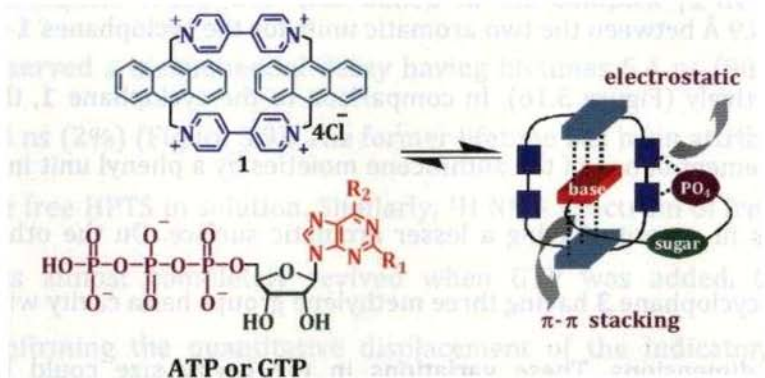


Figure 3.17. Schematic representation of the 1:1 complex formation between the cyclophane **1** and ATP or GTP.

which is further stabilized by π - π stacking of the nucleobase inside the cavity. The presence of a cavity in the molecular system **1** as well as three phosphate groups in ATP or GTP are very essential for the selective recognition and for the formation of a stable 1:1 complex, as evidenced from the negative results obtained with the model system **4** and with various other guest molecules.¹⁸ Evidence for this comes from the fact that the cyclophane **1** exhibits non-negligible interactions with ADP, containing two phosphate groups, while no binding interactions were observed with AMP, adenosine and phosphate.

This mode of complexation was further confirmed by making use of the Debye-Huckel ionic strength function¹⁹ of the medium on

the K_{ass} values and the thermodynamic parameters such as ΔH° and ΔS° ($-11.15 \text{ kJmol}^{-1}$ and $-37.41 \text{ JK}^{-1}\text{mol}^{-1}$), obtained using Van't Hoff's plot²⁰ (Figures 3.18-3.19). Thermodynamic parameters obtained are consistent with the expected non-classical hydrophobic interactions usually observed in the case of the cyclophane systems.^{10a} As a consequence of the complex formation between **1** and ATP, (i) current intensity decreases as observed in the differential pulse and square wave voltammograms,²¹ (ii) shielding of protons of the viologen moiety occurs due to the interactions with the phosphate groups, (iii) broadening of signals corresponding to the methylene

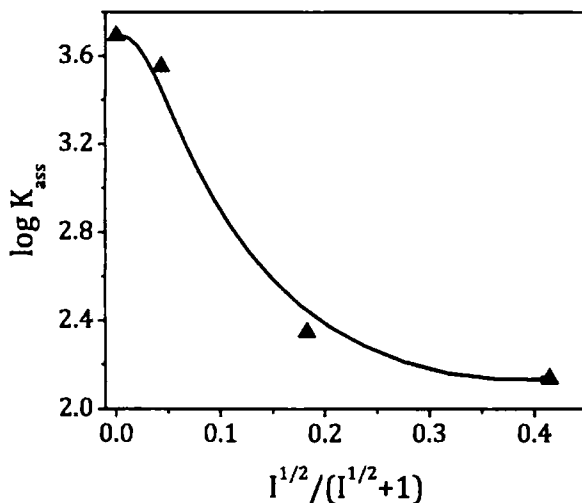


Figure 3.18. Effect of Debye-Huckel ionic strength function of the medium on the association constants for the complex $[\mathbf{1}\cdot\text{ATP}]$ in 10 mM phosphate buffer (pH 7.4) under various salt concentrations. [NaCl] (a) 0, (b) 2, (c) 50 and (d) 500 mM.

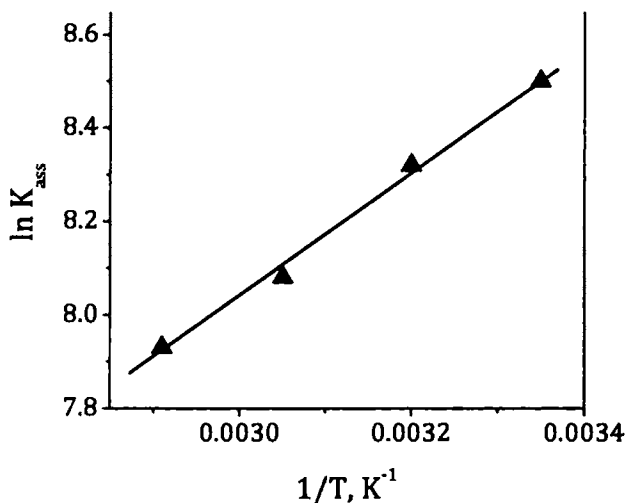


Figure 3.19. Van't Hoff plot of the association constants (K_{ass}) for the complex [1·ATP] at different temperatures (T), (a) 298, (b) 313, (c) 328 and (d) 343 K.

protons is observed because of π -stacking of the aromatic part of ATP, and (iv) decrease in entropy (ΔS°) is observed due to the formation of an ordered complex through non-classical hydrophobic interactions.

As observed with ATP and GTP, the fluorescence indicator, HPTS undergoes efficient complexation with the receptor **1** resulting in complete quenching of its fluorescence. The mechanism of the quenching is due to photoinduced electron transfer process from the excited state of HPTS to the viologen moiety as characterized through experimental evidence and the theoretically

calculated favorable change in free energy ($\Delta G = -1.7$ eV).²² The driving force for such a complexation is attributed to the synergistic effects of π -stacking and electrostatic interactions inside the cavity. This was confirmed by the sigmoidal nature of the relative fluorescence quenching curves obtained at different ionic strengths and the effect of temperature and negative results obtained with the model system 4.

A schematic representation of the selective recognition of GTP by [1.HPTS] and [2.HPTS] is shown in Figure 3.20. In the competitive displacement assay, the fluorescent indicator, HPTS, is successfully displaced from the complex [1·HPTS] by nucleotides and nucleosides. Interestingly, GTP induced maximum displacement resulting in net fluorescence enhancement of *ca.* 150-fold leading to visual changes in fluorescence (Figure 3.21). The time-resolved

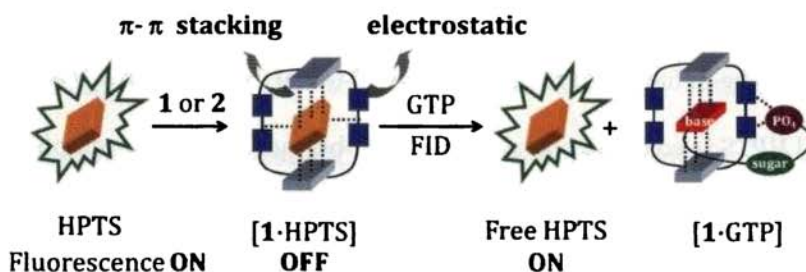


Figure 3.20. Schematic representation of GTP recognition through fluorescence indicator displacement assay (FID).

fluorescence analysis and revival of the original ^1H NMR spectrum of HPTS confirms the quantitative displacement of HPTS from the complex by GTP. The competitive displacement of the indicator, HPTS by various analytes is found to be in the order $\text{GTP (buffer)} \approx \text{GTP (biofluid)} \gg \text{ITP} \approx \text{ATP} > \text{UTP} > \text{CTP} \approx \text{ADP} \approx \text{AMP} \approx \text{Ade}$. By virtue of having a better π -electron cloud and low ionization potential, GTP unusually exhibits better complexing ability with the receptor **1** through synergistic effects of electronic, π -stacking and electrostatic interactions inside the cavity.



Figure 3.21. Visual observation of fluorescence intensity of (a) HPTS alone, (b) complex $[\mathbf{1}\cdot\text{HPTS}]$ and (c) to (f) $[\mathbf{1}\cdot\text{HPTS}]$ in presence of CTP, ATP, GTP (buffer) and GTP (bio-fluid), respectively.

The behavior of the cyclophane **2** towards various nucleotides and HPTS is comparable to the results obtained with the cyclophane **1**, but with lesser sensitivity. In this case, *ca.* 73-fold fluorescence enhancement was observed upon addition of GTP to the complex $[\mathbf{2}\cdot\text{HPTS}]$. Based on our experimental evidence, the observation of

relatively lesser sensitivity for **2** in comparison to **1** can be attributed to the presence of a cavity with lesser aromatic surface. The cyclophane **2** with lesser aromatic surface in the cavity undergoes not so strong π stacking and hydrophobic interactions as compared to the cyclophane **1**. Because of these weak interactions, a less favorable complex between **2** and GTP will be formed and as a result lesser displacement of HPTS occurs from [2.HPTS] by GTP.

The contrasting results obtained with the cyclophane **3**, containing a flexible spacer group with a larger cavity, are indeed interesting, although not completely unexpected. Moreover, it helps to confirm the role played by cavity size in the molecular recognition process.²³ The negligible interactions exhibited by the cyclophane **3** with various guest molecules such as nucleotides and nucleosides indicate that the cyclophane **3** is unable to form a stable complex with these analytes. Eventhough the fluorescence quenching of HPTS by the cyclophane **3** is an indicative of complexation, the investigation of the effect of temperature on their interaction shows that the quenching may be attributed to an outside stacking mechanism involving electrostatic interactions between the viologen moiety of the cyclophane **3** and HPTS.^{22,24}

The investigation of the effect of temperature on fluorescence of a mixture of the cyclophane **3** and HPTS substantiates our hypothesis. Moreover, if a complex is formed between the cyclophane **3** and HPTS, the addition of GTP should, in principle, result in the displacement of HPTS leading to an enhancement in the emission of HPTS. In contrast, we observed non-negligible quenching of the fluorescence of HPTS with the addition of GTP. This observation confirms the fact that the cyclophane **3** is unable to form a stable complex with the fluorescent indicator, HPTS. The inability of the cyclophane **3** in selectively recognizing any of the guest molecules could be attributed to the presence of a larger cavity, which in turn is not favorable for the formation of a tightly packed complex involving various non-covalent interactions such as π -stacking and hydrophobic interactions.

3.5. CONCLUSIONS

In summary, we have investigated the biomolecular recognition properties of a series of selected novel cyclophane derivatives containing anthracene and viologen moieties wherein the cavity size was varied by changing the spacer groups as well as

the aromatic moiety. The cyclophane **1** acts as a selective probe for GTP and ATP through absorption spectroscopy. Subsequently, a highly sensitive and selective fluorescence assay was developed for GTP through the beneficial properties of the cyclophane **1** and the fluorescence indicator, HPTS. The uniqueness of this assay is that it successfully discriminates GTP from ATP, and other nucleotides and nucleosides through an "ON-OFF-ON" fluorescence mechanism with a visual change in fluorescence intensity.

The behavior of the cyclophane **2** towards various guest molecules is similar to that of the cyclophane **1**, but with lesser sensitivity, i.e. *ca.* 73-fold fluorescence enhancement was observed as against *ca.* 150-fold enhancement with the cyclophane **1** towards GTP through FID. On the other hand, the utility of the cyclophane **3** having a larger cavity as a receptor for nucleotides, nucleosides and HPTS is limited due to its larger cavity which leads to less favorable interactions with the guest molecules. These results are important in understanding the role of cavity size and aromatic surface in the biomolecular recognition and in the design of efficient receptors based on cyclophanes for nucleosides and nucleotides.

3.6. EXPERIMENTAL SECTION

3.6.1. General Techniques

The equipment and procedures for melting point determination and spectral recordings have been described elsewhere.²⁵ All melting points are uncorrected and were determined on a Mel-Temp II melting point apparatus. An Elico pH meter was used for pH measurements. ¹H and ¹³C NMR spectra were measured on a 300 MHz or 500 MHz Bruker advanced DPX spectrometer. HRMS were recorded on a JEOL mass spectrometer. The electronic absorption spectra were recorded on a Shimadzu UV-VIS-NIR spectrophotometer. Fluorescence spectra were recorded on a SPEX-Fluorolog F112X spectrofluorimeter. The fluorescence quantum yields were determined by using optically matched solutions. Quinine sulphate ($\Phi_f = 0.54$) in 0.1 N H₂SO₄ was used as the standard.²⁶ The quantum yields of fluorescence were calculated using the equation 3.1, where, A_s and A_u are the absorbance of

$$F_u = \frac{A_s F_u n_s^2}{A_u F_s n_u^2} F_s \quad (3.1)$$

standard and unknown, respectively. F_u and F_s are the areas of fluorescence peaks of the unknown and standard and n_s and n_u are the refractive indices of the standard and unknown solvents, respectively. Φ_s and Φ_u are the fluorescence quantum yields of the standard and unknown. Fluorescence lifetimes were measured using a IBH Picosecond single photon counting system. The fluorescence decay profiles were deconvoluted using IBH data station software V2.1, fitted with monoexponential decay and minimizing the χ^2 values of the fit to 1 ± 0.1 .

3.6.2. Materials

All nucleosides and nucleotides and the fluorescence indicator, HPTS, were purchased from Sigma-Aldrich and used as received. The synthesis of the cyclophane derivatives **1** - **3** and the model derivative **4** used in the present study was achieved as described in Chapter 2 of the present thesis.¹¹ Doubly distilled water was used for all the experiments. All experiments were carried out in 10 mM phosphate buffer (pH 7.4) containing 2 mM NaCl at room temperature (25 ± 1 °C), unless otherwise mentioned.

3.6.2. Measurement of GTP in biofluids²⁷

Fresh blood samples collected from healthy people were immediately treated with EDTA and centrifuged at 3000 rpm for 5 min. The supernatant was collected and divided into two portions. One of the portions was subjected to deproteinization by stirring with 20% trichloroacetic acid for 20 min. followed by centrifugation at 3000 rpm for 5 min. The supernatant was used for further studies after diluting 1000 times with water. The other portion (not subjected to deproteinization) was used as such after dilution with water. The pH of all blood samples used for all the experiments was maintained at 7.4.

3.6.3. Calculation of association constants (K_{ass})

Nucleotides, nucleosides and other analyte solutions were prepared in distilled water. The binding affinities of the cyclophanes and model derivatives were calculated using Benesi-Hildebrand equation 3.2, where, K is the equilibrium constant, A_f is the

$$\frac{1}{A_f - A_{ob}} = \frac{1}{A_f - A_{fc}} + \frac{1}{K(A_f - A_{fc})[\text{Ligand}]} \quad (3.2)$$

absorbance of free host, A_{ob} is the observed absorbance in the presence of various ligands and A_{fc} is the absorbance at saturation. The linear dependence of $1/(A_f - A_{ob})$ on the reciprocal of the ligand concentration indicates the formation of a 1:1 molecular complex between ligands and the host.

3.6.4. Calculation of change in free energy (ΔG_{ET})

The change in free energy (ΔG_{ET}) for the photoinduced electron transfer reaction was evaluated according to Rehm-Weller equation 3, where, $E_{(0,0)}$ is the singlet excitation energy in eV, w_p is

$$\Delta G_{ET} = E_{ox} - E_{red} - w_p - E_{0,0} \quad (3.3)$$

the work term which was taken as -0.056 eV in water,²⁸ E_{ox} is the oxidation potential of the donor and E_{red} is the reduction potential of the acceptor. The oxidation potential of anthracene (1.9 eV), reduction potential of viologen (-0.45 eV) and singlet state energy of anthracene (3.18 eV) were used for calculations.⁵ The change in free energy value for the electron transfer from the singlet excited state of anthracene to the viologen was found to be -0.77 eV, which predicts a facile quenching of the anthracene fluorescence by the viologen moiety through an electron transfer mechanism.

The oxidation potential of HPTS (0.42 eV),²⁹ reduction potential of the viologen moiety (-0.45 eV) and singlet state energy of HPTS (2.59 eV) were used for calculations. The change in free energy value for the electron transfer from the excited state of HPTS to the viologen moiety was found to be -1.72 eV, which predicts a facile quenching of the fluorescence of HPTS by the viologen moiety through an electron transfer mechanism.

3.7. REFERENCES

- 1) (a) R. Martinez-Manez, F. Sancenon, *Chem. Rev.* **2003**, *103*, 4419-4476. (b) A. P. de Silva, H. Q. N. Gunaratne, T. Gunnlaugsson, A. J. M. Huxley, C. P. McCoy, J. T. Rademacher, T. E. Rice, *Chem. Rev.* **1997**, *97*, 1515-1566. (c) C. V. Kumar, A. Buranaprapuk, *Angew. Chem. Int. Ed. Engl.* **1997**, *36*, 2085-2087. (d) M. W. Hosseini, A. J. Blacker, J.-M. Lehn, *J. Am. Chem. Soc.* **1990**, *112*, 3896-3904. (e) L. Vial, P. Dumy, *J. Am. Chem. Soc.* **2007**, *129*, 4884-4885. (f) C. Marquez, U. Pischel, W. M. Nau, *Org. Lett.* **2003**, *5*, 3911-3914.
- 2) (a) B. Alberts, A. Johnson, J. Lewis, M. Raff, K. Roberts, P. Walter, *Molecular Biology of the Cell*, Garland Science, New

- York, **2002**. (b) G. Li, V. B. G. Segu, M. E. Rabaglia, R. -H. Luo, A. Kowluru, S. A. Metz, *Endocrinology* **1998**, *139*, 3752-3762. (c) C. S. Pinto, R. Seifert, *J. Neurochem.* **2006**, *96*, 454-459.
- 3) W. N. Lipscomb, N. Strater, *Chem. Rev.* **1996**, *96*, 2375-2433.
- 4) (a) S. Wang, Y.-T. Chang, *J. Am. Chem. Soc.* **2006**, *128*, 10380-10381. (b) K. Y. Kwon, N. J. Singh, H. N. Kim, S. K. Kim, K. S. Kim, J. Yoon, *J. Am. Chem. Soc.* **2004**, *126*, 8892-8893. (c) S. K. Kim, B.-S. Moon, J. H. Park, Y. I. Seo, H. S. Koh, Y. J. Yoon, K. D. Lee, J. Yoon, *Tetrahedron Lett.* **2005**, *46*, 6617-6620.
- 5) (a) A. Ojida, I. Takashima, T. Kohira, H. Nonaka, I. Hamachi, *J. Am. Chem. Soc.* **2008**, *130*, 12095-12101. (b) F. Zapata, A. Caballero, A. Espinosa, A. Tárraga, P. Molina, *J. Org. Chem.* **2008**, *73*, 4034-4044. (b) C. Li, M. Numata, M. Takeuchi, S. Shinkai, *Angew. Chem. Int. Ed.* **2005**, *44*, 6371-6374. (c) S. C. McCleskey, M. J. Griffin, S. E. Schneider, J. T. McDevitt, E. V. Anslyn, *J. Am. Chem. Soc.* **2003**, *125*, 1114-1115. (d) L. M. Tumir, I. Piantanida, P. Novak, M. Zinic, *M. J. Phys. Org. Chem.* **2002**, *15*, 599-607.
- 6) (a) J. Rebek, Jr. *Angew. Chem. Int. Ed. Engl.* **1990**, *29*, 245-255. (b) I. Piantanida, V. Tomisic, M. Zinic, *J. Chem. Soc., Perkin*

- Trans. 2*, **2000**, 375-383. (c) J. L. Sessler, V. Kral, T. V. Shishkanova, P. A. Gale, *Proc. Natl. Acad. Sci. USA* **2002**, *99*, 4848-4853.
- 7) M. Inouye, K. Kim, T. Kitao, *J. Am. Chem. Soc.* **1992**, *114*, 778-780.
- 8) (a) S. M. Biroš, J. Rebek, Jr. *Chem. Soc. Rev.* **2007**, *36*, 93-104. (b) H. Hayashida, N. Ogawa, M. Uchiyama, *J. Am. Chem. Soc.* **2007**, *129*, 13698-13705. (c) V. Dvornikovs, B. E. House, M. Kaetzel, J. R. Dedman, D. B. Smithrud, *J. Am. Chem. Soc.* **2003**, *125*, 8290-8301. (d) J. Yan, Y. Zhou, P. Yu, L. Su, L. Mao, D. Zhang, D. Zhu, *Chem. Commun.* **2008**, 4330-4332.
- 9) (a) A. H. Flood, Y. Liu, J. F. Stoddart, In *Modern Cyclophane Chemistry*, R. Gleiter, H. Hopf (Eds.) Wiley-VCH, Weinheim, **2004**. (b) F. Diederich, In *Cyclophanes, Monographs in Supramolecular Chemistry*, J. F. Stoddart (Ed.), The Royal Society of Chemistry, London, **1991**.
- 10) (a) E. A. Meyer, R. K. Castellano, F. Diederich, *Angew. Chem. Int. Ed.* **2003**, *42*, 1210-1250. (b) C. G. Claessens, J. F. Stoddart, *J. Phys. Org. Chem.* **1997**, *10*, 254-272.

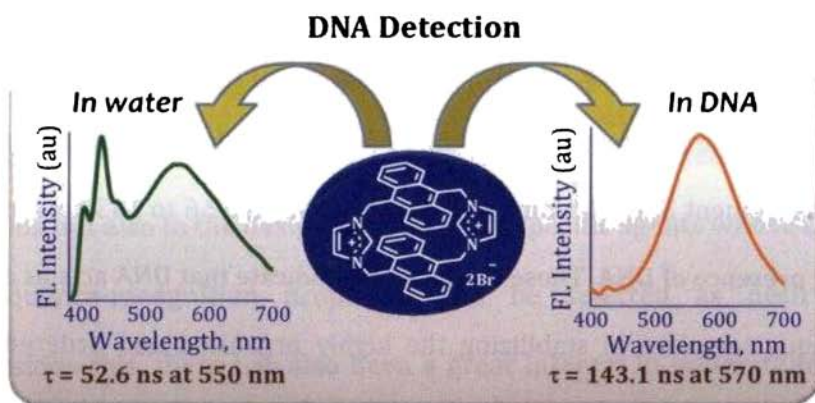
- 11) (a) P. P. Neelakandan, M. Hariharan, D. Ramaiah, *Org. Lett.* **2005**, *7*, 5765-5768. (b) P. P. Neelakandan, M. Hariharan, D. Ramaiah, *J. Am. Chem. Soc.* **2006**, *128*, 11334-11335.
- 12) H. Benesi, J. Hildebrand, *J. Am. Chem. Soc.* **1949**, *71*, 2703-2707.
- 13) (a) C. L. Bird, A. T. Kuhn, *Chem. Soc. Rev.* **1981**, *10*, 49-82. (b) J. Joseph, N. V. Eldho, D. Ramaiah, *J. Phys. Chem. B* **2003**, *107*, 4444-4450.
- 14) H.-J. Schneider, *Angew. Chem. Int. Ed. Engl.* **1991**, *30*, 1417-1436.
- 15) (a) S. L. Wiskur, H. Ait-Haddou, J. J. Lavigne, E. V. Anslyn, *Acc. Chem. Res.* **2001**, *34*, 963-972. (b) B. T. Nguyen, E. V. Anslyn, *Coord. Chem. Rev.* **2006**, *250*, 3118-3127. (c) L. Fabbriizzi, N. Marcotte, F. Stomeo, A. Taglietti, *Angew. Chem. Int. Ed.* **2002**, *41*, 3811-3814.
- 16) E. Pino, A. M. Campos, E. J. Lissi, *J. Photochem. Photobiol. A Chem.* **2003**, *155*, 63-68.
- 17) Gaussian 03 (Revision-D.01), M. J. Frisch, G. W. Trucks, H. B. Schlegel, G. E. Scuseria, M. A. Robb, J. R. Cheeseman, J. A. Montgomery, Jr., T. Vreven, K. N. Kudin, J. C. Burant, J. M.

- Millam, S. S. Iyengar, J. Tomasi, V. Barone, B. Mennucci, M. Cossi, G. Scalmani, N. Rega, G. A. Petersson, H. Nakatsuji, M. Hada, M. Ehara, K. Toyota, R. Fukuda, J. Hasegawa, M. Ishida, T. Nakajima, Y. Honda, O. Kitao, H. Nakai, M. Klene, X. Li, J. E. Knox, H. P. Hratchian, J. B. Cross, C. Adamo, J. Jaramillo, R. Gomperts, R. E. Stratmann, O. Yazyev, A. J. Austin, R. Cammi, C. Pomelli, J. W. Ochterski, P. Y. Ayala, K. Morokuma, G. A. Voth, P. Salvador, J. J. Dannenberg, V. G. Zakrzewski, S. Dapprich, A. D. Daniels, M. C. Strain, O. Farkas, D. K. Malick, A. D. Rabuck, K. Raghavachari, J. B. Foresman, J. V. Ortiz, Q. Cui, A. G. Baboul, S. Clifford, J. Cioslowski, B. B. Stefanov, G. Liu, A. Liashenko, P. Piskorz, I. Komaromi, R. L. Martin, D. J. Fox, T. Keith, M. A. Al-Laham, C. Y. Peng, A. Nanayakkara, M. Challacombe, P. M. W. Gill, B. Johnson, W. Chen, M. W. Wong, C. Gonzalez, and J. A. Pople, Gaussian, Inc., Pittsburgh, PA, **2003**.
- 18) C. A. Hunter, K. R. Lawson, J. Perkins, C. J. Urch, *J. Chem. Soc., Perkin Trans. 2* **2001**, 651-669.
- 19) H.-J. Schneider, R. Kramer, S. Simova, U. Schneider, *J. Am. Chem. Soc.* **1988**, *110*, 6442-6448.

- 20) C. Carmona, M. Balon, A. S. Coronilla, M. A. Munoz, *J. Phys. Chem. A* **2004**, *108*, 1910-1918.
- 21) P. L. Boulas, M. G. Kaifer, L. Echegoyen, *Angew. Chem. Int. Ed.* **1998**, *37*, 216-247.
- 22) E. B. de Borba, C. L. C. Amaral, M. J. Politi, R. Villalobos, M. S. Baptista, *Langmuir* **2000**, *16*, 5900-5907.
- 23) (a) B. J. Whitlock, H. W. Whitlock, in *Comprehensive Supramolecular Chemistry, Vol. 2. Molecular Recognition: Receptors for Molecular Guests*; J. L. Atwood, J. E. D. Davies, D. D. Macnicol, F. Vogtle, J.-M. Lehn, Eds.; Elsevier Science Ltd., Oxford, **1996**. (b) B. R. Peterson, T. Mordasini-Denti, F. Diederich, *Chem. Biol.* **1995**, *2*, 139-146. (c) M. E. Haeg, B. J. Whitlock, H. W. Whitlock, Jr. *J. Am. Chem. Soc.* **1989**, *111*, 692-696.
- 24) S. Gamsey, A. Miller, M. M. Olmstead, C. M. Beavers, L.C. Hirayama, S. Pradhan, R. A. Wessling, B. Singaram, *J. Am. Chem. Soc.* **2007**, *129*, 1278-1286.
- 25) (a) R. R. Avirah, K. Jyothish, D. Ramaiah, *J. Org. Chem.* **2008**, *73*, 274-279. (b) M. Hariharan, P. P. Neelakandan, D. Ramaiah, *J. Phys. Chem. B* **2007**, *111*, 11940-11947. (c) K. Jyothish, M.

- Hariharan, D. Ramaiah, *Chem. Eur. J.* **2007**, *13*, 5944-5951. (d)
- E. Kuruvilla, D. Ramaiah, *J. Phys. Chem. B* **2007**, *111*, 6549-6556.
- 26) A. R. Roshal, J. A. Organero, A. Douhal, *Chem. Phys. Lett.* **2003**, *379*, 53-59.
- 27) I. Koshiishi, T. Imanari, *Anal. Chem.* **1997**, *69*, 216-220.
- 28) J. Joseph, N. V. Eldho, D. Ramaiah, *Chem. Eur. J.* **2003**, *9*, 5926-5935.
- 29) C. Prayer, T.-H. Tran-Thi, S. Pommeret, P. d'Oliveira, P. Meynadier, *Chem. Phys. Lett.* **2000**, *323*, 467-473.

4 BIOMOLECULAR RECOGNITION: INVESTIGATION OF INTERACTIONS OF A FEW CYCLOPHANES WITH DNA



4.1. ABSTRACT

With the objective of understanding how cyclophanes interact with DNA and also to evaluate their potential use as probes, we have studied the interactions of a few selected cyclophane derivatives with calf thymus DNA and polyoligonucleotides. Addition of DNA to the aqueous solution of the cyclophane **1** resulted in significant hypochromicity in its absorption spectrum, whereas only negligible changes were observed in the emission spectrum. The cyclophane **2**, on the other hand, exhibited significant hypochromicity in its

absorption spectrum, along with red shifted excimer emission with increased intensity and lifetimes, leading to the visual detection of DNA. In contrast, the cyclophane **3** containing only one anthracene moiety showed negligible changes in its absorption and fluorescence spectra in the presence of DNA. Time-resolved fluorescence measurements of the cyclophane **2** showed significant enhancement in the lifetime of the excimer from 52.6 to 143.1 ns in the presence of DNA. These observations indicate that DNA acts as a unique template in stabilizing the highly organized and ordered conformer of **2** leading to the formation of excimer favorably. The driving force for the formation of excimer in the presence of DNA could be attributed to the synergistic effects of both hydrophobic interactions in the minor groove and the electrostatic interactions between the cationic cyclophane with the phosphate backbone. The uniqueness of the cyclophane **2** is that it selectively undergoes sequence selective interactions with DNA in buffer and under agarose gel electrophoresis conditions and signals the event through a "turn on" excimer emission mechanism.

4.2. INTRODUCTION

Study of interactions of small molecules with nucleic acids has assumed great significance over the past few decades because of their importance in biochemical and medicinal applications. Such studies not only give insights into the molecular basis of nucleic acid interactions, development and analysis of drugs targeted to nucleic acids but also in the design of new highly specific agents whose DNA sequence-recognition properties can be selected as desired.¹ Besides this, there has also been a great interest in understanding the natural process of DNA recognition by biomolecules such as proteins and enzymes.²

Most natural DNA recognition and modification processes involve the use of non-covalent (reversible) interactions. For example, proteins, restriction enzymes and related biomolecules undergo specific interactions with DNA during various biological events, including DNA replication and transcription. Several attempts have been made to mimic nature's design and architecture through the synthesis of DNA targeted molecules.³ The essence of these efforts is to develop molecules, which can be used in various

DNA mediated applications ranging from the design of new drugs to probes useful in studying electron transfer properties of DNA.⁴

As mentioned in the Chapter 1 of the present thesis, there are two principal ways through which small molecules can bind with DNA - covalent and non-covalent interactions. The non-covalent interactions in turn can be further subdivided into electrostatic, groove binding and intercalative interactions. The study of interactions of small molecules with DNA through non-covalent interactions can have potential applications in biology and medicine. As described in the Chapters 2 and 3 of this thesis, the water soluble cyclophane derivatives based on the anthracene chromophore have favorable photophysical properties and undergo selective interactions with nucleotides such as ATP and GTP.⁵ Our next objective was to investigate how efficiently these systems interact with polyoligonucleotides and DNA. Moreover, investigation of the interaction of cyclophane derivatives with DNA is challenging due to their inherent steric constraints.

In this context, we chose a few selected cyclophane derivatives **1** - **3** and the model compound **4** (Chart 4.1) and investigated their interactions with polyoligonucleotides, DNA and

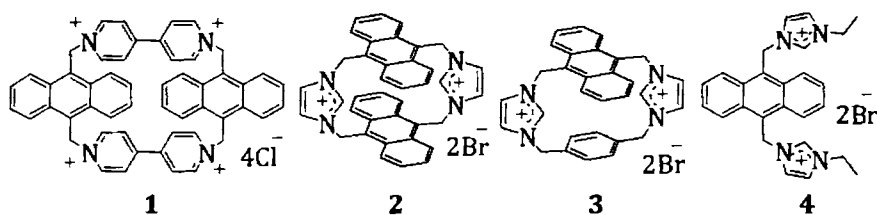


Chart 4.1

proteins through various photophysical and biophysical techniques.⁶ Our results indicate that the imidazolium bridged cyclophane **2** undergoes efficient interactions with DNA leading to the formation of a highly ordered *sandwich*-type excimer with red shifted emission maximum and enhanced fluorescence intensity and lifetimes. The uniqueness of cyclophane **2** is that it selectively recognizes DNA in buffer and under agarose gel electrophoresis conditions and signals the event through a "turn on" excimer emission mechanism.

4.3. RESULTS

4.3.1. Interactions with DNA

We have chosen a few novel cyclophane derivatives **1-3** to investigate the influence of spacer length, cavity size and the

bridging units in the interaction of cyclophanes with DNA and a model open derivative **4**, for comparison. We synthesized these derivatives as described in the Chapter 2 of this thesis and have studied their interactions with DNA employing absorption, fluorescence, thermal denaturation, viscometry, circular dichroism (CD) and agarose gel electrophoresis techniques. Figure 4.1 shows the changes in the absorption spectrum of the cyclophane **1** upon the addition of DNA. The successive addition of calf thymus (CT) DNA to a solution of the cyclophane **1** in buffer (10 mM phosphate, pH 7.4) containing 2 mM NaCl resulted in gradual decrease in

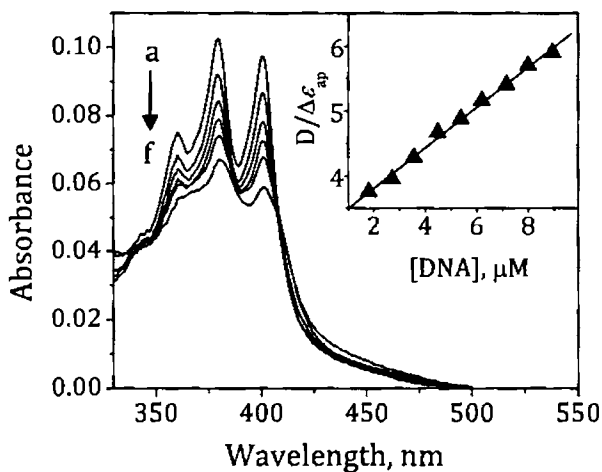


Figure 4.1. Changes in the absorption spectrum of **1** (21 μM) in the presence of CT DNA in phosphate buffer (10 mM, pH 7.4) containing 2 mM NaCl. [DNA], (a) 0 and (f) 55 μM. Inset shows the corresponding half-reciprocal analysis for the binding of the cyclophane **1** with DNA.

absorbance at 379 nm, corresponding to the anthracene chromophore. The maximum hypochromism (ca. 40%) was observed at 55 μM of DNA along with a bathochromic shift of 2 nm. As shown in the inset of Figure 4.1, half-reciprocal analysis of the absorption data gave a linear plot. The binding constant for the complex between the cyclophane **1** and DNA was determined and is found to be $K_{\text{DNA}} = 9.7 \pm 0.4 \times 10^4 \text{ M}^{-1}$. In the emission spectrum, we observed negligible changes with the addition of DNA (Figure 4.2).

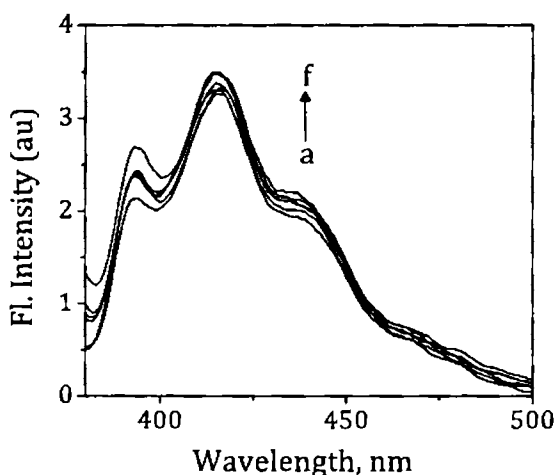


Figure 4.2. Changes in the emission spectrum of the cyclophane **1** (21 μM) in the presence of CT DNA in phosphate buffer (10 mM, pH 7.4) containing 2 mM NaCl. [DNA], (a) 0 and (f) 55 μM . Excitation wavelength, 350 nm.

We have further investigated the interaction of the imidazolium based derivatives **2** – **4** with DNA under identical

conditions. The gradual addition of CT DNA to a solution of the cyclophane **2** in buffer resulted in a regular decrease in the absorbance at 375 nm (Figure 4.3). At 40 μM of DNA, we observed 45% hypochromicity and a bathochromic shift of *ca.* 5 nm in the absorption spectrum along with three isosbestic points at 332, 382 and 402 nm. On the other hand, with the gradual addition of DNA, in the emission spectrum of the cyclophane **2** (which exhibited dual emission in buffer with an I_{550}/I_{430} ratio of 0.8, Section 2.3.3), we observed a regular and non-negligible decrease in the fluorescence intensity of the monomer at 430 nm, whereas a significant

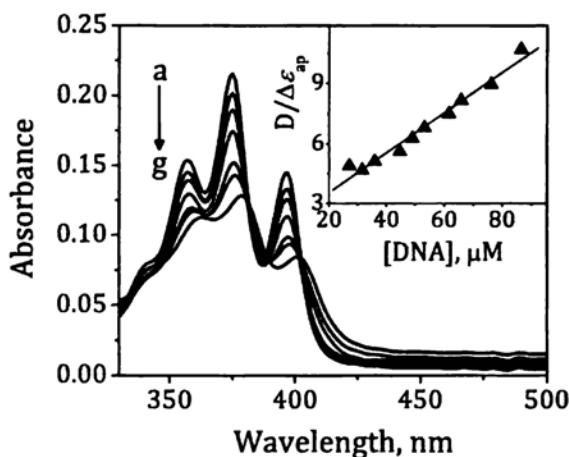


Figure 4.3. Changes in the absorption spectrum of the cyclophane **2** (14 μM) with the addition of DNA in phosphate buffer (10 mM, pH 7.4). Inset shows the half-reciprocal analysis of the absorption data for the binding of **2** to DNA. $[\text{DNA}]$, (a) 0 and (g) 40 μM .

enhancement was observed in the excimer emission intensity at 570 nm (Figure 4.4). At 40 μM of DNA, we observed *ca.* 9-fold enhancement in the I_{570}/I_{430} ratio along with a bathochromic shift of 20 nm leading to visual detection of DNA in buffer (inset of Figure 4.4) through 'turn-on' excimer fluorescence. The association constant (K_{DNA}) between the cyclophane **2** and DNA was determined using the absorption and emission spectral data by half-reciprocal (Inset of Figure 4.3) and Scatchard methods, respectively.^{7,8} Both these methods gave a value of $K_{\text{DNA}} = 7.6 \pm 1 \times 10^4 \text{ M}^{-1}$, indicating the strong binding affinity of the cyclophane **2** towards DNA.

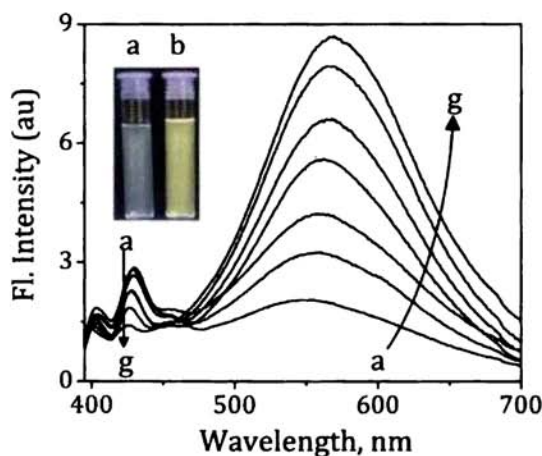


Figure 4.4. Changes in the emission spectra of **2** (14 μM) with addition of DNA in phosphate buffer (pH 7.4). [DNA], (a) 0 and (g) 40 μM . Excitation wavelength, 385 nm. Inset shows the fluorescence of **2** in (a) buffer and (b) presence of DNA (40 μM).

Figure 4.5 shows the changes observed in the photophysical properties of the model cyclophane derivative **3** with the gradual addition of CT DNA. The successive addition of DNA to a solution of the cyclophane **3** in buffer resulted in a marginal hypochromicity of 13% in the absorbance of the cyclophane **3** as compared to *ca.* 40% and 45% in the case of the cyclophanes **1** and **2**, respectively.

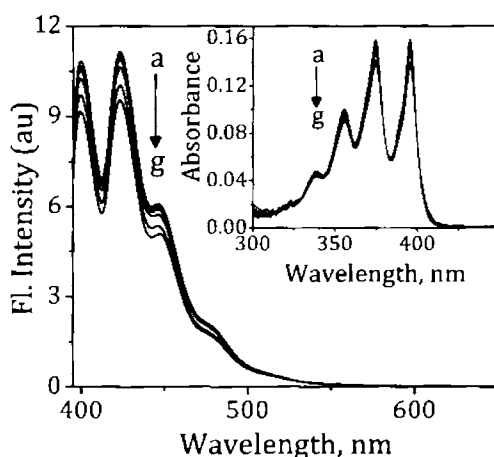


Figure 4.5. Changes in fluorescence emission and absorption (inset) spectra of the cyclophane **3** (17.2 μM) in phosphate buffer (10 mM, pH 7.4) with addition of DNA. [DNA], (a) 0 and (g) 45 μM. Excitation wavelength, 385 nm.

Similarly, we observed negligible quenching in the emission spectra of the cyclophane **3** upon the addition of 45 μM of DNA. On the other hand, the addition of DNA to the model open derivative **4** resulted in more prominent changes in its photophysical properties (Figure

4.6). For example, the addition of DNA to a solution of **4** resulted in *ca.* 23% hypochromicity in its absorption spectrum along with a gradual quenching in its emission intensity at 422 nm. Eventually, at 52 μM of DNA we observed a net quenching of 45% in the emission spectrum of the model derivative **4**.

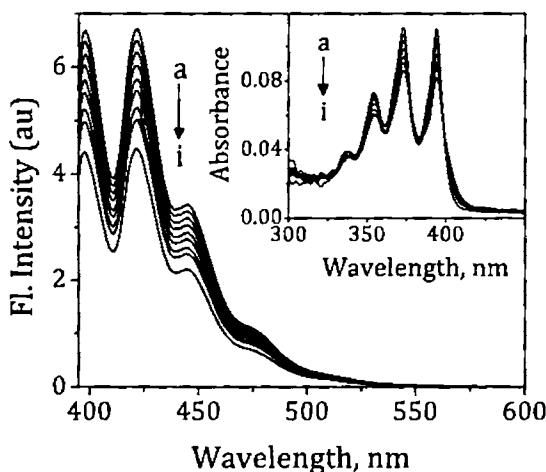


Figure 4.6. Changes in fluorescence emission and absorption (inset) spectra of the model derivative **4** (22 μM) in phosphate buffer (10 mM, pH 7.4) with addition of DNA. [DNA], (a) 0 and (i) 52 μM . Excitation wavelength, 385 nm.

4.3.2. Time Resolved Fluorescence Analysis

To understand the excited state properties of the cyclophanes in the presence of DNA, we have carried out picosecond time resolved fluorescence measurements. As described above, while the

viologen bridged cyclophane **1** showed negligible changes in the fluorescence spectrum in the presence of DNA, the imidazolium bridged cyclophane **2** exhibited an enhancement in the excimer emission. Therefore, we chose the cyclophane **2** as a representative example to carry out time resolved fluorescence measurements. As discussed in Chapter 2 of the thesis, picosecond time-resolved fluorescence analysis of the cyclophane **2** in buffer exhibited bi-exponential decay having lifetimes of 13.4 ± 0.5 and 52.6 ± 2 ns, corresponding to monomer and excimer. When we monitored the lifetimes at 550 nm, the species having longer lifetime (excimer) was observed to be the major component (96%), while at 430 nm, both these species were observed in equal amplitudes (Section 2.3.4).

When the lifetime measurements of the cyclophane **2** were carried out in the presence of DNA, we observed significant enhancement in the lifetime of excimer with a concomitant decrease in the monomer lifetime (Figure 4.7). The successive additions of DNA to a solution of the cyclophane **2** in buffer resulted in gradual increase in the excimer lifetimes when monitored at 570 nm. As compared to the lifetime of 52.6 ns in buffer, the cyclophane **2**

exhibited a significantly enhanced fluorescence lifetime of 143.1 ns at 40 μM DNA. In contrast, the monomer lifetime at 430 nm showed a gradual decrease and at 40 μM DNA we observed a lifetime of 11.5 ns as compared to 13.4 ns in the absence of DNA.

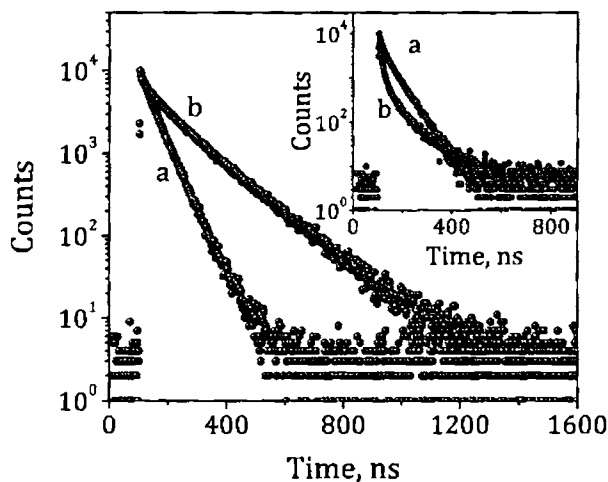


Figure 4.7. Fluorescence decay profiles of the cyclophane **2** (14 μM) (a) alone and (b) in the presence of DNA (40 μM) in phosphate buffer (10 mM, pH 7.4) monitored at 550 and 430 nm (inset). Excitation wavelength, 375 nm.

As DNA induced excimer emission in the cyclophane **2**, it was of our interest to investigate the cyclophane – DNA interaction through time resolved emission spectroscopy (TRES). TRES analysis of the cyclophane **2** in buffer showed a single peak at 420 nm corresponding to the monomer immediately after excitation (60 ps) (Section 2.3.4). In buffer, in the absence of DNA, the formation of

excimer could be detected only at a time scale of 0.46 ns. On the other hand, the addition of DNA led to more efficient excimer formation in the cyclophane **2**. In the presence of 40 μM DNA, the formation of excimer in **2** could be detected even at 60 ps, albeit with less intensity, indicating thereby the role played by DNA in facilitating the excimer formation (Figure 4.8). Subsequently, the

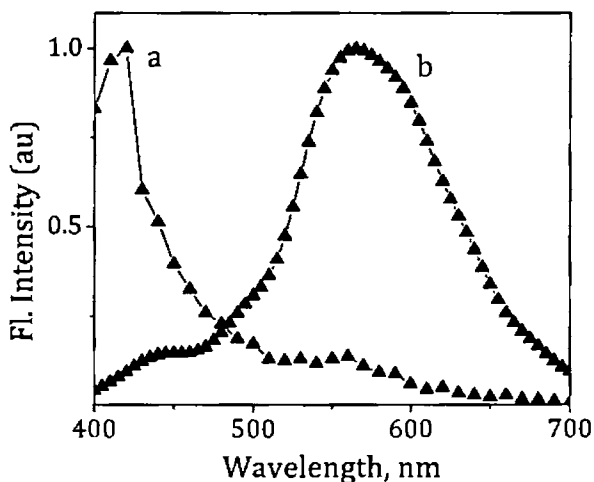


Figure 4.8. Time-resolved emission spectra of the cyclophane **2** in the presence of DNA monitored (a) 60 ps and (b) 96 ns after excitation. Excitation wavelength, 375 nm.

emission spectrum evolved with time and when the emission was monitored after 96 ns, the spectrum dominated exclusively with the excimer emission with $\lambda_{\text{max}} = 570$ nm.

4.3.3. Nature of DNA Binding Interactions

Since the cyclophanes under investigation are sterically bulky, it could be expected that their planar anthracene chromophore can intercalate between the base pairs of DNA and at the same time, the positively charged bridging units can interact electrostatically with the phosphate backbone of the DNA.⁹ To determine the binding mode of the cyclophane **2** with DNA, we have carried out the DNA binding studies under different ionic strengths (Figures 4.9 and 4.10). Interestingly, the binding of the cyclophane **2** to DNA was found to be highly dependent on the ionic strength of the buffer. For

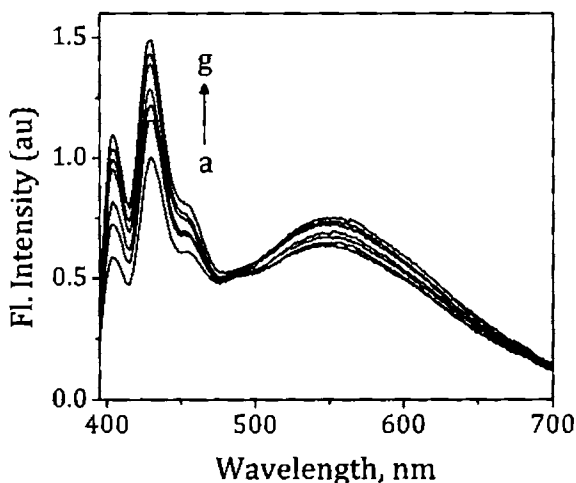


Figure 4.9. Changes in emission spectra of **2** (14 μM) in phosphate buffer (10 mM, pH 7.4) containing 50 mM NaCl with increasing addition of DNA. [DNA], (a) 0 and (g) 40 μM . Excitation wavelength, 385 nm.

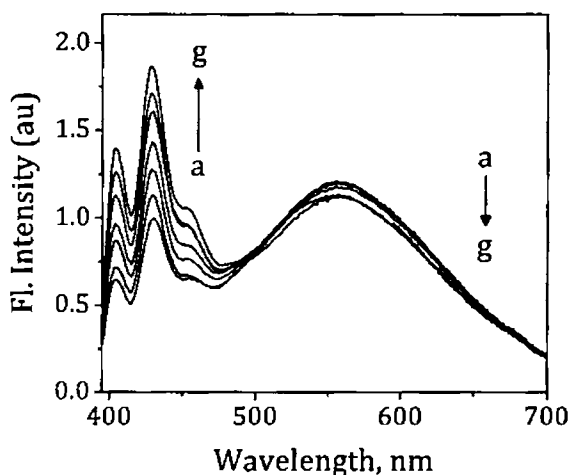


Figure 4.10. Changes in emission spectra of **2** ($14 \mu\text{M}$) in phosphate buffer (10 mM , $\text{pH } 7.4$) containing 500 mM NaCl with increasing addition of DNA. $[\text{DNA}]$, (a) 0 and (g) $40 \mu\text{M}$. Excitation wavelength, 385 nm .

example, when DNA was successively added to a solution of the cyclophane **2** in buffer containing 50 mM of NaCl , we observed an I_{550}/I_{430} ratio of 0.42 as compared to 7.1 observed in the absence of NaCl . Similarly, as shown in Figure 4.10, when the DNA binding studies were carried out in buffer containing 500 mM NaCl , we observed only negligible changes in the excimer emission of **2**.

Circular dichroism (CD) studies are useful in identifying the binding modes of organic ligands with DNA. Binding of an achiral molecule within a chiral environment, such as DNA, can induce optical activity in the bound species.¹⁰ In this context, we have

monitored the changes in the CD spectrum of DNA upon the successive addition of the cyclophane **2**. The CD spectrum of CT DNA in buffer is shown in Figure 4.11, which consisted of a positive peak at 290 nm and a negative band at 260 nm. When the cyclophane **2** was added to DNA, an induced CD (ICD) signal corresponding to the anthracene chromophore was observed at 375 nm. The successive additions of a solution of the cyclophane **2** to DNA resulted in the regular development of a bisignated ICD signal with a negative band at 405 nm and a positive peak around 375 nm. The corresponding absorption spectra, on the other hand, showed

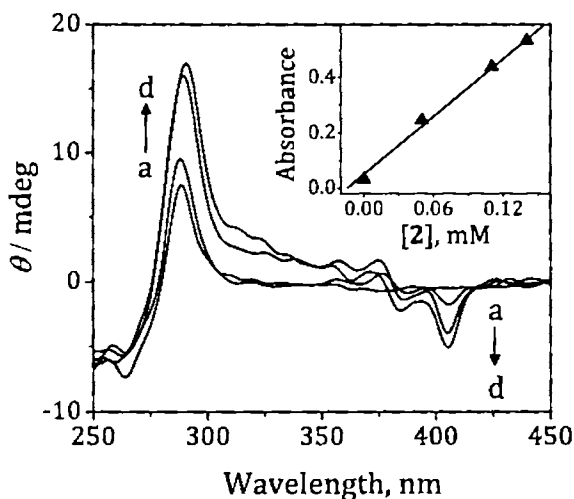


Figure 4.11. Changes in the circular dichroism spectrum of DNA (0.72 mM) in the presence of the cyclophane **2** in phosphate buffer (10 mM, pH 7.4) at 25 °C. Inset shows the corresponding variation in the absorption spectra. [**2**], (a) 0 and (d) 0.14 mM.

linearity with concentration, thereby ruling out the formation of aggregates under these conditions. These results indicate that the cyclophane **2** undergoes both electrostatic as well as non-classical intercalative interactions in the minor grooves of DNA.¹¹

4.3.4. DNA Thermal Denaturation Studies

Intercalation of the ligands with duplex DNA and interstrand crosslink formation during irradiation are known to increase the DNA melting temperature (T_m), i.e. the temperature at which the double helix denatures to single strand DNA.¹² The extinction coefficient of DNA bases at 260 nm in the double helical form is much less than that of the single strand form; hence, melting of the helix leads to an increase in the absorption at this wavelength. Thus, the helix to coil transformation can be determined by monitoring the absorbance of the duplex at 260 nm as a function of temperature.^{12,13} In order to understand the extent of interaction of the cyclophane **2** with DNA, we have examined the stabilization of CT DNA in the presence of the cyclophane **2**. Figure 4.12 shows the thermal denaturation curves for CT DNA in the absence and presence of the cyclophane **2** and the DNA melting temperature was

evaluated from the corresponding first derivative plots. DNA alone showed a melting temperature (T_m) of 55 °C without any additive, while in the presence of the cyclophane **2**, the melting temperature was found to be 65 °C, indicating significant stabilization of the duplex in the presence of the cyclophane **2**.

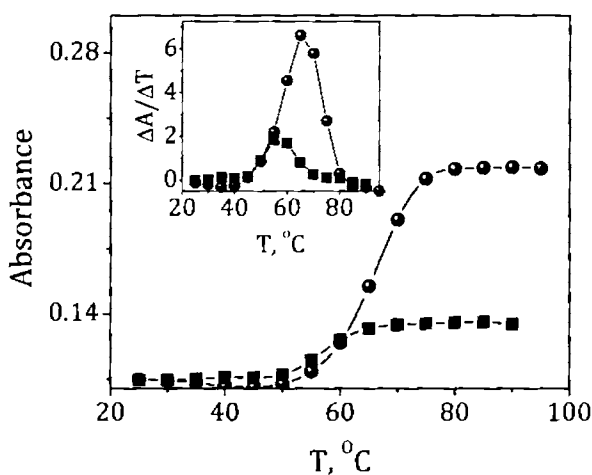


Figure 4.12. Thermal denaturation and (inset) differential thermal denaturation curves for CT DNA, in the (■) absence ($T_m = 55$ °C) and (●) presence of cyclophane **2** (8.3 μ M, $T_m = 65$ °C).

4.3.5. Viscosity Measurements

Viscosity of DNA is known to be sensitive to the mode of interaction of a ligand with DNA. For example, if a ligand binds through classical intercalative interactions, it exhibits significant increase in the length of the DNA resulting in enhancement in the

viscosity of DNA (Figure 4.13).¹⁴ In contrast, a partial, non-classical intercalation of ligand could bend (or kink) the DNA helix and hence reduce its effective length resulting in reduction in its viscosity.¹⁵ To have a better understanding of the mode of binding of the cyclophane **2** with DNA, the viscosity measurements of DNA were

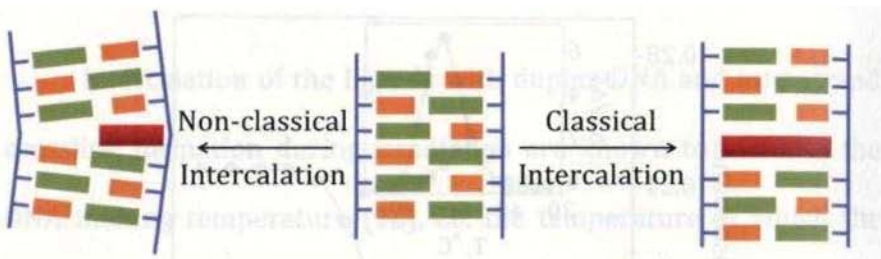


Figure 4.13. Schematic representation of DNA structural changes induced by classical and non-classical intercalative interactions.

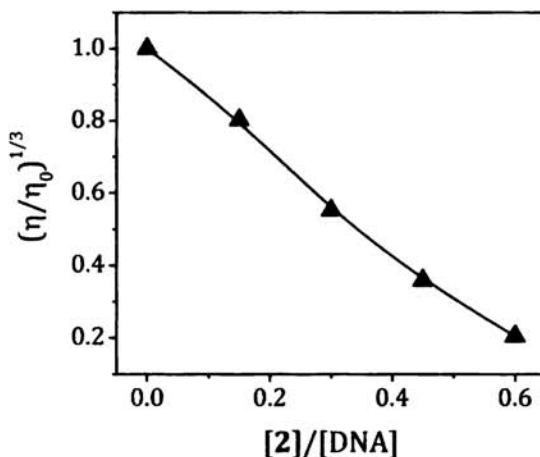


Figure 4.14. The effect of increasing concentrations of the cyclophane **2** on the relative viscosity of CT DNA (0.25 mM) at 25 ± 0.2 °C in phosphate buffer (10 mM, pH 7.4).

carried out in the presence and absence of the cyclophane **2**. Figure 4.14 shows the changes in viscosity of DNA with the increase in addition of the cyclophane **2**. We observed a dramatic decrease in the viscosity of DNA in the presence of the cyclophane **2** thereby, indicating a partial intercalative binding mode for **2**.

4.3.6. Interactions with Micelles and Proteins

To understand the uniqueness of the DNA template in inducing the excimer formation with enhanced emission, we investigated the changes in the excimer emission of the cyclophane **2** in the presence of surfactants and proteins. Above a certain concentration range, surfactant molecules aggregate in aqueous solution to form particles of colloidal dimensions called micelles. In a micelle, the alkyl chains of the surfactant form the interior hydrophobic core, whereas, the polar heads point towards the bulk aqueous medium. Therefore, the unique micellar structure confers in them both hydrophobic and hydrophilic environments.¹⁶

We have investigated the effect of sodium dodecyl sulphate (SDS) micelles on the photophysical properties of the cyclophane **2** because the anionic nature of SDS is expected to facilitate

electrostatic interactions with the cyclophane. The successive additions of SDS at and above critical micellar concentration (8.3 to 32.3 mM) to a solution of the cyclophane **2** led to a gradual increase in the monomer emission at 430 nm along with non-negligible decrease in the excimer emission at 550 nm (Figure 4.15). It is

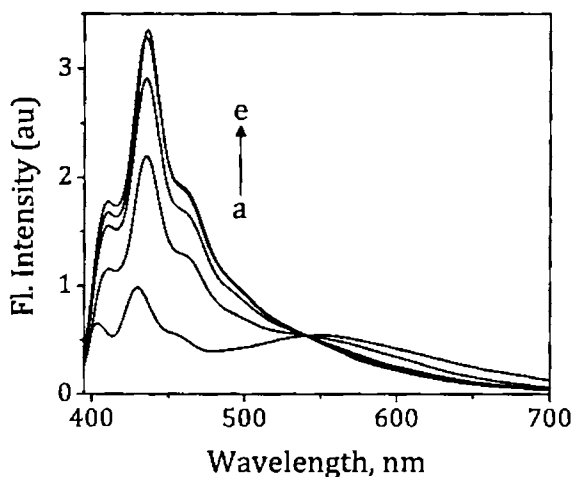


Figure 4.15. Changes in emission spectrum of **2** ($14 \mu\text{M}$) with increasing addition of sodium dodecyl sulphate (SDS) micelles. [SDS], (a) 0 and (e) 32.3 mM. Excitation wavelength, 385 nm.

expected that the cyclophane **2** gets encapsulated inside the micelles where the polarity is comparatively less as compared to the bulk. The excimer formation in the cyclophane **2**, which is strongly dependent on the polarity of the medium (Section 2.3.3), is suppressed under these conditions leading to enhancement in the

monomer emission. Further, we have investigated the effect of proteins on the fluorescence properties of the cyclophane **2**. We chose bovine serum albumin (BSA) and fibrinogen as two representative examples because they are reported to bind ligands through hydrophobic and electrostatic interactions.¹⁷ The successive addition of both BSA (0 - 21.6 μM) and fibrinogen (0 - 7 mM) led to negligible changes in the fluorescence spectrum of **2** as compared to that observed in buffer (Figure 4.16), indicating thereby that the **2** undergoes less efficient interactions with these proteins.

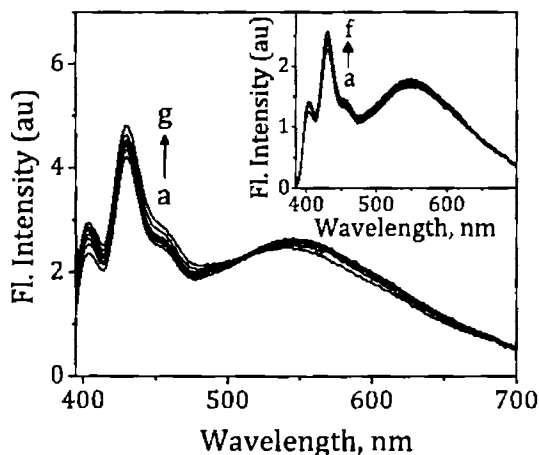


Figure 4.16. Changes in emission spectrum of **2** (14 μM) in phosphate buffer (10 mM, pH 7.4) with increasing concentration of bovine serum albumin (BSA) and (inset) fibrinogen. [BSA], (a) 0 and (g) 21.6 μM . [Fibrinogen], (a) 0 and (f) 7.01 mM. Excitation wavelength, 385 nm.

4.3.7. Gel Electrophoretic DNA Detection

As the DNA template alone induced excimer formation in the cyclophane **2** as compared to the micelles and proteins, it was of our interest to examine its potential use for the detection of DNA under agarose gel electrophoresis conditions. Agarose gel electrophoresis is a method used to separate and analyze DNA, which is achieved by moving negatively charged nucleic acid molecules through an agarose matrix using an electric field. After electrophoresis, DNA is visualized by staining with a suitable dye and the most common dye used for agarose gel electrophoresis is ethidium bromide (EB). In the bulk, EB is negligibly fluorescent, whereas when intercalated into DNA it becomes highly fluorescent and thus DNA can be visualized by illuminating the gel with UV light.¹⁸ The major drawback associated with EB is that it is highly carcinogenic. Moreover, its fluorescence lifetime after intercalating to DNA is *ca.* 20 ns, which makes it difficult to differentiate from the background fluorescence of biological samples. Therefore, it was of our interest to investigate the potential application of the cyclophane **2** as a staining agent under agarose gel electrophoresis conditions. Since **2**

exhibits turn on excimer emission with long fluorescence lifetime (143.1 ns) in the presence of DNA, it is expected that it can, in principle, act a staining agent whose fluorescence can be effectively differentiated from the background fluorescence. In this context, different concentrations of DNA solutions were prepared and electrophoresis was carried out on a 1% agarose gel. After electrophoresis, when the gel was stained with the cyclophane **2**, we observed DNA concentration dependent excimer intensity (Figure 4.17). Such a “turn on” excimer emission under electrophoresis conditions can be effectively used for the quantification of DNA.



Figure 4.17. Recognition of plasmid PUC18 DNA by the cyclophane **2** after gel electrophoresis through excimer emission. Lanes: (a) 0.05 and (b) 0.1 $\mu\text{g}/\mu\text{L}$ of DNA.

4.3.8. DNA Sequence Selective Interactions

Since the cyclophane **2** exhibited selective interactions with DNA, we were interested to evaluate their DNA sequence selectivity.

It is well established that most of the inherited and acquired diseases are transferred via disease-related sequences and ligands that can bind selectively to a particular DNA sequence can have potential medicinal applications.¹⁹ In this context, we have studied the interactions of the cyclophane **2** with polyoligonucleotides such as the non-alternating poly(dA).poly(dT) and poly(dG).poly(dC) sequences as well as alternating poly(dG.dC)-poly(dG.dC) sequences. The addition of poly(dA).poly(dT) to a solution of the cyclophane **2** in buffer gave initially an enhancement in the excimer emission at 565 nm (Figure 4.18). However, the subsequent additions from 32.8 to 68.6 μM yielded significant enhancement in

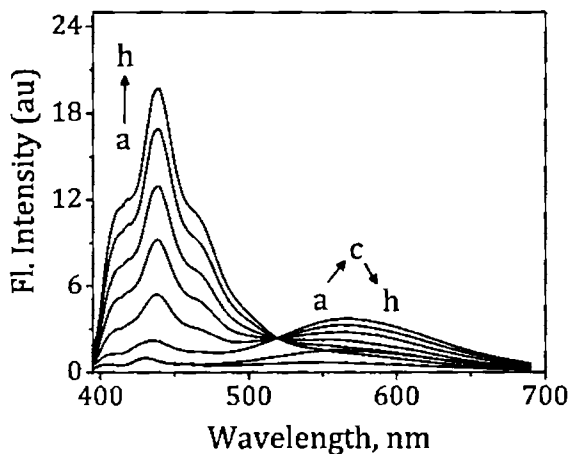


Figure 4.18. Changes in the emission spectrum of the cyclophane **2** (10 μM) with the addition of poly(dA).poly(dT) in phosphate buffer (10 mM, pH 7.4). [Poly(dA).poly(dT)], (a) 0, (c) 23.6 and (h) 68.6 μM . Excitation wavelength, 385 nm.

the monomer emission at 438 nm along with a concomitant decrease in the excimer emission intensity at 565 nm. In contrast, the addition of poly(dG).poly(dC) and poly(dG-dC).poly(dG-dC) under similar conditions, exhibited enhancement in the excimer emission of the cyclophane **2** as shown in Figures 4.19 and 4.20.

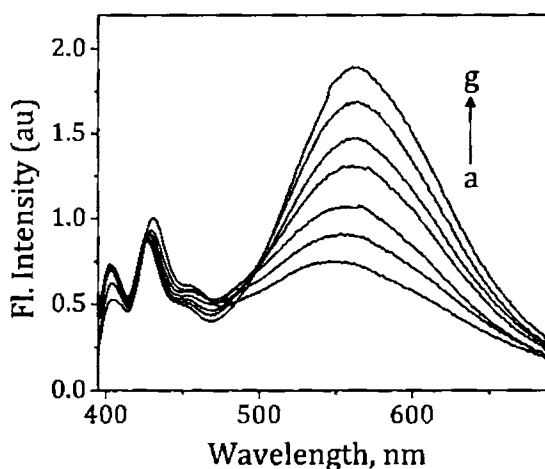


Figure 4.19. Changes in the emission spectrum of the cyclophane **2** (10 μ M) with the addition of poly(dG).poly(dC) in phosphate buffer (10 mM, pH 7.4). [Poly(dG).poly(dC)], (a) 0 and (g) 64.8 μ M. Excitation wavelength, 385 nm.

These observations are comparable to those obtained with CT DNA, but the extent of enhancement in the excimer emission was found to be less, *ca.* 3-fold and 2.5-fold enhancement in the I_{570}/I_{430} ratio for poly(dG).poly(dC) and poly(dG-dC).poly(dG-dC), respectively as compared to *ca.* 9-fold observed in the case of CT DNA. These

observations clearly indicate that the excimer formation in the cyclophane **2** is strongly dependant on the DNA sequence.

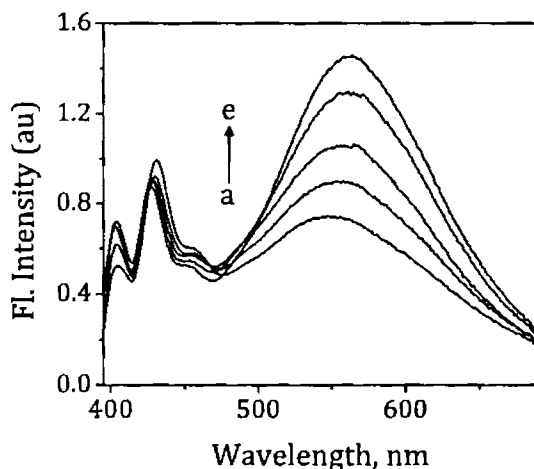


Figure 4.20. Changes in the emission spectrum of the cyclophane **2** ($10 \mu\text{M}$) with the addition of poly(dG-dC).poly(dG-dC) in phosphate buffer (10 mM , pH 7.4). [Poly(dG-dC).poly(dG-dC)], (a) 0 and (e) $57.4 \mu\text{M}$. Excitation wavelength, 385 nm .

4.4. DISCUSSION

The cyclophane derivatives used in the present investigation exhibited favorable photophysical properties in the aqueous medium and undergoes efficient interactions with DNA, as compared to proteins and micelles. Eventhough the interaction of the cyclophane **1** with DNA resulted in hypochromicity in the absorption, only negligible changes were observed in its emission spectrum. The marginal bathochromic shift (*ca.* 1 nm) along with *ca.*

40% hypochromicity in the absorption spectrum of the cyclophane **1** in the presence of DNA clearly indicates that the classical intercalative interactions can be ruled out. Based on the fact that substantially large substituents on the ligands inhibit intercalation through steric blockage,^{11a} the rigid cyclophane **1** can be considered to bind to DNA within the grooves.

On the other hand, the interaction of the cyclophane **2** with DNA results in significant hypochromicity in the absorption spectrum along with a bathochromic shift of 5 nm. The change in the optical properties of this cyclophane indicates its strong affinity for DNA. The binding of the cyclophane **2** to DNA could be attributed to the π - π stacking of the anthracene chromophore between DNA bases through partial intercalation. In addition to this, electrostatic interaction between the cationic cyclophane and the phosphate backbone of DNA is expected to facilitate the formation of a stable complex as evidenced through the results obtained at different ionic strengths of the medium. This interpretation is based on the experimental evidence and literature reports.²⁰ The observation of decrease in DNA association constants of the cyclophane **2** upon increasing ionic strength of the medium clearly suggests that

electrostatic interactions play an important role in binding interactions with DNA. Similarly, the decrease in DNA viscosity in presence of the cyclophane **2** and the bisignated induced CD signal corresponding to the anthracene chromophore confirms that these systems undergo predominantly non-classical intercalative interactions with DNA.

The cyclophane **3** containing only one anthracene chromophore, on the other hand, exhibited only negligible binding with DNA. The observations with the cyclophane **3** are rather unexpected, but indeed interesting. Moreover, these results help in determining the driving forces behind the interaction of cyclophanes with DNA. The replacement of one anthracene moiety by a phenyl group in the cyclophane **3** results in significantly reduced aromatic surface. This reduction in the aromatic surface, in turn, results in significantly decreased π - π stacking interactions with the nucleobases of DNA, thereby resulting in negligible binding. The results with the cyclophane **3**, moreover, prove that electrostatic interactions are not the decisive factors which govern DNA binding interactions of cyclophanes. In contrary to the observations with the cyclophane **2**, the model open derivative

showed less significant binding affinity towards DNA. It is expected that this open derivative binds to the DNA double helix through intercalative binding mechanism thereby resulting in the quenching of its fluorescence.

The interaction of the cyclophane **2** with DNA is novel since it resulted in the exclusive formation of the intramolecular excimer with bathochromically shifted emission maximum at 570 nm along with significantly enhanced intensity (*ca.* 9-fold enhancement in excimer to monomer ratio) and lifetimes (143.1 ns). These observations indicate that DNA acts as a unique template in stabilizing the highly organized *sandwich*-type conformer of the cyclophane **2**.²¹ The observation of fluorescence quenching at 422 nm, without the formation of any long wavelength bands in the emission spectrum of the open derivative **4** in the presence of DNA rules out the possibility of intermolecular excimer formation.

Based on the negative results obtained with proteins and micellar medium, the driving force for the formation of an excimer in the presence of DNA could be attributed to the synergistic effects of both hydrophobic interactions in the minor groove and the electrostatic interactions between the cationic cyclophane **2** and the

phosphate backbone of DNA. The involvement of electrostatic interactions was established through the observation of negligible influence of DNA on the excimer formation at the higher ionic strengths of the buffer. Based on the steric considerations, the classical intercalative binding of the cyclophane **2** with DNA could be ruled out, but it can undergo non-classical intercalative interactions in the minor grooves of DNA, as evidenced from the observation of bisignated ICD signal and the sequence dependent excimer formation.²²

4.5. CONCLUSIONS

In conclusion, we have demonstrated the potential use of the cyclophanes as probes for DNA. Of all the cyclophane derivatives under study, the imidazolium bridged cyclophane **2** undergoes sequence selective interactions with DNA, resulting in the exclusive formation of a highly organized *sandwich*-type excimer having bathochromic shifted emission at 570 nm and significant enhancement in intensity and lifetime of 143.1 ns. The viologen linked cyclophane **1**, on the other hand, undergoes less significant interactions with DNA, whereas, the model cyclophane **3** exhibits

negligible binding with DNA. As far as we know this is the first report wherein DNA assists the formation of an excimer which has the longest lifetime at 25 °C. The uniqueness of the cyclophane **2** is that it selectively recognizes DNA as compared to micelles and proteins in buffer and under agarose gel electrophoretic conditions and signals the event interestingly through “turn on” excimer emission mechanism.

4.6. EXPERIMENTAL SECTION

4.6.1. General Techniques

An Elico pH meter was used for pH measurements. The electronic absorption spectra were recorded on a Shimadzu UV-VIS-NIR spectrophotometer. Fluorescence spectra were recorded on a SPEX-Fluorolog F112X spectrofluorimeter. The fluorescence quantum yields were determined by using optically matched solutions. Fluorescence lifetimes were measured using a IBH picosecond single photon counting system. The fluorescence decay profiles were deconvoluted using IBH data station software V2.1, and minimizing the χ^2 values of the fit to 1 ± 0.1 . Circular dichroism spectra were recorded on a Jasco J-810 spectropolarimeter.

A solution of calf thymus DNA was sonicated for 1 h to minimize complexities arising from DNA flexibility¹⁴ and filtered through a 0.45 μm Millipore filter ($M_w = 3 \times 10^5 \text{ g mol}^{-1}$). The concentrations of DNA solutions were determined by using the average value of $6600 \text{ M}^{-1} \text{ cm}^{-1}$ for the extinction coefficient of a single nucleotide at 260 nm.¹⁴ Polynucleotides were dissolved in phosphate buffer, and the concentrations were determined by using the average extinction coefficient value of $7400 \text{ M}^{-1} \text{ cm}^{-1}$ at 253 nm for poly(dG).poly(dC) and $6000 \text{ M}^{-1} \text{ cm}^{-1}$ at 260 nm for poly(dA).poly(dT).²³ Viscosity measurements of DNA were carried out using calf thymus DNA (0.25 mM) in phosphate buffer (10 mM) containing 2 mM NaCl (pH 7.4) at 25 °C and also in the presence of the cyclophanes under similar conditions.

4.6.2. Materials

Calf thymus DNA and polynucleotides, purchased from Sigma-Aldrich and Amersham Pharmacia Biotech Inc. respectively, were used as received. The synthesis of the cyclophane derivatives **1** – **3** and the model derivative **4** used in the present study has been achieved as described in Chapter 2 of the present thesis.^{5,6} Doubly

distilled water was used for all the experiments. All experiments were carried out in 10 mM phosphate buffer (pH 7.4) containing 2 mM NaCl at room temperature (25 ± 1 °C), unless otherwise mentioned.

4.6.2. DNA Binding Studies

The DNA binding studies were carried out in 10 mM phosphate buffer (pH 7.4) containing 2, 100 and 500 mM NaCl. The intrinsic binding constant of the cyclophane derivatives with CT DNA was determined using absorbance at the respective maxima recorded after each addition of CT DNA. The intrinsic binding constant K_{DNA} was determined from the half reciprocal plot of $D/\Delta\epsilon_{ap}$ vs D , where D is the concentration of DNA in base pairs, $\Delta\epsilon_{ap} = [\epsilon_a - \epsilon_F]$ and $\Delta\epsilon = [\epsilon_b - \epsilon_F]$.^{7,24} The apparent extinction coefficient, ϵ_a , is obtained by calculating $A_{[obsd]} / [\text{cyclophane derivatives}]$. ϵ_b and ϵ_F correspond to the extinction coefficient of the bound form of the cyclophane derivatives and the extinction coefficient of the free cyclophanes, respectively. The data were fitted to Equation 4.1,

$$D/\Delta\epsilon_{ap} = D/\Delta\epsilon + 1/(\Delta\epsilon K_{DNA}) \quad (4.1)$$

with a slope equal to $1/\Delta\varepsilon$ and a y-intercept equal to $1/(\Delta\varepsilon K_{\text{DNA}})$. ε_b was determined from $\Delta\varepsilon$ and K_{DNA} was obtained from the ratio of the slope to the y-intercept.

4.6.3. Gel Electrophoresis

Agarose gel electrophoresis experiments were carried out using a Hoefer PS3000 system (Hoefer Scientific Instruments, San Francisco, CA) and the gel pictures were captured using a GelDoc 2000 series system (BioRad Laboratories, Segrate, Milan, Italy). Agarose, plasmid DNA, bromophenol blue, xylene cyanol FF and all other chemicals for gel electrophoresis experiments were obtained from Sigma-Aldrich. Agarose gel was prepared in 0.5X TBE buffer (45 mM Tris-borate, 1 mM EDTA, pH 7.4). The analysis was carried out by electrophoresis in a 1% agarose gel followed by autoradiography.²⁵ The gel was run at 60 V for 2 h. After electrophoresis, the gel was stained using the cyclophane **2**.

4.7. REFERENCES

1. (a) P. B. Dervan, *Science* **1986**, 232, 464-471. (b) *Molecular aspects of anticancer drug-DNA interactions*; S. N. Neidle, M. J.

- Waring, (Eds.), The Macmillan Press, Ltd. **1993**, Vol. 2. (c) M. J. Waring, *Annu. Rev. Biochem.* **1981**, *50*, 159. (d) M. Tomasz, In *Molecular Aspects of Anticancer-Drug Interactions*; S. N. Neidle, M. J. Waring, (Eds.), Macmillan Press, Boca Raton, FL, **1994**, Vol. 2. (e) D. M. Tidd, In *Molecular Aspects of Anticancer Drug-DNA Interactions*; S. N. Neidle, M. J. Waring, (Eds.), CRC, Boca Raton, FL, **1993**, Vol. 1.
2. (a) S. C. Harrison, R. T. Saeur, *Curr. Opinion Struc. Biol.* **1994**, *4*, 1-2. (b) S. E. V. Philips, D. Moras, *Curr. Opinion Struc. Biol.* **1992**, *2*, 69-70. (c) M. E. A. Churchill, A. A. Travers, *Trends Biochem. Sci.* **1991**, *16*, 92-97.
3. (a) P. E. Nielsen, *Bioconjugate Chem.* **1991**, *2*, 1-12. (b) M. Hansen, S.-J. Lee, J. M. Cassady, L. H. Hurley, *J. Am. Chem. Soc.* **1996**, *118*, 5553-5561.
4. (a) G. B. Schuster, *Acc. Chem. Res.* **2000**, *33*, 253-260. (b) M. D. Purugganan, C. V. Kumar, N. J. Turro, J. K. Barton, *Science*, **1988**, *241*, 1645-1649.
5. (a) P. P. Neelakandan, M. Hariharan, D. Ramaiah, *Org. Lett.* **2005**, *7*, 5765-5768. (b) P. P. Neelakandan, M. Hariharan, D. Ramaiah, *J. Am. Chem. Soc.* **2006**, *128*, 11334-11335.

6. P. P. Neelakandan, D. Ramaiah, *Angew. Chem. Int. Ed.* **2008**, *47*, 8407-8411.
7. (a) E. Kuruvilla, D. Ramaiah, *J. Phys. Chem. B* **2007**, *111*, 6549-6556. (b) J. Joseph, E. Kuruvilla, A. T. Achuthan, D. Ramaiah, G. B. Schuster, *Bioconjugate Chem.* **2004**, *15*, 1230-1235. (c) C. V. Kumar, E. H. Asuncion, *J. Am. Chem. Soc.* **1993**, *115*, 8541-8553.
8. (a) G. Scatchard, *Ann. N. Y. Acad. Sci.* **1949**, *51*, 660-662. (b) J. D. McGhee, P. H. Von Hippel, *J. Mol. Biol.* **1974**, *86*, 469-489. (c) E. Kuruvilla, J. Joseph, D. Ramaiah, *J. Phys. Chem. B* **2005**, *109*, 21997-22002.
9. J. Joseph, N. V. Eldho, D. Ramaiah, *Chem. Eur. J.* **2003**, *9*, 5926-5935.
10. (a) D. G. Dalglish, A. R. Peacocke, *Biopolymers* **1971**, *10*, 1853-1863. (b) R. J. Fiel, B. R. Munson, *Nucleic Acids Res.* **1980**, *8*, 2835-2842. (c) B. Nordén, F. Tjerneld, *Biopolymers* **1982**, *21*, 1713-1734. (d) M. Kubista, B. Aakerman, B. Nordén, *J. Phys. Chem.* **1988**, *92*, 2352-2356.
11. (a) W. B. Tan, A. Bhambhani, M. R. Duff, A. Rodger, C. V. Kumar, *Photochem. Photobiol.* **2006**, *82*, 20-30. (b) H. Ihmels, D. Otto,

- Top. Curr. Chem.* **2005**, *258*, 161-204. (c) S. Satyanarayana, J. C. Dabrowiak, J. B. Chaires, *Biochemistry* **1992**, *31*, 9319-9324.
12. (a) F. P. Gasparro, *Psoralen DNA Photobiology*, CRC Press Inc. Boca Raton, Florida, **1988**. (b) D. J. Patel, L. Cannel, *Proc. Natl. Acad. Sci. USA* **1976**, *73*, 674-678.
13. W. Adam, M. Berger, J. Cadet, F. Dall'Acqua, B. Epe, S. Frank, D. Ramaiah, S. Raoul, C. R. Saha-Moller, D. Vedaldi, *Photochem. Photobiol.* **1996**, *63*, 768-778.
14. (a) B. C. Baguley, E.-M. Falkenhaus, *Nucleic Acids Res.* **1978**, *5*, 161-171. (b) H. Deng, J. Cai, H. Xu, H. Zhang, L. Ji, *J. Chem. Soc. Dalton Trans.* **2003**, 325-330.
15. (a) Y. Xiong, X.-F. He, X.-H. Zou, J.-Z. Wu, X.-M. Chen, L.-N. Ji, R.-H. Li, J.-Y. Zhou, K.-B. Yu, *J. Chem. Soc. Dalton Trans.* **1999**, 19-23. (b) L. Kapicak, E. J. Gabbay, *J. Am. Chem. Soc.* **1975**, *97*, 403-408. (a) S. Satyanarayana, J. C. Dabrowiak, J. B. Chaires, *Biochemistry* **1992**, *31*, 9319-9324. (b) S. Satyanarayana, J. C. Dabrowiak, J. B. Chaires, *Biochemistry* **1993**, *32*, 2573-2584.
16. K. Kalyanasundaram, In *Photochemistry in Microheterogeneous Systems*, Academic Press, New York, **1987**.

17. V. Lhiaubet-Vallet, Z. Sarabia, F. Bosca, M. A. Miranda, *J. Am. Chem. Soc.* **2004**, *126*, 9538-9539.
18. (a) A. A. Marti, X. Li, S. Jockusch, Z. Li, B. Raveendra, S. Kalachikov, J. J. Russo, I. Morozova, S. V. Puthanveetil, J. Ju, N. J. Turro, *Nucleic Acids Res.* **2006**, *34*, 3161-3168. (b) C. J. Yang, S. Jockusch, M. Vicens, N. J. Turro, W. Tan, *Proc. Natl. Acad. Sci. USA* **2005**, *102*, 17278-17283.
19. (a) D. M. Chenoweth, A. Viger, P. B. Dervan, *J. Am. Chem. Soc.* **2007**, *129*, 2216-2217. (b) P. L. Paris, J. M. Langenhan, E. T. Kool, *Nucleic Acids Res.* **1998**, *26*, 3789-3793.
20. (a) E. C. Long, J. K. Barton, *Acc. Chem. Res.* **1990**, *23*, 271-273. (b) H. M. Berman, P. R. Young, *Annu. Rev. Biophys. Bioeng.* **1981**, *10*, 87-96. (c) G. Dougherty, W. J. Prigram, *Crit. Rev. Biochem.* **1982**, *12*, 103-125. (d) C. Cantor, P. R. Schimmel, In *Biophysical Chemistry*, W. H. Freeman (Ed.), San Fransisco, **1980**, Vol 2.
21. (a) Y. Molard, D. M. Bassani, J. P. Desvergne, N. Moran, J. H. R. Tucker, *J. Org. Chem.* **2006**, *71*, 8523-8531. (b) L. S. Kaanumalle, C. L. D. Gibb, B. C. Gibb, V. Ramamurthy, *J. Am. Chem. Soc.* **2005**, *127*, 3674-3675. (c) T. Hayashi, N. Mataga, Y.

- Sakata, S. Misumi, M. Morita, J. Tanaka, *J. Am. Chem. Soc.* **1976**, *76*, 5910-5913.
22. (a) *Circular Dichroism. Principles and Applications*, N. Berova, K. Nakanishi, R. W. Woody, (Eds.) Wiley-VCH, New York. **2000**. (b) A. Bhambhani, C. V. Kumar *Adv. Mater.* **2006**, *18*, 939-942. (c) M. Hariharan, J. Joseph, D. Ramaiah, *J. Phys. Chem. B* **2006**, *110*, 24678-24686. (d) F. D. Lewis, L. Zhang, X. Liu, X. Zuo, D. M. Tiede, H. Long, G. C. Schatz, *J. Am. Chem. Soc.* **2005**, *127*, 14445-14453.
23. S. Takenaka, T. Ihara, M. Takagi, *J. Chem. Soc. Chem. Commun.* **1990**, 1485-1487.
24. W. D. Wilson, L. Ratmeyer, M. Zhao, L. Strekovski, D. Boykin, *Biochemistry* **1993**, *32*, 4098-4104.
25. D. Ramaiah, Y. Kan, T. Koch, H. Orum, G. B. Schuster, *Proc. Natl. Acad. Sci. USA* **1998**, *95*, 12902-12905.

LIST OF PUBLICATIONS OF Mr. PRAKASH P. N.

1. DNA assisted long lived excimer formation in a cyclophane, **Prakash P. Neelakandan** and Danaboyina Ramaiah, *Angew. Chem. Int. Ed.* **2008**, *47*, 8407-8411.
2. Encapsulation of electron donor-acceptor dyads in β -cyclodextrin cavity: Unusual planarization and enhancement in rate of electron transfer reaction, Mahesh Hariharan, **Prakash P. Neelakandan** and Danaboyina Ramaiah, *J. Phys. Chem. B* **2007**, *111*, 11940-11947.
3. A supramolecular ON-OFF-ON fluorescence assay for selective recognition of GTP, **Prakash P. Neelakandan**, Mahesh Hariharan and Danaboyina Ramaiah, *J. Am. Chem. Soc.* **2006**, *128*, 11334 -11335.
4. Synthesis of a novel cyclic donor-acceptor conjugate for selective recognition of ATP, **Prakash P. Neelakandan**, Mahesh Hariharan and Danaboyina Ramaiah, *Org. Lett.* **2005**, *7*, 5765-5768.
5. Allosteric selective recognition of GMP by a novel metallocyclophane, Akhil K. Nair, **Prakash P. Neelakandan** and Danaboyina Ramaiah, (Communicated to *Angew. Chem.*).
6. Energy transfer between a cyclophane and ethidium bromide on a DNA scaffold, **Prakash P. Neelakandan**, Krishnankutty S. Sanju and Danaboyina Ramaiah (Communicated to *J. Am. Chem. Soc.*).
7. Molecular packing and solid-state fluorescence properties of a few anthracene containing cyclophanes, **Prakash P. Neelakandan** and Danaboyina Ramaiah, (To be communicated to *Adv. Mater.*).
8. A supramolecular fluorescent marker for the detection and quantification of GTP and ATP in buffer and biological fluids, Danaboyina Ramaiah, **Prakash P. Neelakandan** and Mahesh Hariharan, *CSIR # 0169NF2006* dated July 22, 2006.

PAPERS PRESENTED AT CONFERENCES

1. DNA recognition by a novel cyclophane through formation of an intramolecular excimer, **Prakash P. Neelakandan** and Danaboyina Ramaiah, a paper presented at the *IVth JNC Research Conference on Chemistry of Materials*, Hotel Lake Palace, Alleppey, Kerala, India, **2008**, Sept. 27-29.
2. Novel anthracenophanes: synthesis and study of their interactions with DNA and nucleotides, **Prakash P. Neelakandan** and Danaboyina Ramaiah, a poster presented at the *Recent Trends in Molecular Materials Research* under the India-Japan Cooperative Programme (IJCSP), Kovalam, Kerala, India, **2008** Jan. 19-22.
3. Synthesis of a few cyclic conjugates and study of their interactions with nucleotides and DNA, **Prakash P. Neelakandan** and Danaboyina Ramaiah, a paper presented at the *IIIrd JNC Research Conference on Chemistry of Materials*, Munnar, Kerala, India, **2007**, Sept. 29-Oct. 1.
4. A supramolecular ON-OFF-ON fluorescence assay for selective recognition of GTP in buffer and biofluids, **Prakash P. Neelakandan**, Mahesh Hariharan and Danaboyina Ramaiah, a poster presented at the *9th CRSI National Symposium in Chemistry*, University of Delhi, New Delhi, India, **2007**, Feb. 1-4.
5. Synthesis of a novel cyclic conjugate for selective recognition of purine nucleotides in aqueous medium, **Prakash P. Neelakandan**, Mahesh Hariharan and Danaboyina Ramaiah, a poster presented at the *IInd JNC Research Conference on Chemistry of Materials*, Quilon, Kerala, India, **2006**, Oct. 29-31 (Adjudged best poster).